NASA Conference Publication 2107

Nuclear-Pumped Lasers

Proceedings of a workshop held at
NASA Langley Research Center
Hampton, Virginia
July 25-26, 1979

NASA

NASA Conference Publication 2107

Nuclear-Pumped Lasers

Proceedings of a workshop held at
NASA Langley Research Center
Hampton, Virginia
July 25-26, 1979

National Aeronautics
and Space Administration

**Scientific and Technical
Information Branch**

1979

Foreword

For the past five years NASA has supported a nuclear-pumped laser program involving a number of universities and other laboratories. NASA is interested in nuclear-pumped lasers primarily because of their potential applications to space power transmission and propulsion. The primary aim of the nuclear-pumped laser research is to develop methods to allow efficient conversion of the energy liberated in nuclear reactions directly to coherent radiation. Conventional conversion of nuclear energy to electricity requires degenerating the fission fragment energy ($\sim$ 100 MeV) to thermal energy ($<$ 1 eV) with the resultant low ($\sim$ 30%) conversion efficiency. Gaseous core self-critical nuclear laser reactors have the potential of uniformly exciting large laser volumes with high efficiencies resulting in selfcontained very high power lasers. However, before such systems can become reality, considerable research is required to solve problems related to the compatibility of the lasing gas with the fissile fuel, the radiation extraction efficiency, and many other laser kinetics and nuclear related areas. It should be noted that the basic feasibility of gaseous core reactors has been demonstrated in the NASA gas core reactor program.

Considerable progress has already been made in the relatively new field of direct nuclear-pumped lasers. Direct nuclear pumping has been achieved for a large number of lasing systems and power output is in excess of 100 W.

The objectives of this workshop were to provide an interchange of research results and ideas among researchers in the field of nuclear-pumped lasers and to review the NASA nuclear-pumped laser program. This document contains a synopsis of the talks and the figures presented at the workshop.

The use of trade names or manufacturers names does not constitute endorsement, either expressed or implied, by the National Aeronautics and Space Administration.

Frank Hohl
Workshop Organizer

CONTENTS

UNIVERSITY OF FLORIDA NUCLEAR PUMPED LASER PROGRAM

by

Richard T. Schneider

ABSTRACT

The contribution towards design and construction of a nuclear pumped laser by the basic research program at the University of Florida consists of fundamental research into the mechanism of excitation of laser gases by fast ions (triton, proton or fission fragments) and especially any role UF_6 might play in non-radiative deexcitation of these gases.

For research on excitation mechanism spectroscopic methods were used to obtain population densities of excited states important for laser action.

Also, basic research on nuclear pumped CW-laser systems, especially He-Ne and CO_2, is under way using steady state reactors. It was demonstrated that He-Ne lases in a CW-mode with nuclear pumping at both the red and the infrared transition. The infrared transition was observed to be superradiant.

Studies into the compatibility of UF_6 with laser gases are necessary, because ultimately the fission fragments exciting the laser gas will have to come from a gaseous medium. For this purpose, measurement of the excited states lifetimes are carried out using the Cf^{252} radioactive isotope as a fission fragment source.

Another important question in this connection is the chemical stability of UF_6 under neutron and fission fragment irradiation. An incore reactor experiment is under way to irradiate UF_6 for an extended period of time and observe its decomposition using spectroscopy methods.

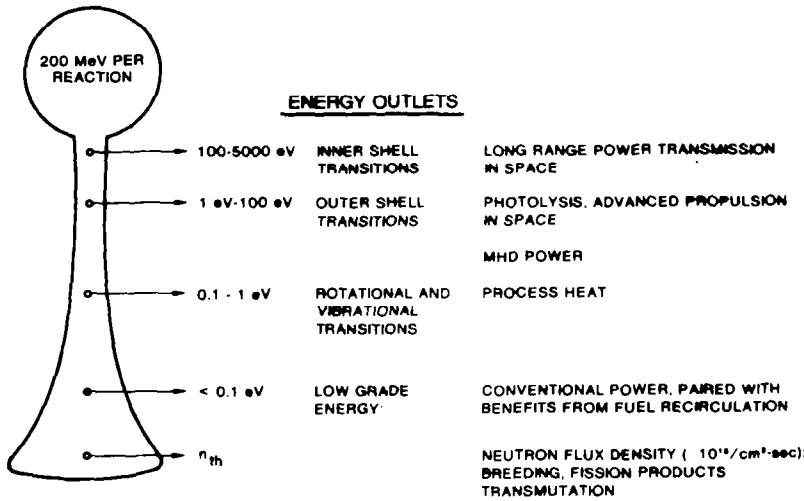

Gaseous fuel reactor. Principle of minimum entropy production.

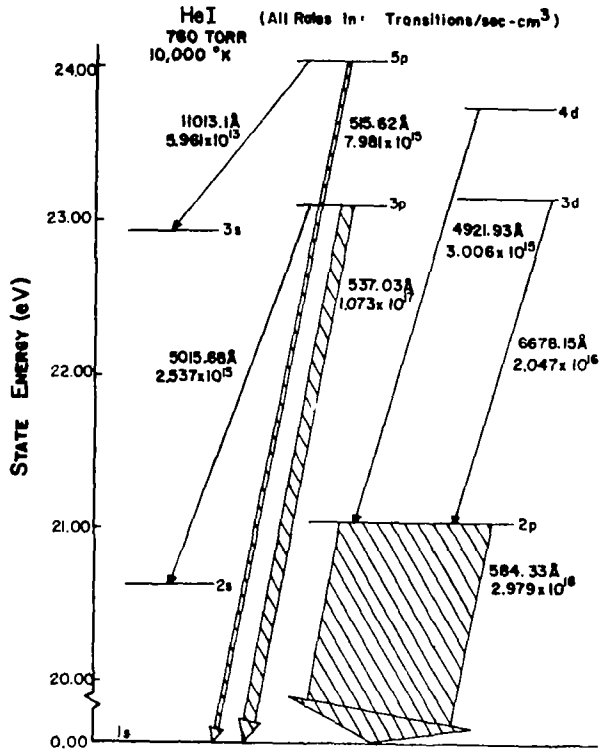

Relative transition rates.

EXPERIMENT FACILITY DESCRIPTION

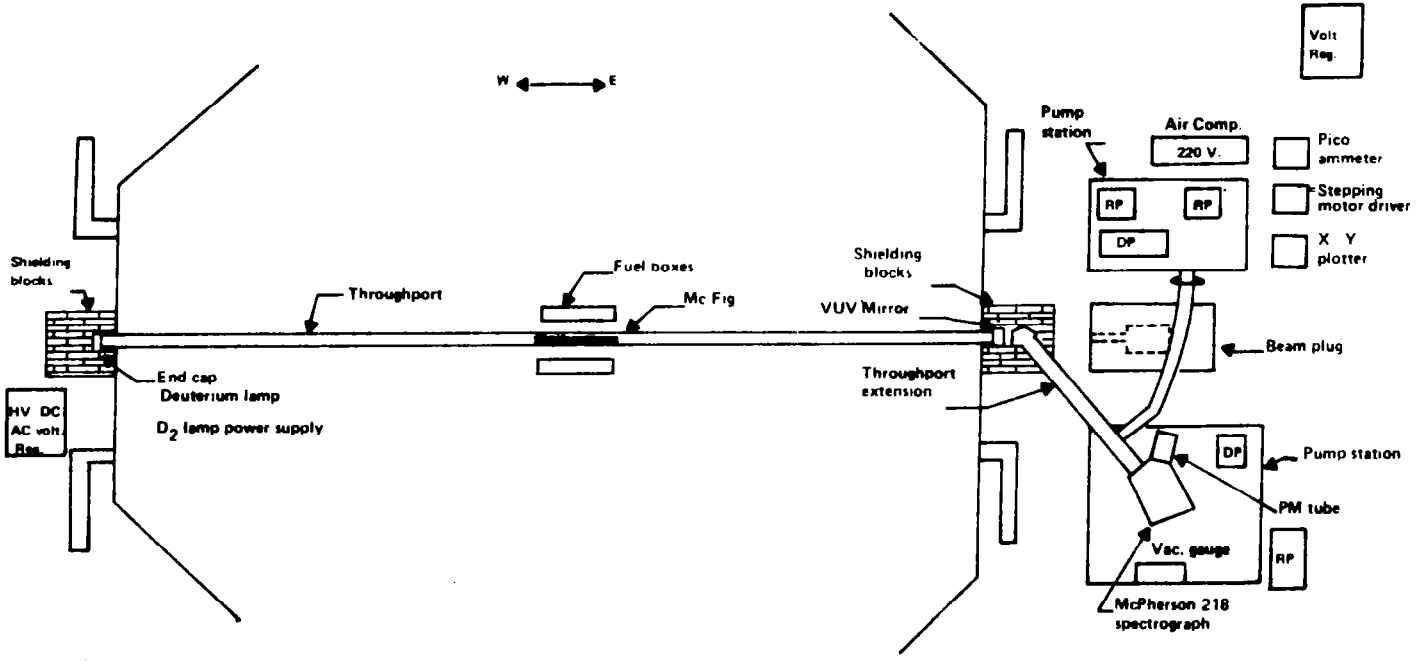

Research facility for vacuum-ultraviolet spectroscopy. (McFig is multipurpose capsule for irradiating gases.)

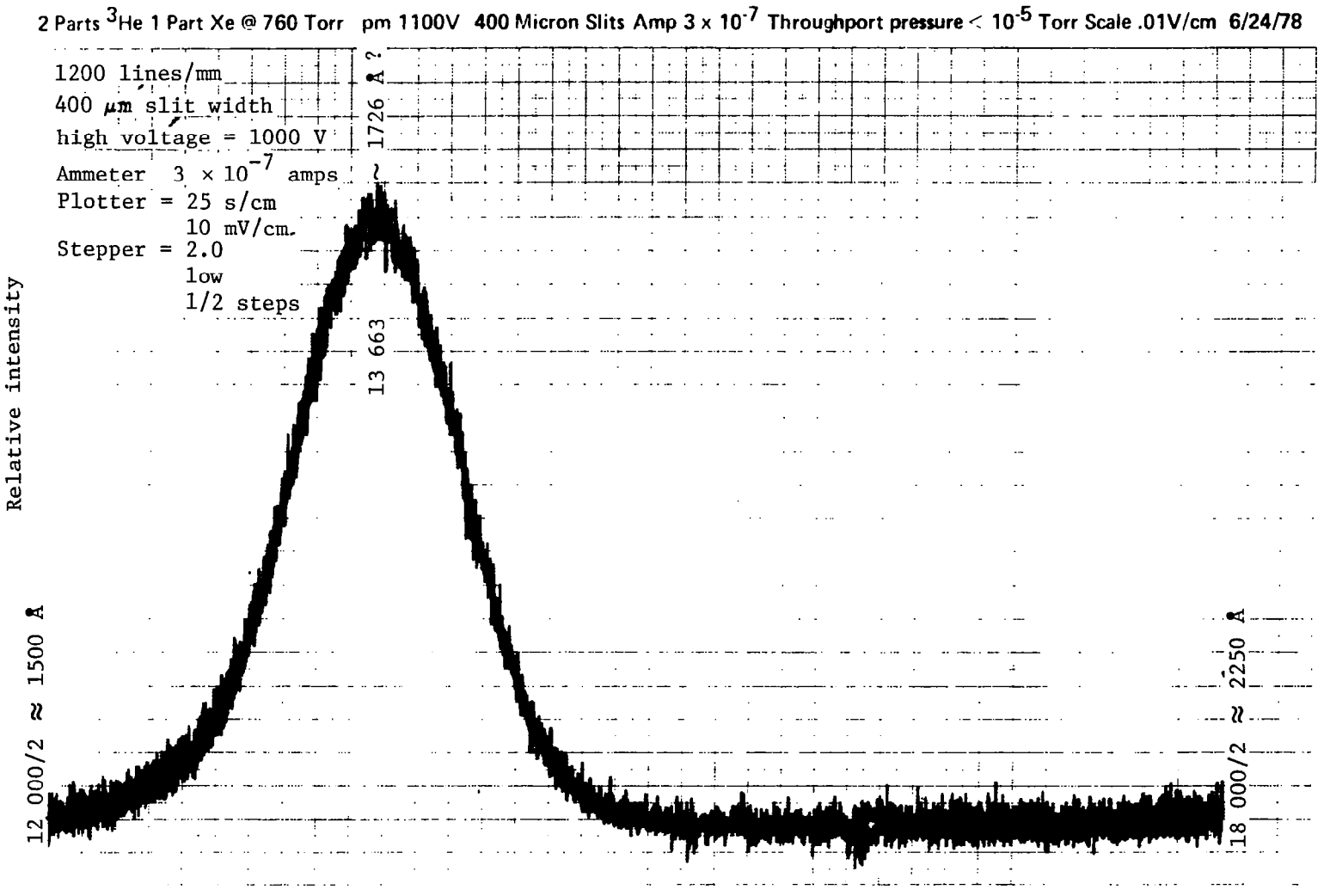

Xe_2^* spectrum.

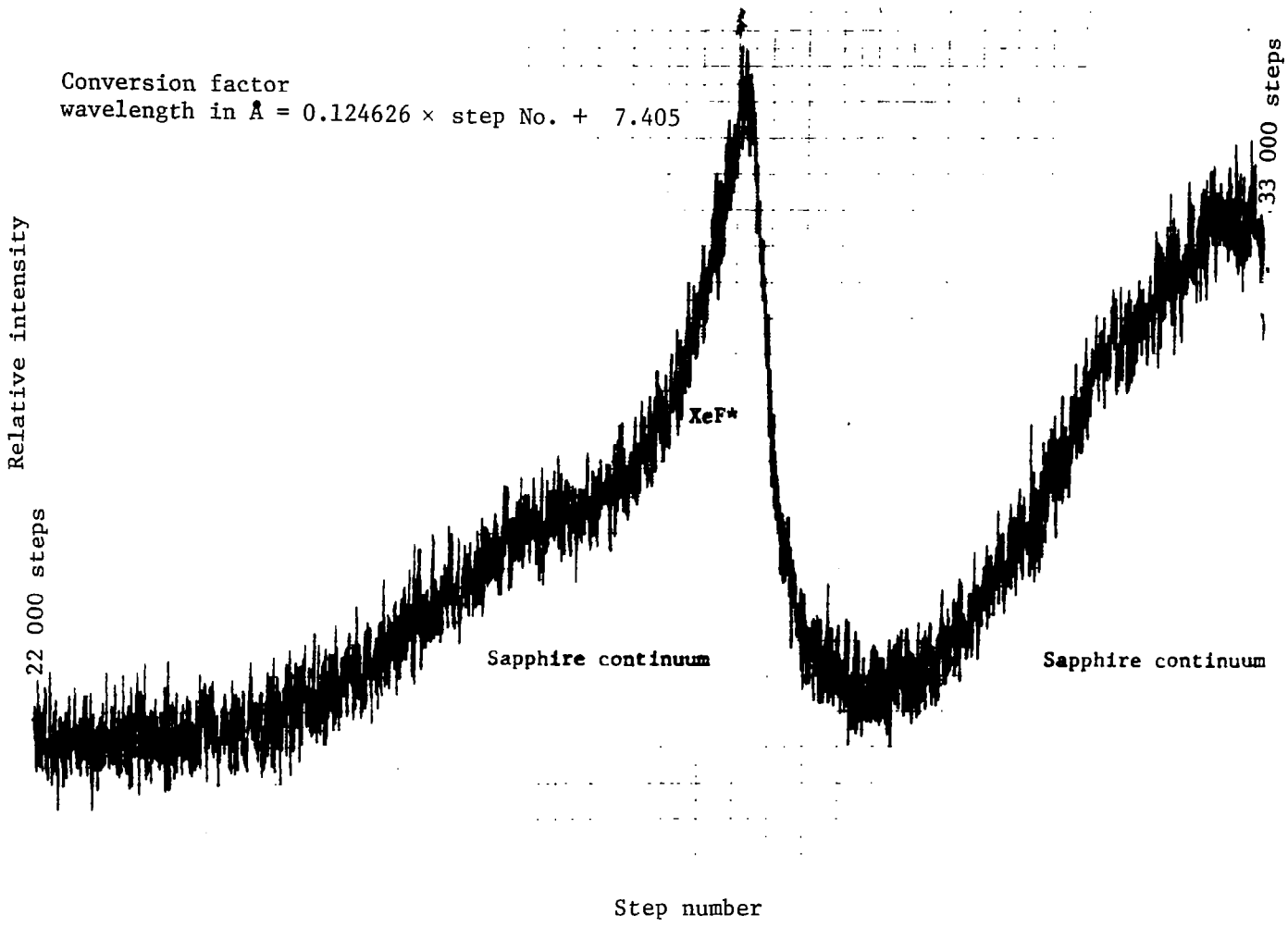

XeF* spectrum.

Gas	Fill Pressures torr	λ max nm	FWHM nm	Integrated Power Out watts	Input Power watts	Efficiency %	Small Signal gain/meter
Xe_2^*	^3He - 507 Xe - 233	172.2	14.9	0.218	0.32	68	1.5×10^{-8}
	^3He - 507 Xe - 233	172.2	14.9	0.126	.192	66	
XeF^*	^3He - 660 Xe - 70 NF_3 - 7	355.0	7.5	6.3×10^{-4}	0.39	0.14	9.61×10^{-9} (2)
	^3He - 660 Xe - 66 NF_2 - 6.6	355.0	7.5	6.3×10^{-4}	0.39	0.14	
	^3He - 660 Xe - 66 NF_3 - 6.6	355.0	7.5	3.5×10^{-4}	0.39	0.10 (1)	
KrF^*	^3He - 600 Kr - 100 NF_3 - 7	245.0	5.2	8.2×10^{-4}	0.35	0.23	1.9×10^{-9} (2)

(1) Suspected air contamination.
(2) Effective excited state lifetime not defined for CW case.

Energy transfer.

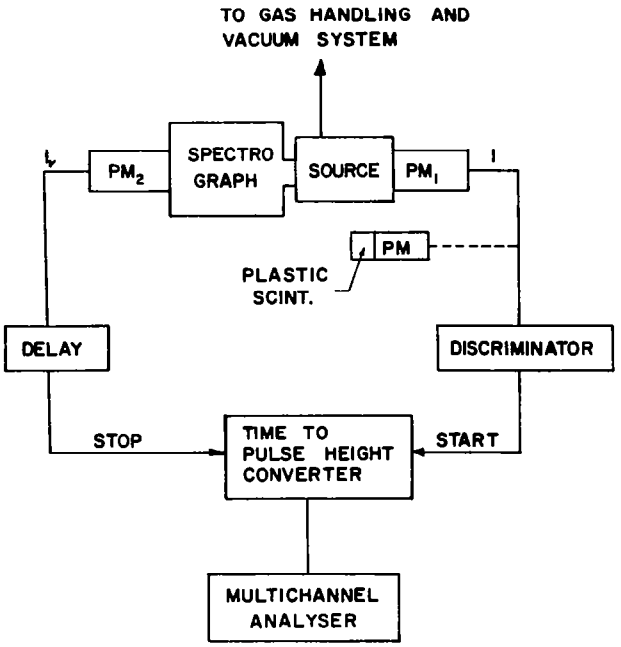

System for lifetime measurement.

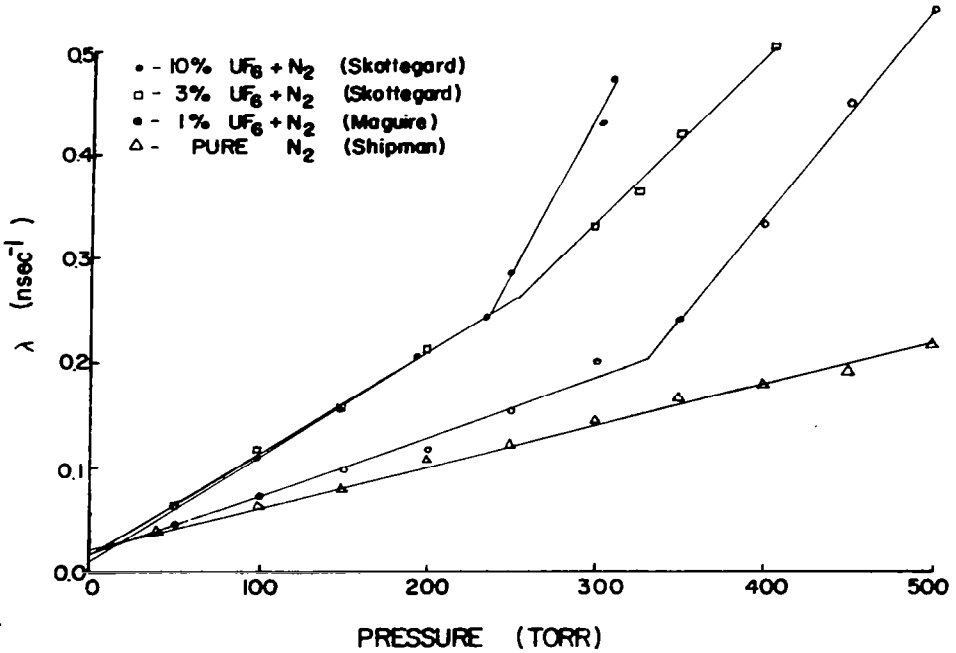

Inverse lifetime of N_2 as a function of pressure.

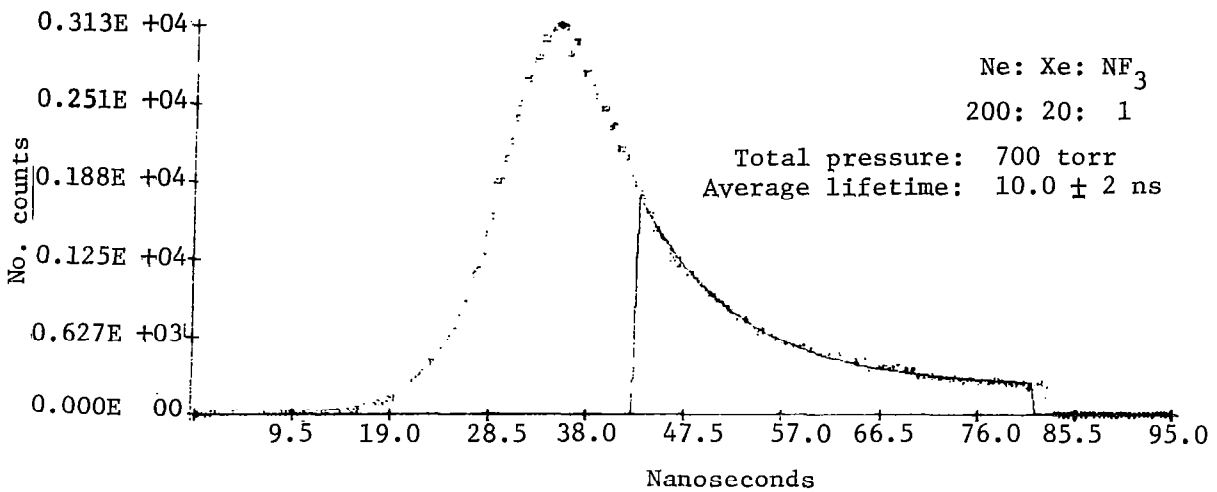

Printout of lifetime measurements.

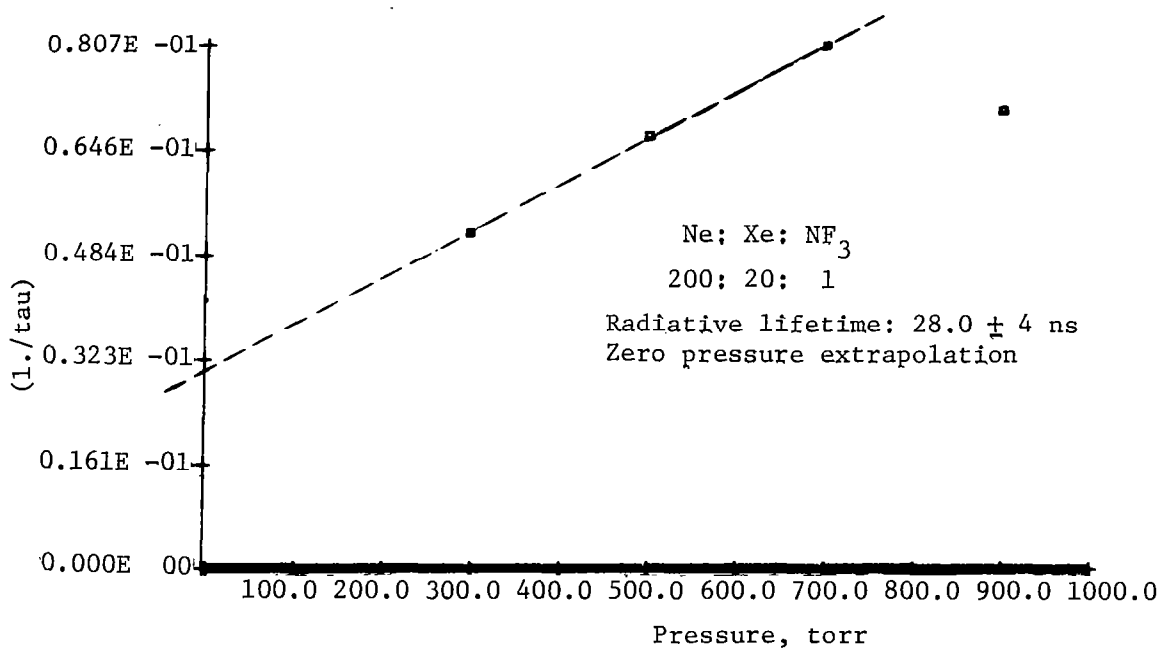

Lifetime of XeF as a function of pressure.

Gas	Fill Pressures torr	max nm	FWHM nm	Integrated Power Out watts	Input Power watts	Efficiency %	Partial Pressure UF_6-torr	Attenuation % of maximum
XeF*	^3He - 660 Xe - 70 NF_3 - 7	355.0	7.5	6.3×10^{-4}	.39	.14	0	100
(43)	^3He - 600 Xe - 70 NF_3 - 7 UF_6 - 1.6	355.0	7.5	1.95×10^{-4}	.34	.057	1.6	41(1)
(49)	^3He - 600 Xe - 66 NF_3 - 6.6 UF_6 - 3.2	355.0	7.5	4.35×10^{-5}	.176	.0245	3.2	18(1)
KrF*	^3He - 568 Xe - 82 UF_6 - 80	--	--	--	.39	0	80	0

(1) A large increase in N_2^+ Bands noted.

UF_6 effects.

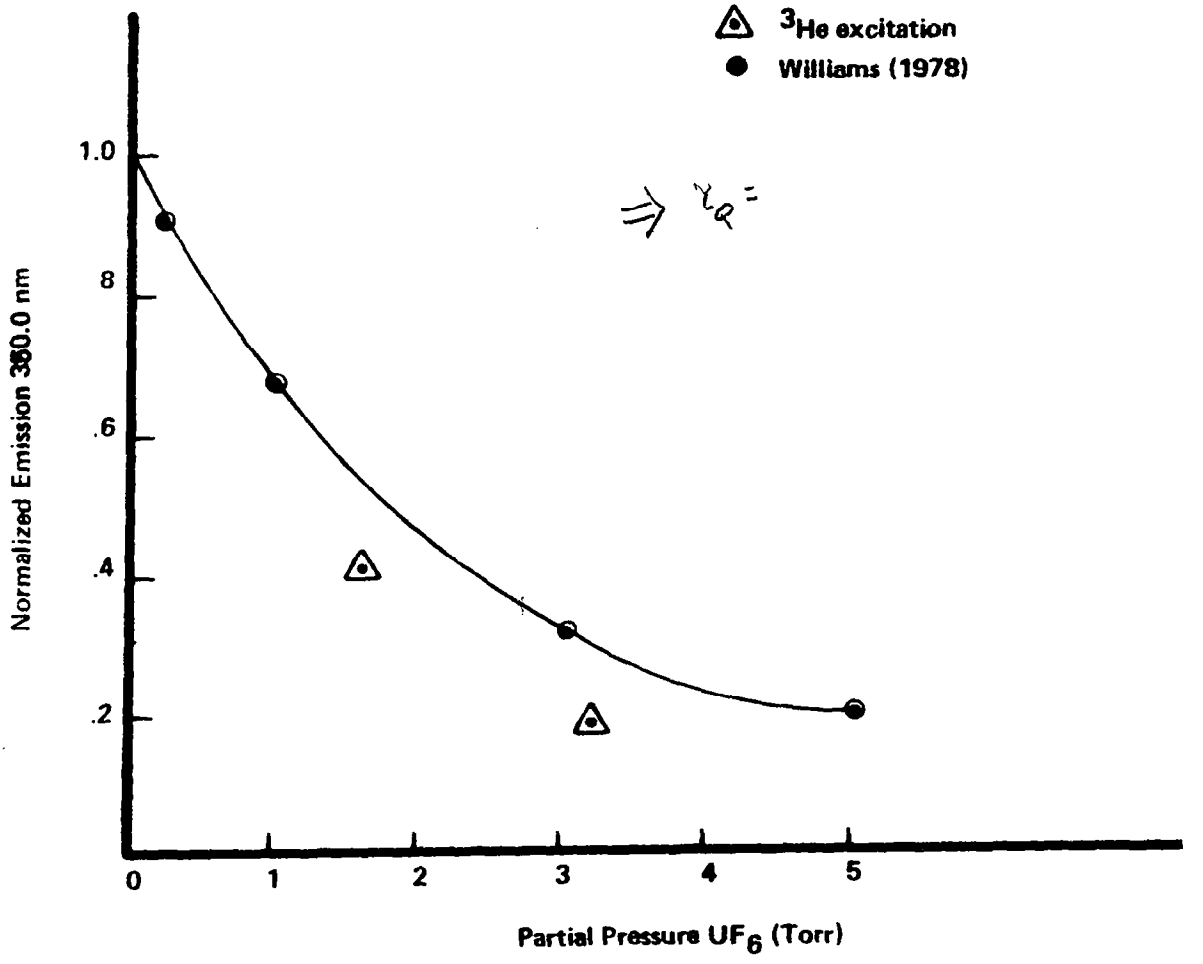

Effects of UF_6 on XeF* emission.

NUCLEAR-PUMPED CO_2 LASER

Michael Rowe
University of Florida

ABSTRACT

The objective of this was to study the $He^3(n,p)T$ reaction as an energy source for a CO_2 laser. For this purpose He^3 was added to a functioning CO_2 electrically excited laser. Initially the laser was run electrically with 12 torr total pressure. The gas mixture was 1:1:8, CO_2:N_2:He. At zero reactor power, the laser was tested in place next to the core of the Georgia Tech. Research Reactor. After verification of laser action He^3 was added to the system. He^3 partial pressures of 10 torr, 50 torr and 300 torr were added in three separate reactor runs. Reactor power ranged from zero to 5×10^6 watts, which corresponds to a peak flux of 10^{14} neutrons/cm^2-sec. At reactor powers greater than 10 kW, gain of up to 30% was shown. However, indications are this may be due to gamma excitation rather than caused by the $He^3(n,p)T$ reaction. These results do agree with the data of past CO_2 nuclear-pumped laser experiments.

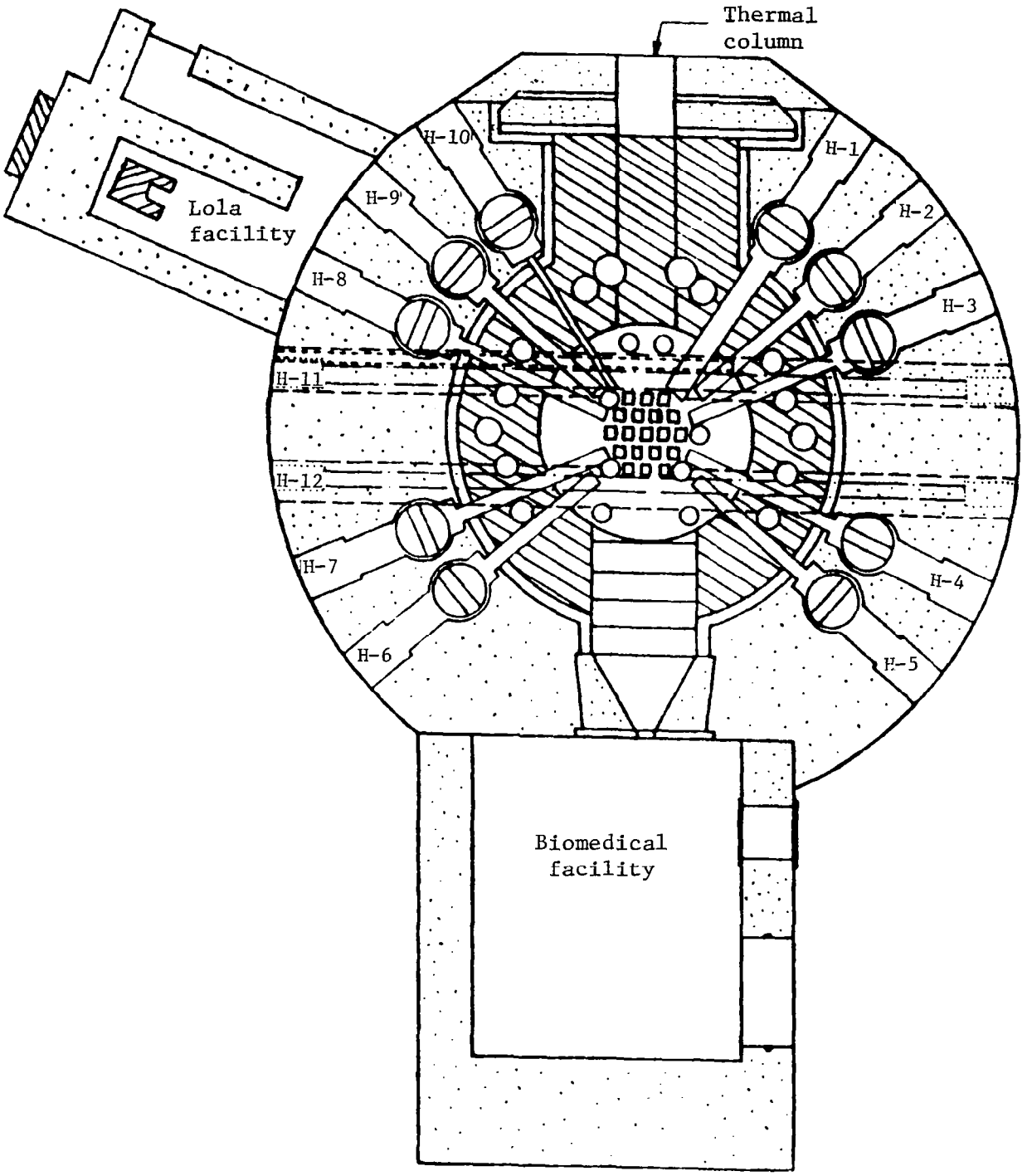

Figure 1.- Layout of Georgia Institute of Technology reactor.

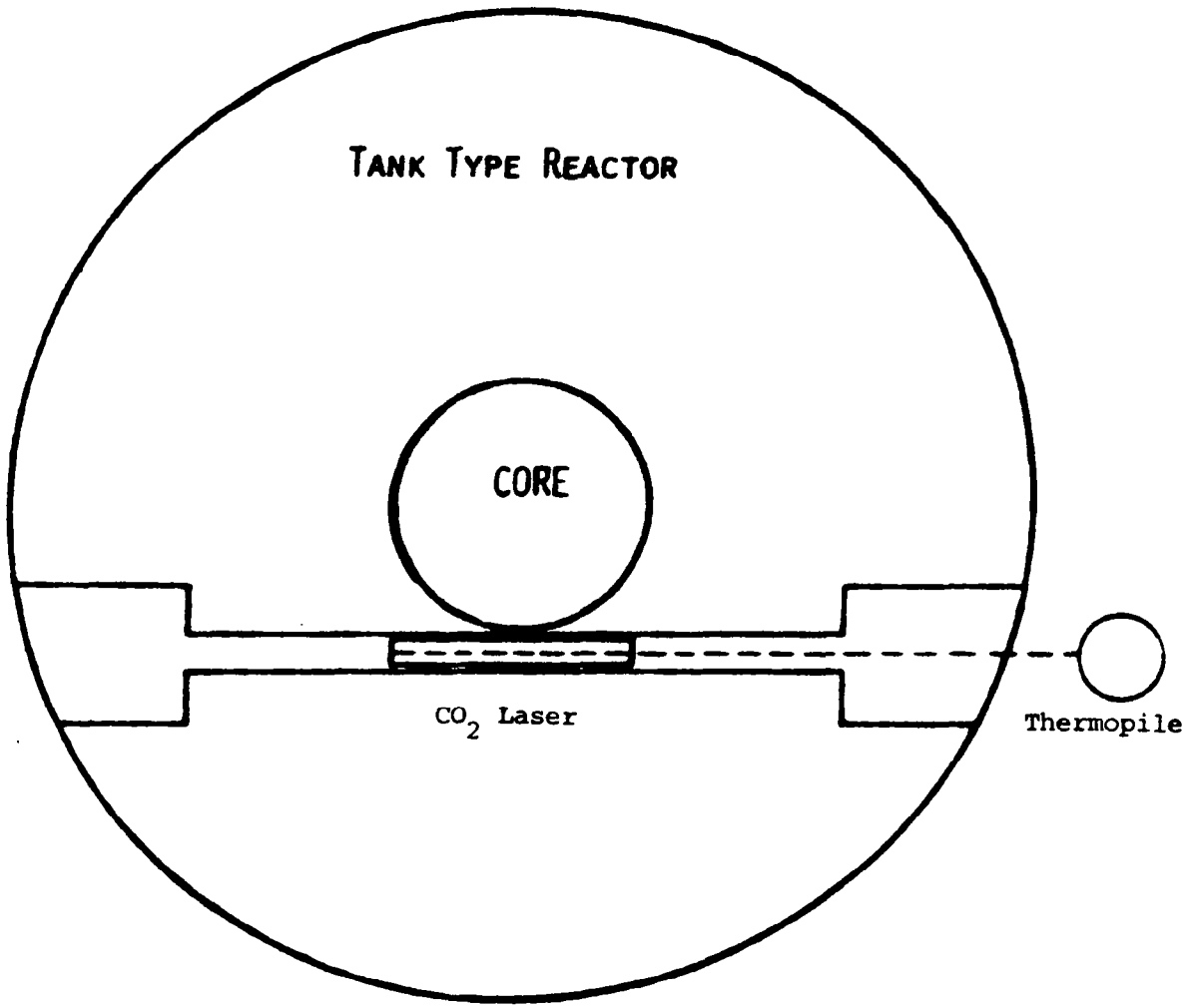

Figure 3.- Beam port used for CO_2 laser experiment.

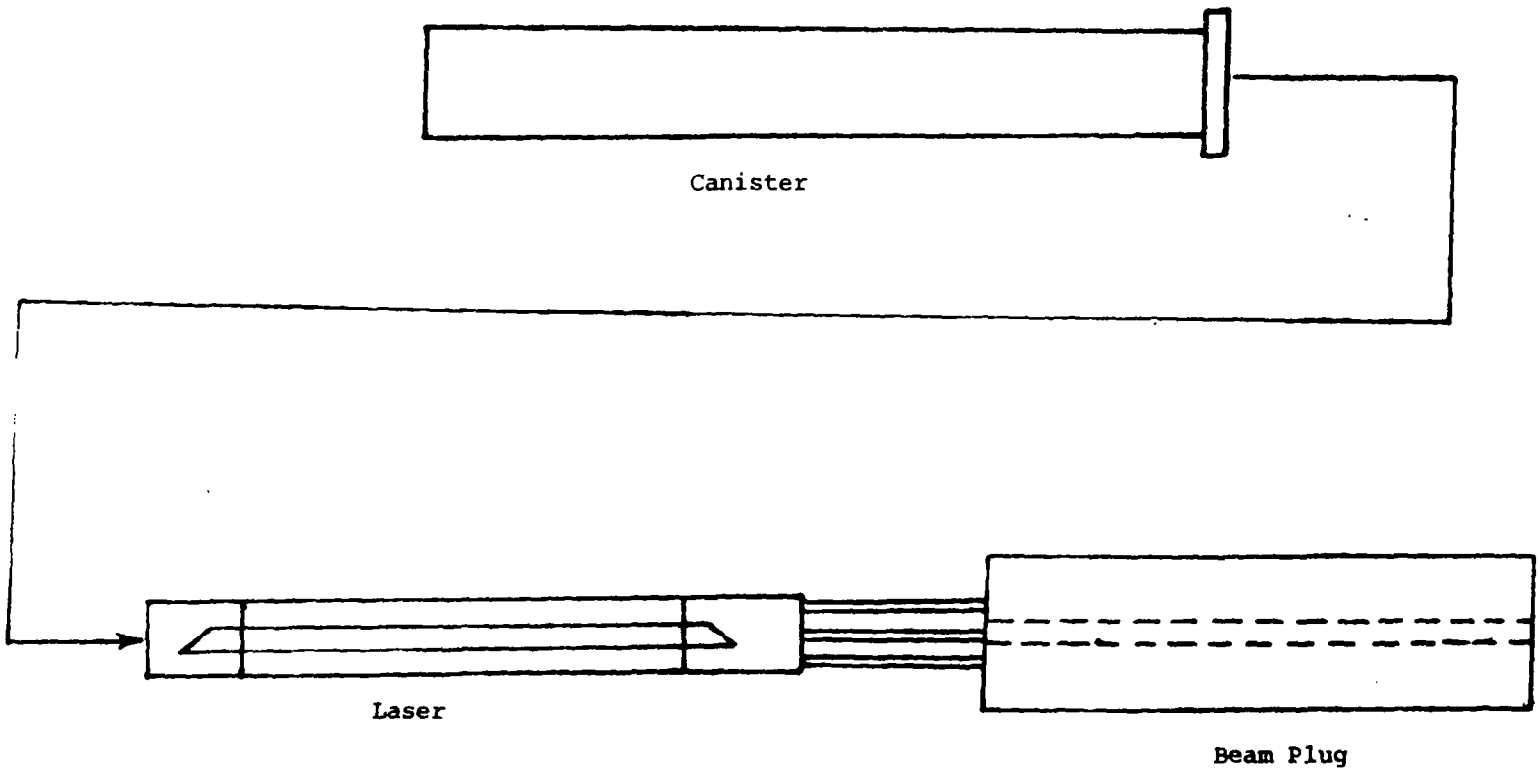

Figure 4.- Diagram of CO_2 laser and beam plugs.

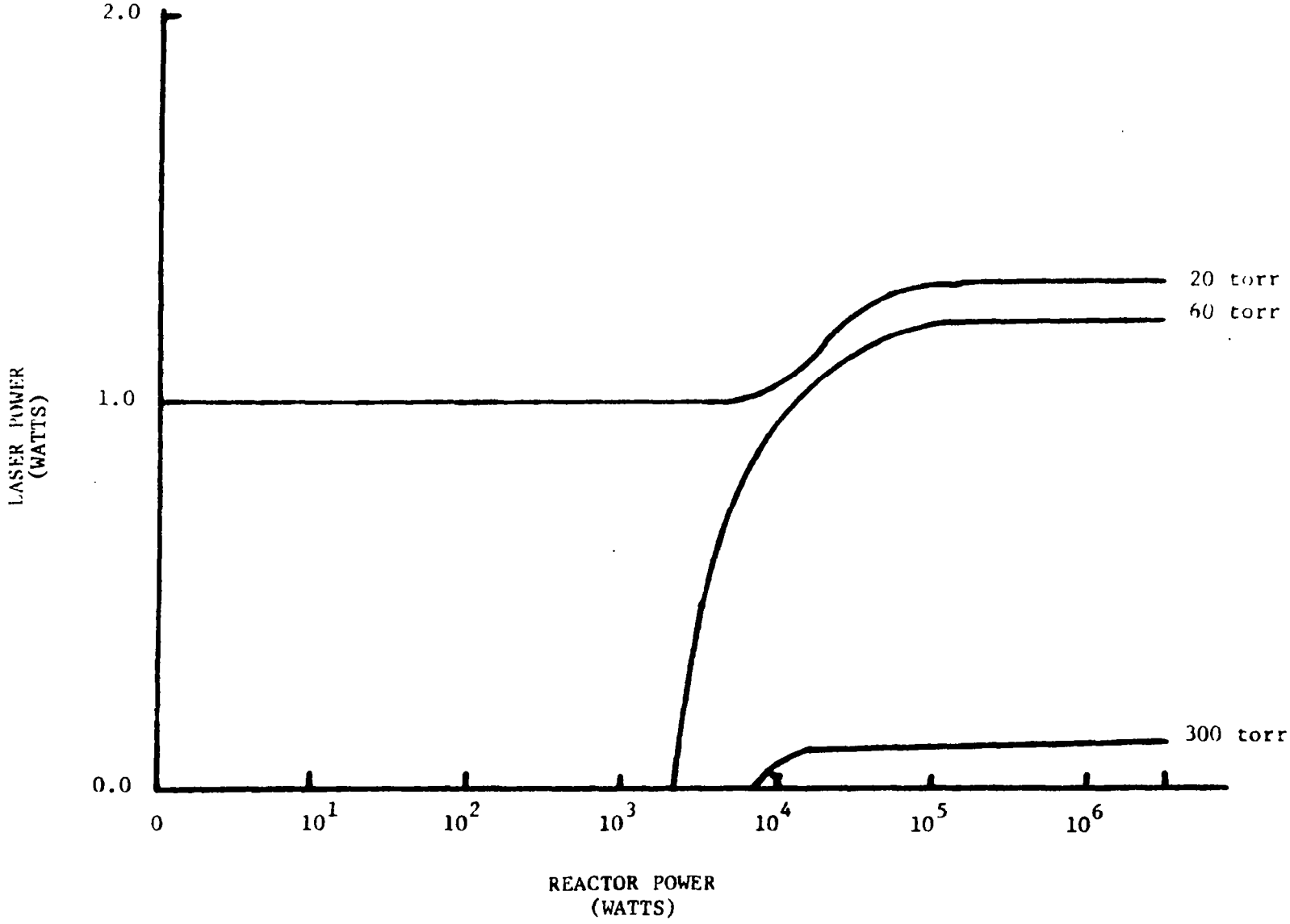

Figure 5.- CO_2 laser output as a function of reactor power.

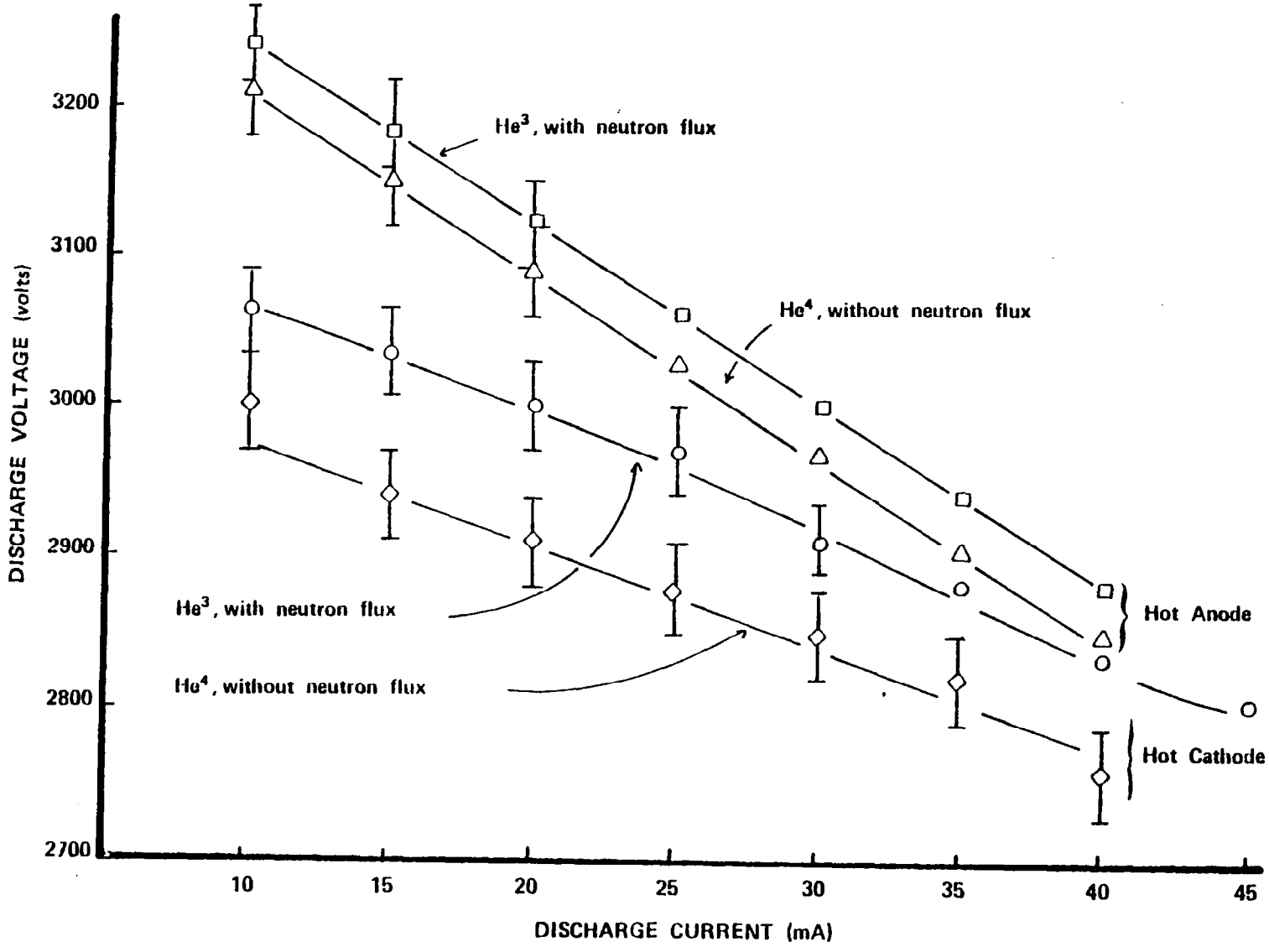

Figure 6.- I-V characteristic of laser with and without neutron irradiation.

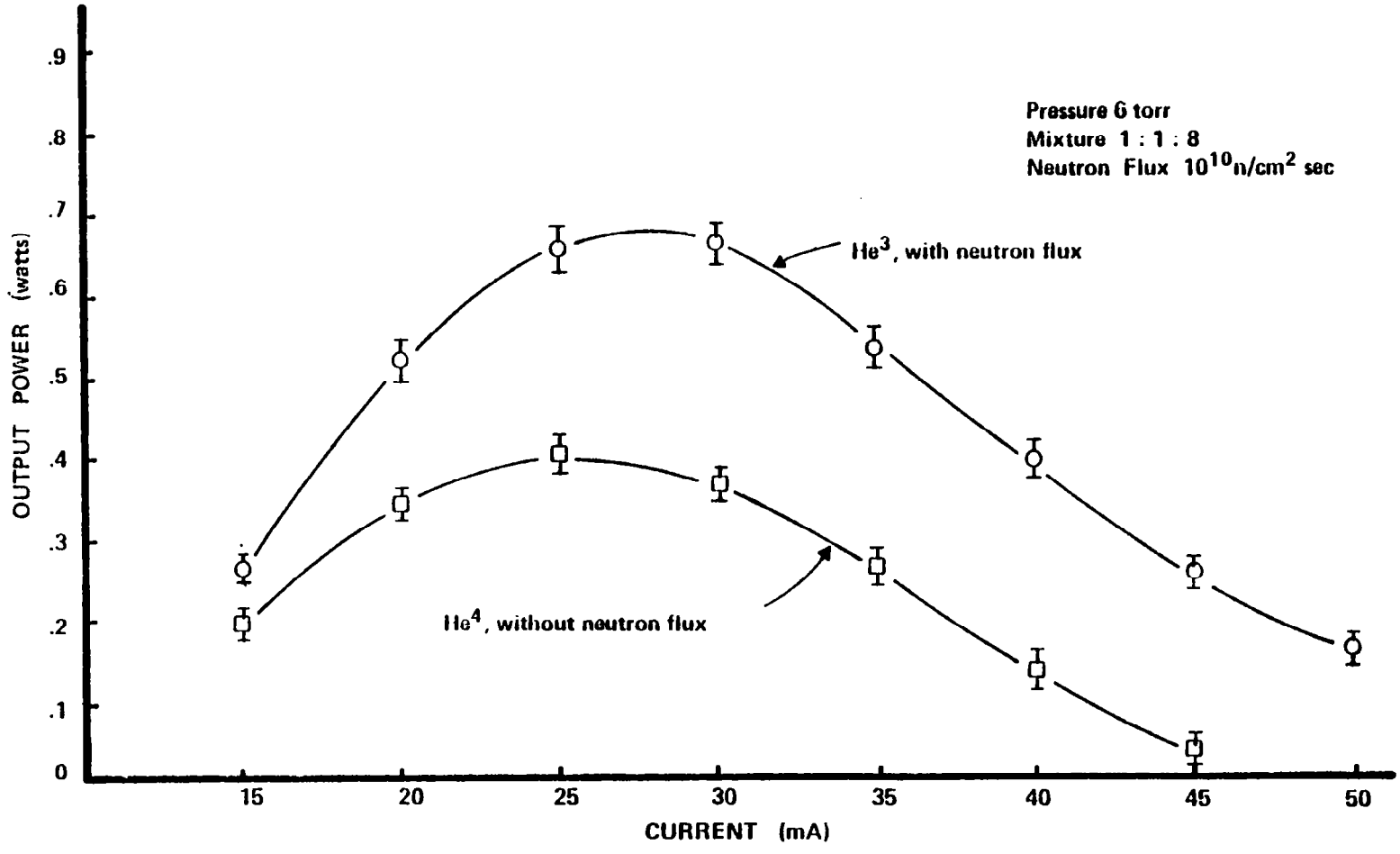

Figure 7.- Laser power enhancement with neutron irradiation.

EXPERIMENTAL SETUP FOR DECOMPOSITION OF UF_6

by

Michael Rowe
University of Florida

ABSTRACT

The purpose of this experiment is to determine the rate at which UF_6 decomposes into UF_5 and UF_4 as a function of neutron fluence. To study UF_6 decomposition rate, an absorption cell for VUV and the associated VUV spectroscopy system is used to measure UF_6 while under irradiation in University of Florida Training Reactor. The cell contains 50 torr of UF_6 at room temperature to insure that the UF_6 is in a gaseous state. By determining the absorption coefficient below 2100Å for UF_6, above 2100Å for F_2 and at 4100Å for cell degradation; UF_6 decomposition can be measured at a neutron flux of 10^{12} neutron/cm^2sec for 72 continuous hours.

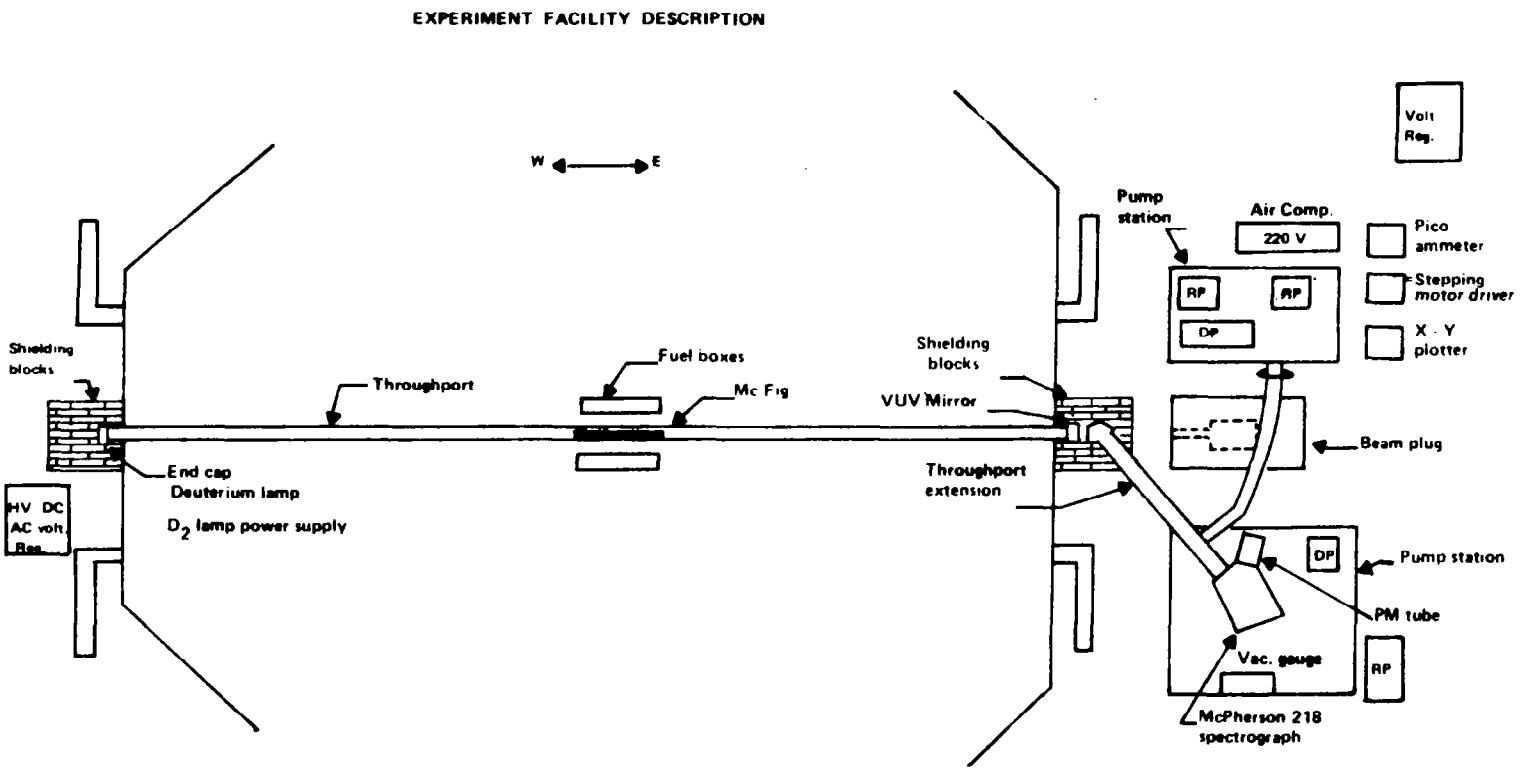

Research facility for vacuum-ultraviolet spectroscopy. (McFig is multipurpose capsule for irradiating gases.)

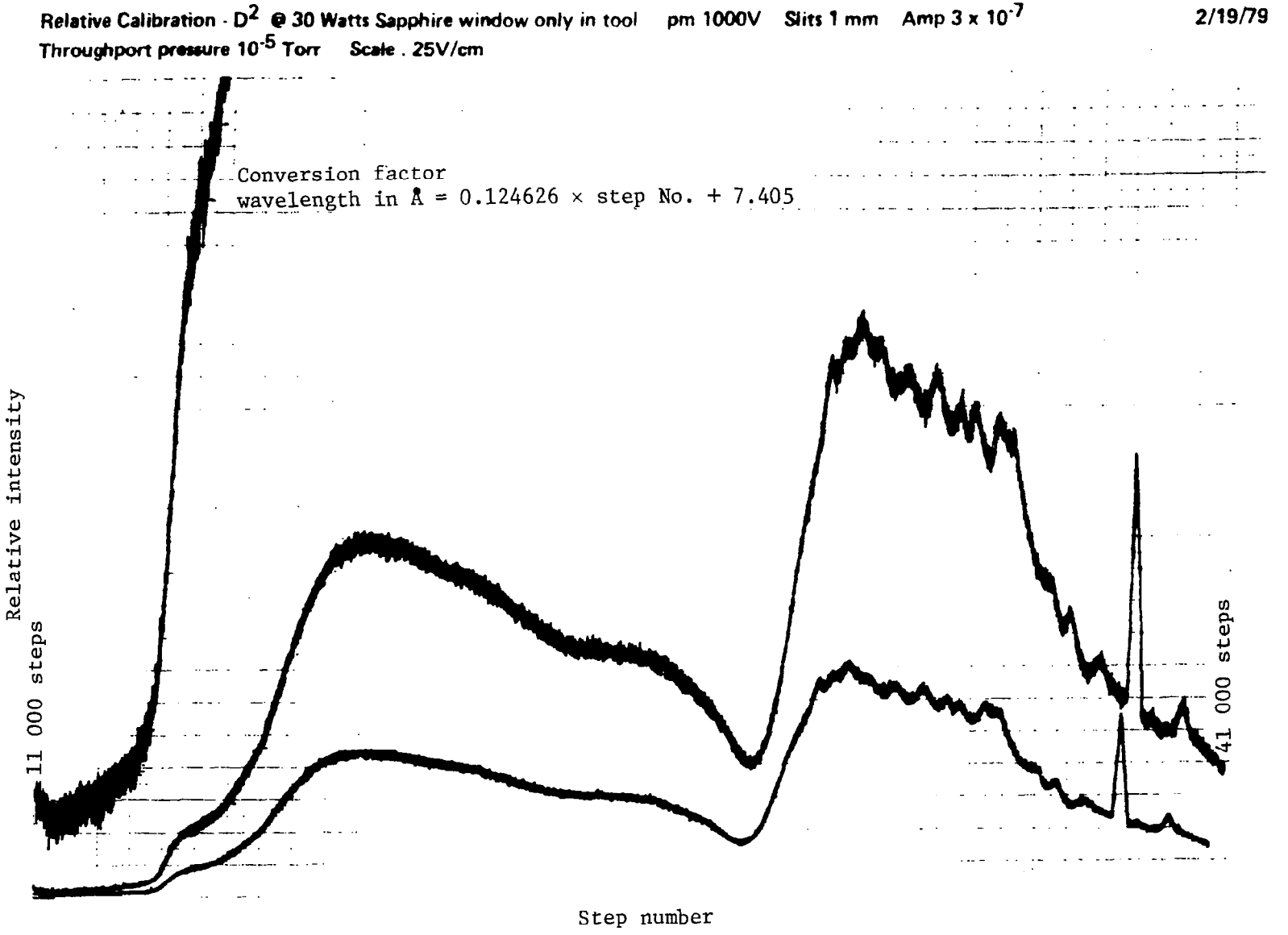

Calibration of deuterium lamp.

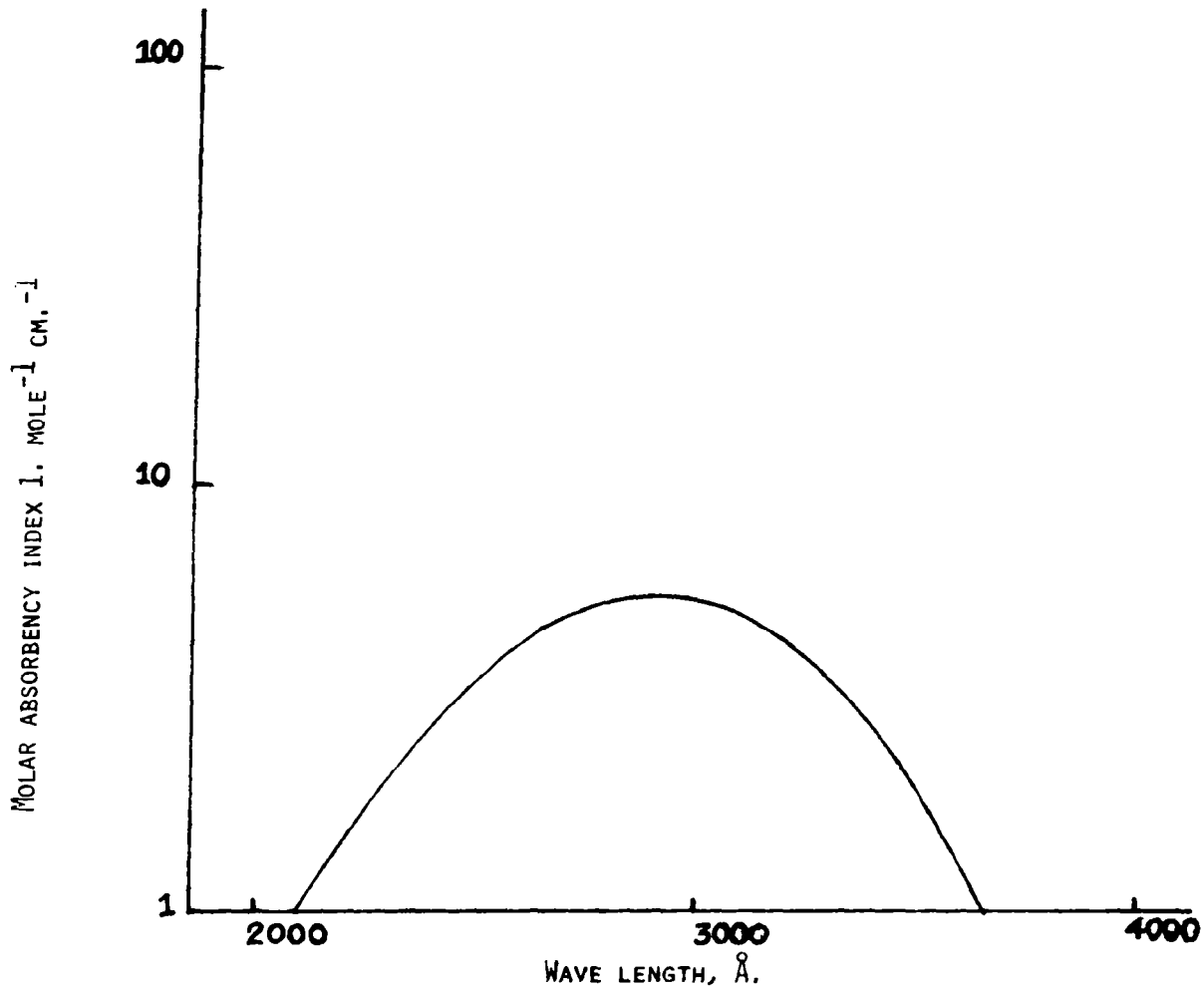

Absorption spectra of F_2.

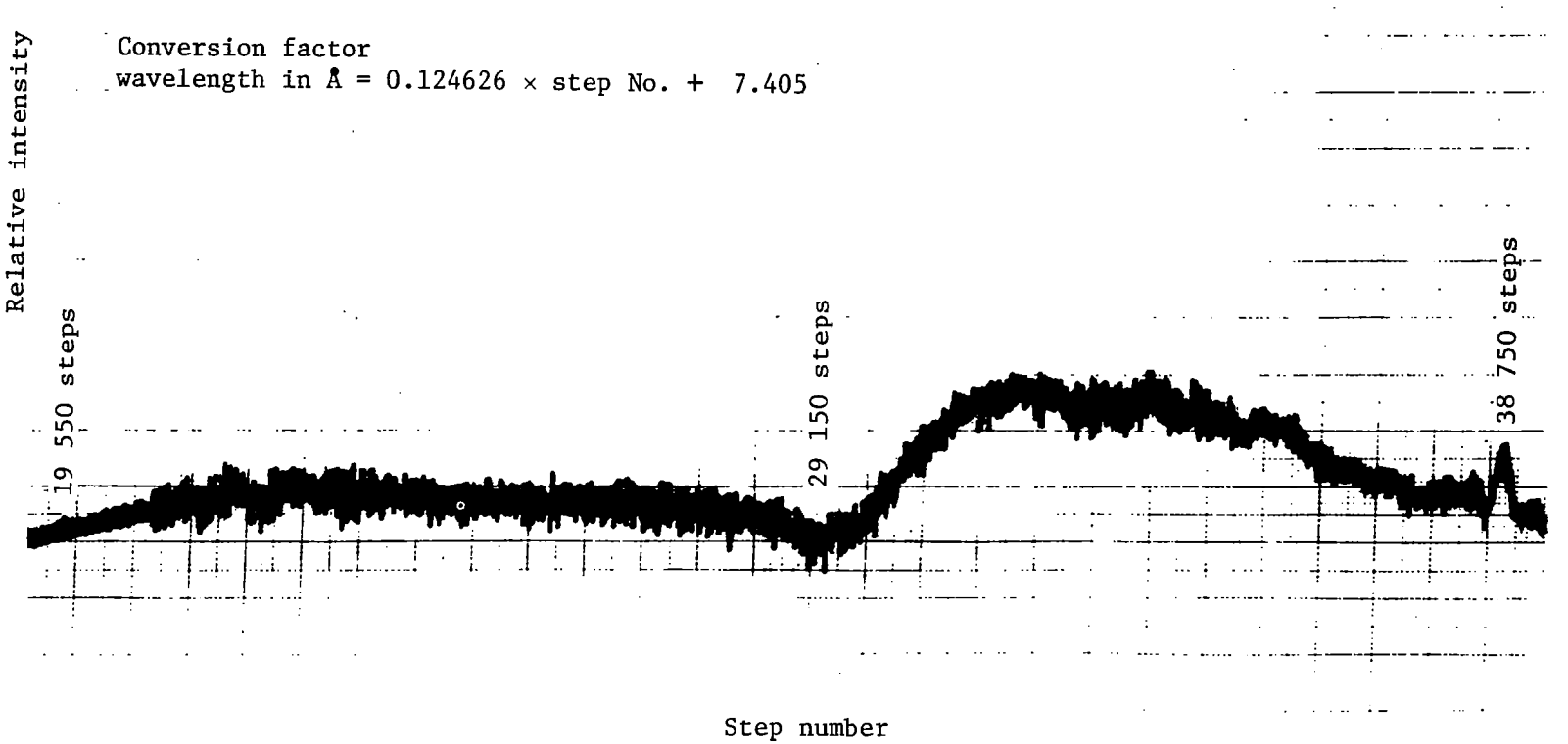

UF_6 absorption scan.

	mpc		Concentration
Sr^{84}	54 µCi	vs	420 µCi
Sr^{90}	1.8 µCi		2.4 µCi
Y^{91}	54 µCi		435 µCi
Zr^{93}	180 µCi		.05 µCi
Zr^{95}	180 µCi		434 µCi
Zr^{97}	180 µCi		36600 µCi
Mo^{99}	360 µCi		9450 µCi
Ru^{103}	900 µCi		333 µCi
I^{131}	16.2 µCi		1540 µCi
I^{132}	360 µCi		198000 µCi
I^{133}	54 µCi		32000 µCi
I^{134}	360 µCi		900000 µCi
I^{135}	180 µCi		91000 µCi
Cs^{137}	18 µCi		1.0 µCi
Ba^{140}	180 µCi		2110 µCi
Ce^{141}	360 µCi		77 µCi
Ce^{143}	360 µCi		18500 µCi
Ce^{144}	10.8 µCi		83 µCi
Nd^{147}	360 µCi		864 µCi

List of most hazardous fission fragments produced and calculated activity. List of occupation level maximum permissible concentration (mpc).

CW NUCLEAR PUMPED LASING OF ^{3}He-Ne

B. Dudley Carter, University of Florida

ABSTRACT

Presented are the results of a two-year study on the CW nuclear pumped lasing of He-Ne system. Preliminary experiments measured single pass gain for the 6328.2Å laser transition at neutron fluxes up to 1 x 10^{14} n/cm^2-sec. Peak gain for a 300 torr ^{3}He-Ne (5:1 mixture) was found to be 8.84 dB/meter at a 2 x 10^{12} n/cm^2-sec neutron flux. Further experiments measured the gain in the flux region from 1 x 10^6 to 2 x 10^{12}n/cm^2-sec. In addition, gain vs. probe laser intensity at various neutron fluxes was measured. These measurements resulted in the construction of a laser cavity and the subsequent CW nuclear pumped lasing at 6328.2Å in ^{3}He-Ne. Experiments were also carried out on the 3.39 μm superradiant line in ^{3}He-Ne. On three separate occasions, at two different facilities, lasing was observed. Although ^{3}He-Ne was found to have the lowest threshold for lasing found so far; unfortunately, it also had the lowest output power on the order of tens of microwatts.

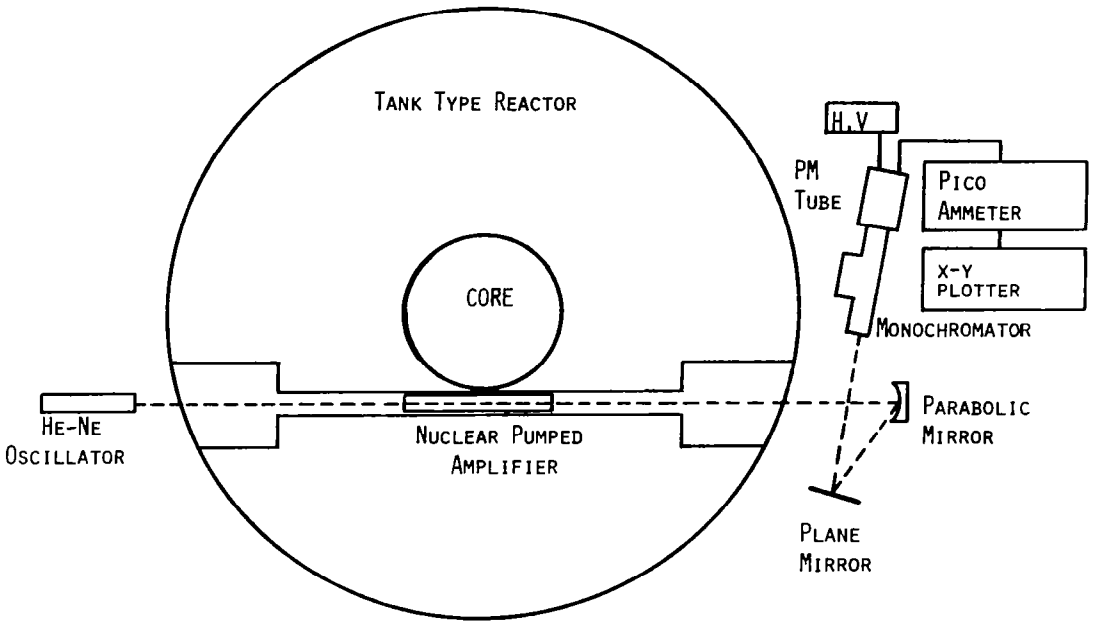

Laser setup at the Georgia Institute of Technology research reactor.

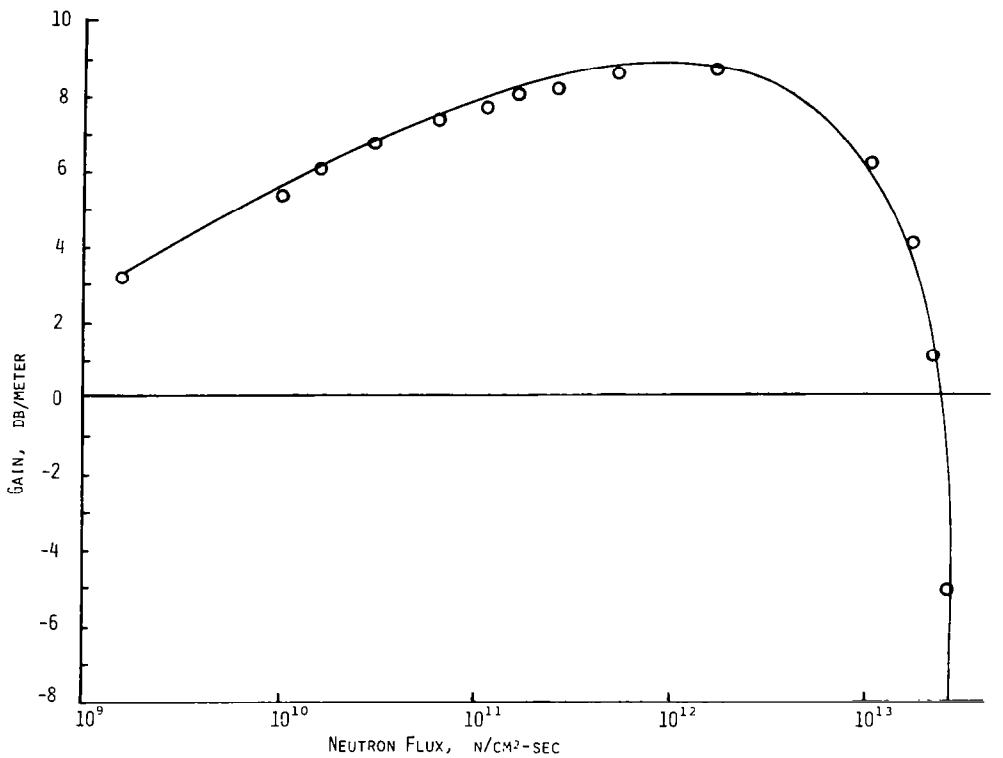

Results of gain measurements.

TRANSITION	$3S_2$-$2P_4$
WAVELENGTH	6328.2 Å
TOTAL PRESSURE	300 TORR
He^3: Ne	5:1
PEAK GAIN	8.84 dB/METER
NEUTRON FLUX AT	$2x10^{12}$ N/CM^2-SEC
POWER DEPOSITION	12 mW/CM^3
POWER EXTRACTION	LESS THAN $4x10^{-3}$ mW/CM^3
EFFICIENCY	LESS THAN .04%

Pertinent values for maximum amplification.

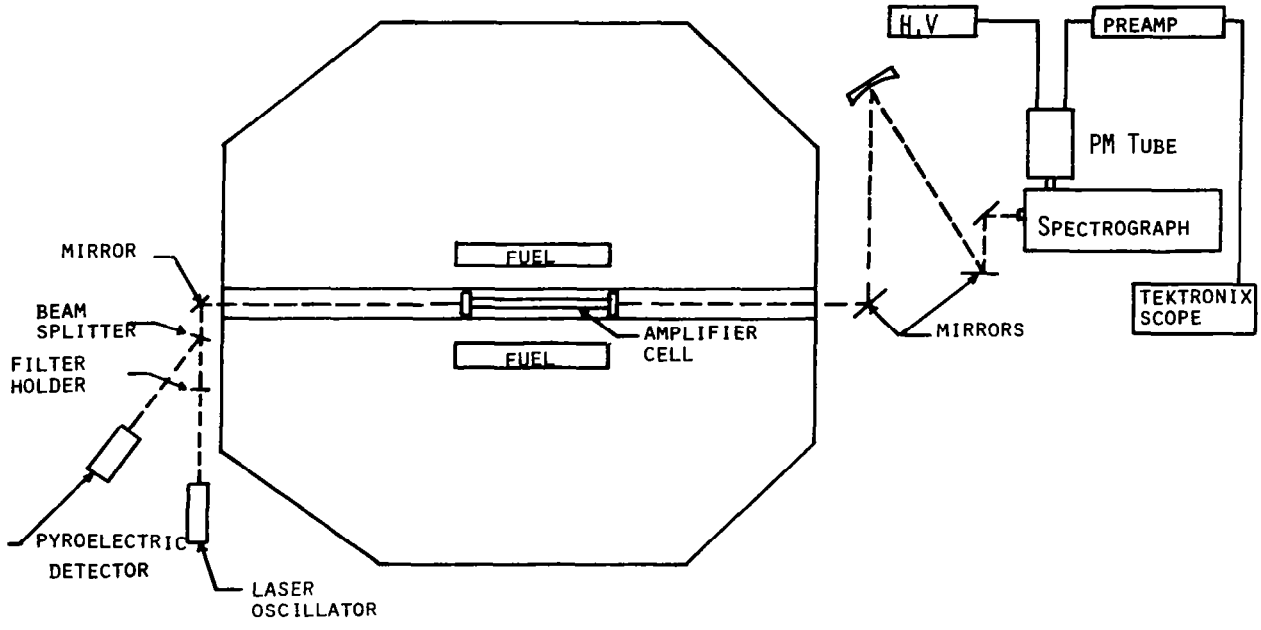

Horizontal throughport at the University of Florida training reactor.

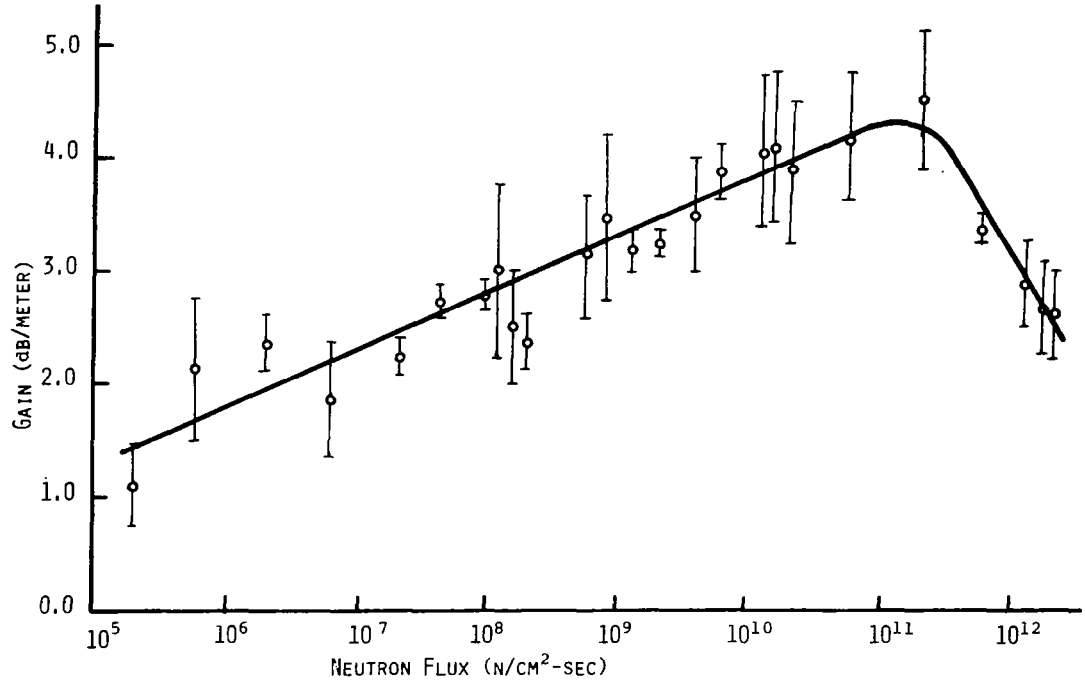

Results of measurements at the University of Florida research reactor.

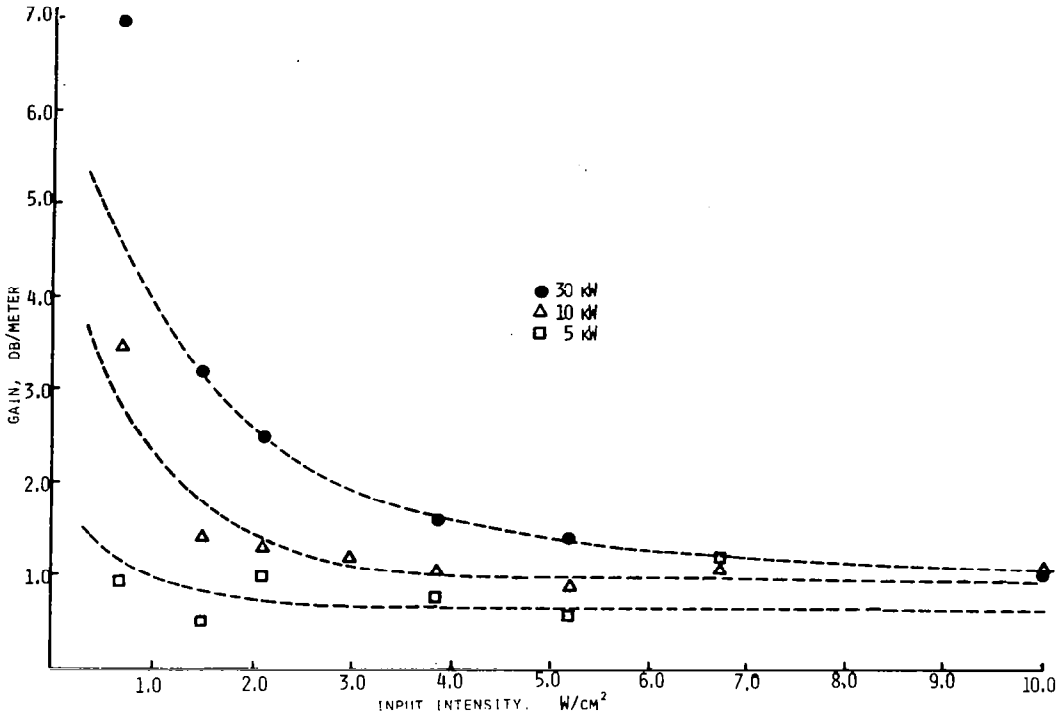

Determination of small signal gain.

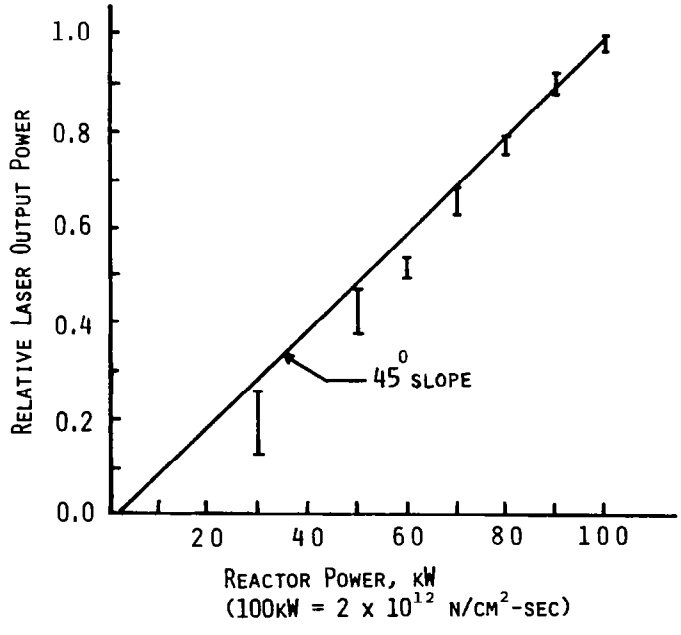

Laser output as a function of reactor power.

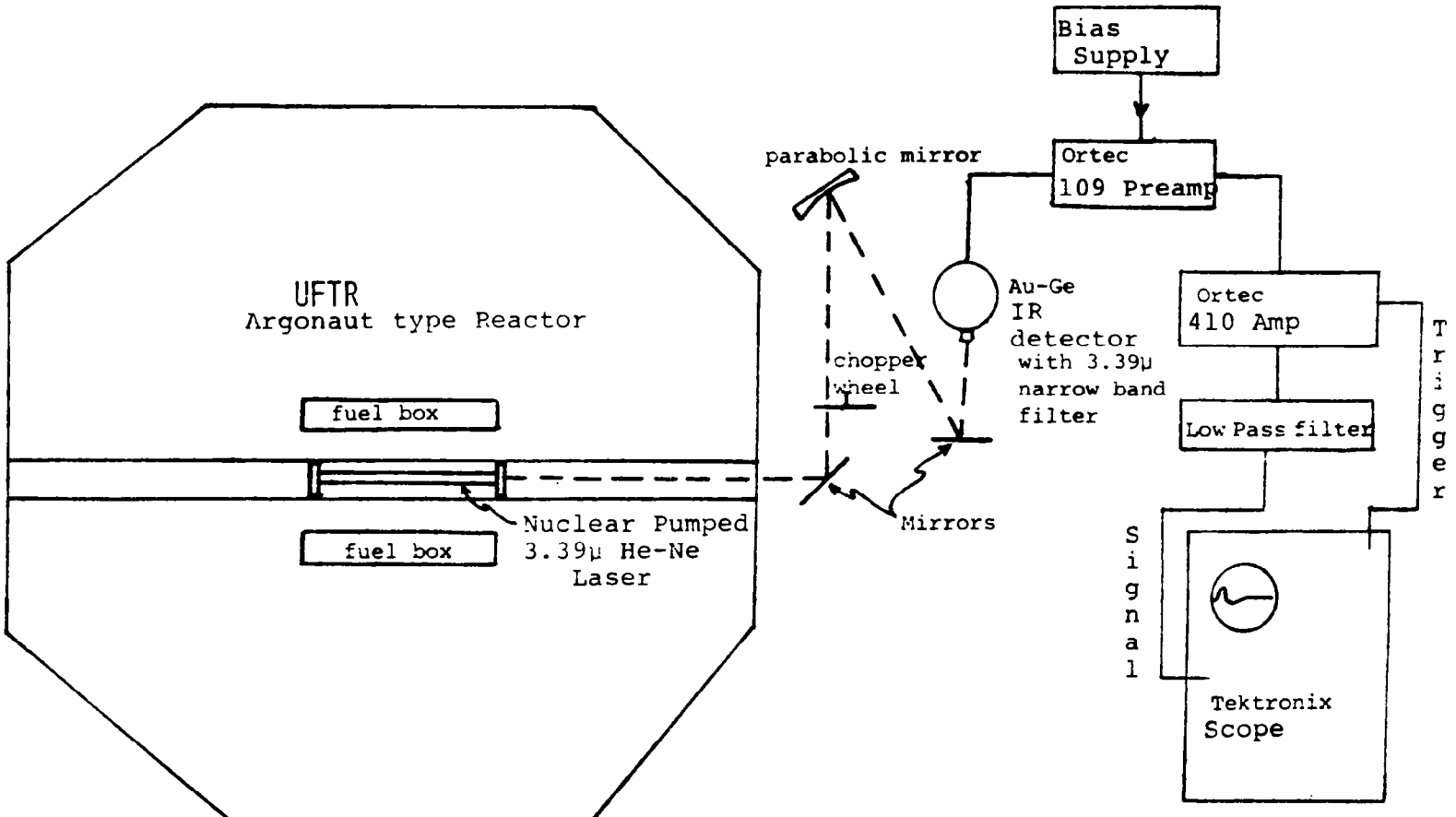

Experimental arrangement for measuring superradiant laser output.

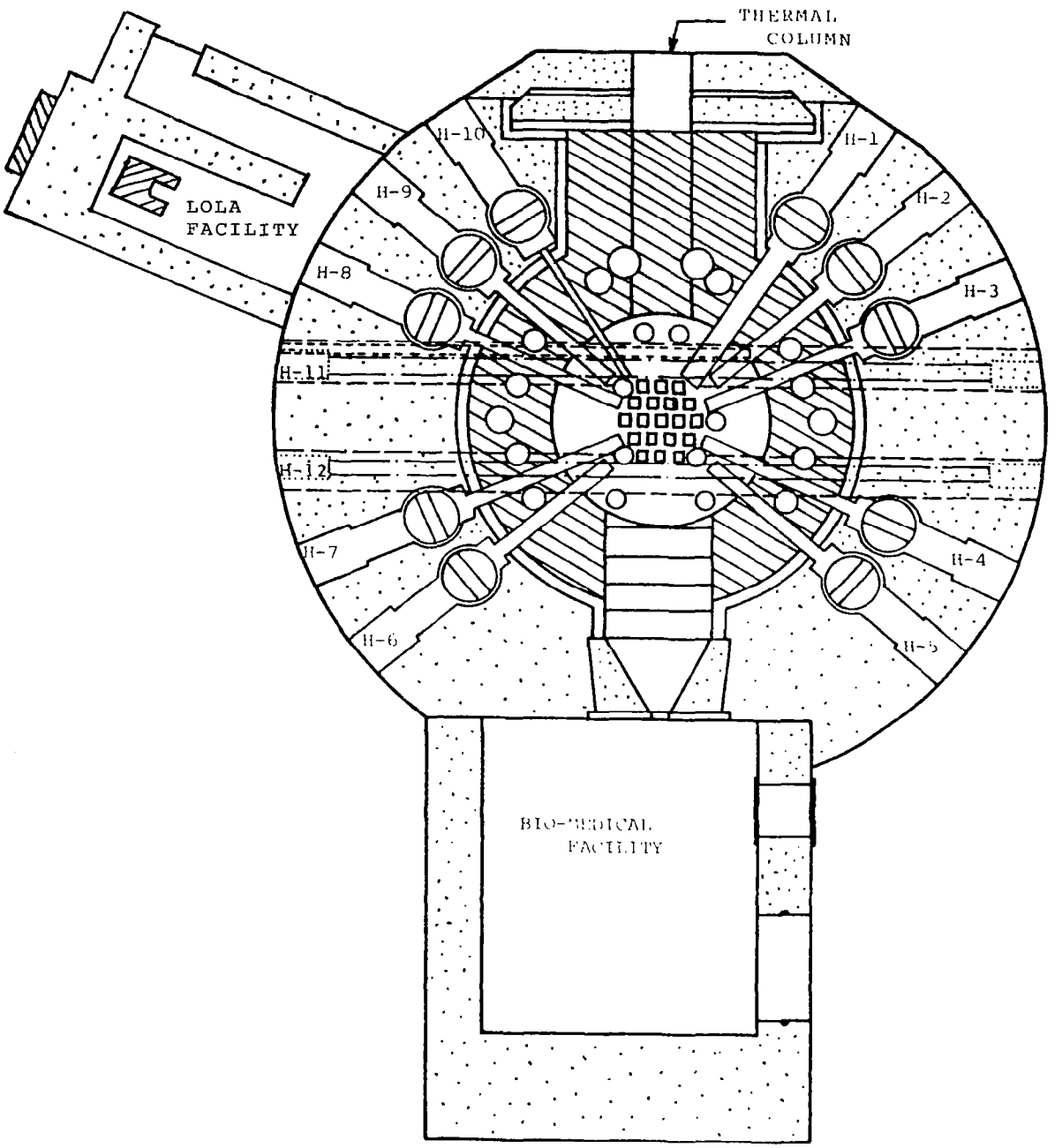

Georgia Institute of Technology research reactor.

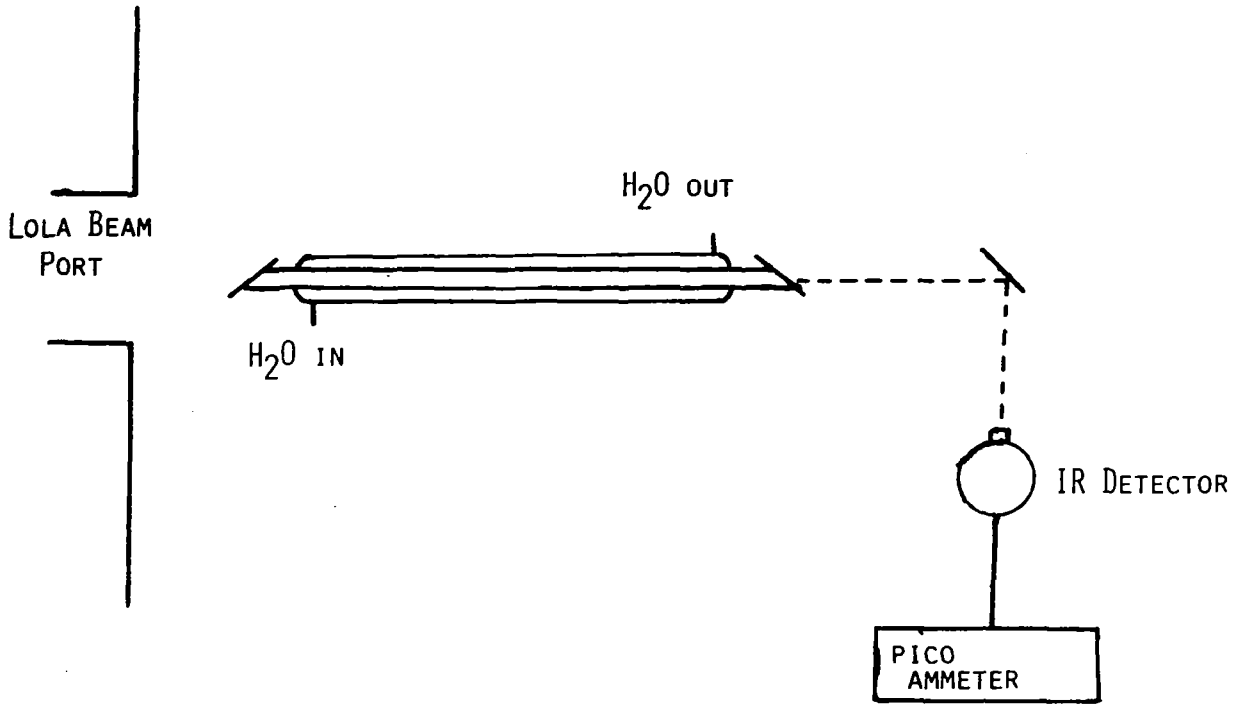

CO_2 nuclear laser system.

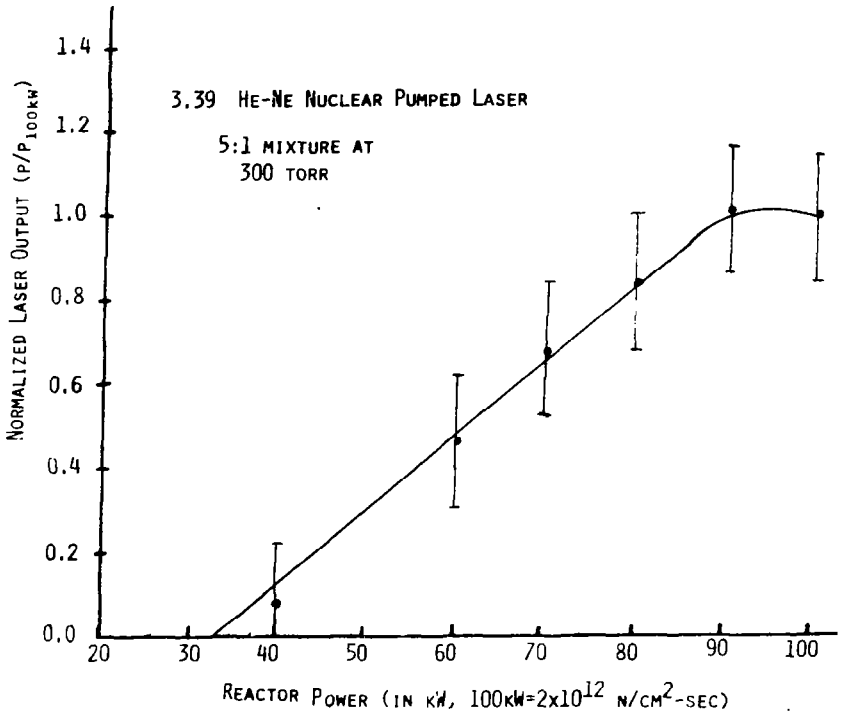

Laser output as a function of neutron flux.

SPECTRAL EMISSION OF NUCLEAR EXCITED XeBr*

R. A. Walters
University of Florida, Gainesville, Florida

ABSTRACT

The ultraviolet emission of XeBr* in a band peaking at 282 nm overlaps the absorption band peak of C_3F_7I. Nuclear photolytic pumping of the long lifetime C_3F_7I laser state via XeBr* emission is possible with an adequate pumping rate. This has been shown with electron beam pumping (Swingle, 1976). The University of Florida vacuum-ultraviolet spectroscopy system and MCFIG capsule (Walters, 1979) were filled with a ^{3}He:Ar:Xe:Br (534:195:12:6) torr mixture and irradiated by a CW flux of 17×10^{11} n/cm^2-sec. XeBr* emission was observed as shown in figure 1, but the Br_2 emission normally observed in argon-bromine mixtures (Pearse, 1965) predominates. This spectrum is typical of these mixtures (Swingle, 1976), with XeBr* probably peaking with 0.1% Bromine in 2 atmosphere argon with 2% xenon. The addition of a large partial pressure of ^{3}He produces additional unknowns. The typical vibrational structure of XeBr* (Tellinghuisen, 1976) was not observed. Sapphire emission continuums were present as noted in figure 2.

Energy deposition was 0.43 watts and the capsule output under the XeBr* and Br_2 bands was 1.6×10^{-3} watts, giving an efficiency of 0.37%.

REFERENCES

1. Pearse, R.W. and Gaydon, A.G., "The Identification of Molecular Spectra," Chapman and Hall LTD, London, 1965.

2. Swingle, J.C., et. al., "Photolytic Pumping of the Iodine Laser by XeBr*," Applied Physics Letters, Vol. 28, No. 7, 1 April 1976.

3. Tellinghuisen, J., et. al., "Spectroscopic Studies of Diatomic Noble Gas Halides. II Analysis of Bound-Free Emission from XeBr, Xe and Krf," Journal of Chemical Physics, Vol. 65, No. 11, 1 Dec. 1976.

4. Walters, R.A., Cox, J.D. and Schneider, R.T., "UV Diagnostics of Charged Particle Excited Gases," BMDATL Contract DASG60-78-C0045, Univ. of Florida, Gainesville, May 22, 1979. (Available from DDC as AD-B038933L.)

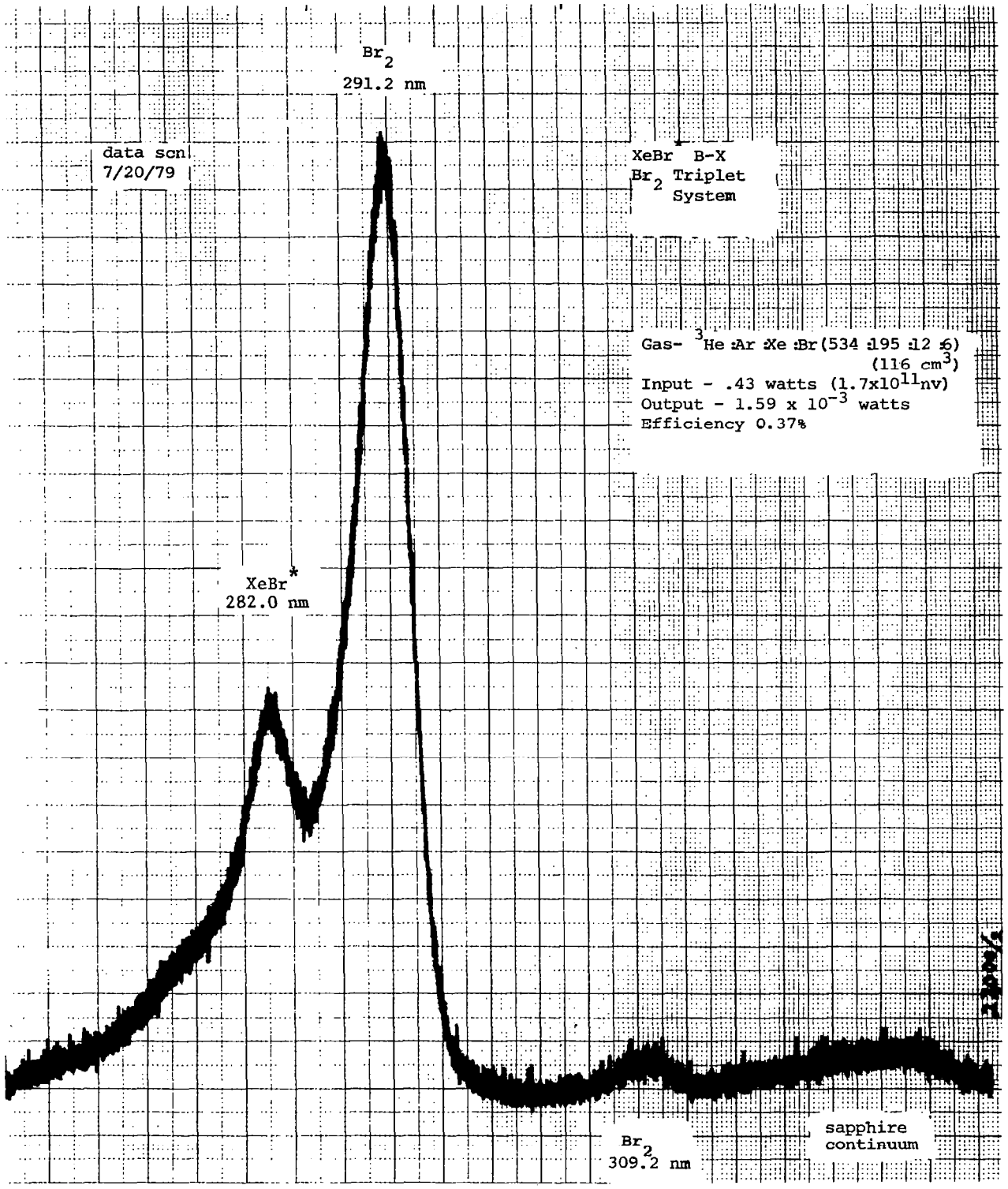

Figure 1.- XeBr* and Br_2 emission bands.

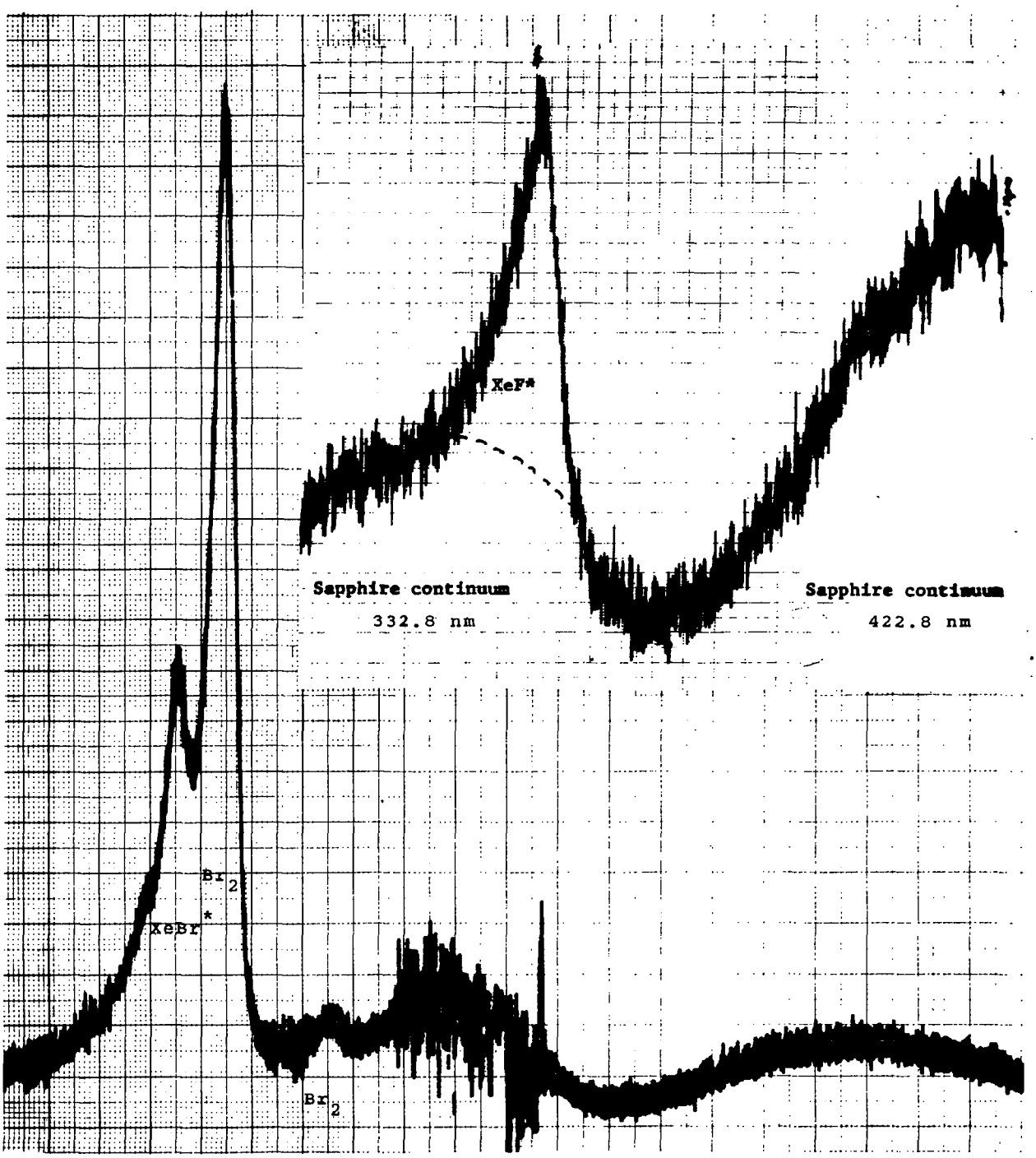

Figure 2.- Comparison of sapphire continuums.

University of Illinois Nuclear Pumped Laser Program

by

George H. Miley

Fusion Studies Laboratory
Nuclear Engineering Program
University of Illinois
Urbana, Illinois 61801

Earlier nuclear pumped laser (NPL) experiments [1,2] at the University of Illinois were aimed at identifying lasers that could operate at neutron flux levels available with the Illinois TRIGA reactor. This led to the development of the simulated emission ratio (SER) technique for multipass in-core gain measurements and the discovery of a new category of "impurity" NPLs that includes both the atomic nitrogen and atomic carbon lasers which use noble gas - N_2 or CO_2 mixtures. Also, operation of a visible laser (He-Hg) was demonstrated for the first time. Concurrently, theoretical/experimental studies have successfully modeled the kinetics of these lasers, despite the occurrence of complex multistep collision process in several cases, with one exception: anamolous production of atomic nitrogen in absorbed surface layers remains under study.

Current research is attempting to build on this previous experience to develop NPL systems with three important characteristics: higher efficiency, energy storage capability, and UF_6 volume pumping. Ideally these characteristics would be combined in one laser, but at the present stage of development each is under separate study.

Excimer lasers are viewed as a prime candidate for efficiency and indeed previous studies at Illinois verified that, like the electrical case,

efficient channeling into the upper level of XeF* occurs with nuclear pumping.[3] Careful selection of buffer gas mixture ratios may make achievement of oscillation possible in a fast burst reactor, but the high flux threshold appears to relegate the excimers to a position of a nuclear "flashlamp" for photolytic pumping of a second gas. This could still be attractive, especially with UF_6 addition to the flashlamp region, which is under study. Experiments under preparation involve adding UF_6 (both natural and enriched) to the boron-coated XeF* gain cell used in previous work. SER measurements are then possible and will be used for parametric studies of optimum in-core mixtures for UF_6 and buffer. Further, facilities to examine the effect of elevated temperature on excimer - UF_6 systems - have been designed.

Energy storage studies to date have concentrated on the atomic carbon laser where millisecond delays have been observed between the reactor pulse and lasing. As described in a companion paper by M. Prelas,[4] this is attributed to metastables involved in the pumping steps, as opposed to the lifetime of the upper state. A prime candidate for achieving nuclear pumping with a long-lived upper state is the iodine laser. Various methods of pumping I* are now being investigated, including XeBr* photolytic pumping and $O_2(a'\Delta)$ collisional pumping. In conclusion, it might be noted that ours is the only group currently carrying out NPL experiments with a TRIGA-type pulsed reactor. Compared to the fast burst reactors used by others, the TRIGA has a broader pulse (~ 10 vs ~ 0.1 msec thermal pulse FWHM) with a somewhat lower peak flux (> 10^{15} vs ~ 10^{17} n/cm^2-sec). This puts the TRIGA at a disadvantage in pumping high threshold lasers, but from the view point of practical applications, these fluxes seem more realistic.

Further the ease of access via beam ports combined with a good repetition rate (~ 1 pulse per 20 min) make the TRIGA an ideal facility for accumulating data needed for studies of basic mechanisms and parametric variations for NPLs. Consequently, it appears that our group could play two vital roles in the NASA NPL research effort, namely

(1) to perform detailed knetic/parametric studies on NPLs developed at fast burst facilities, or elsewhere, and

(2) to provide reactor-based verification of predictions from simulation experiments using e-beams.

References

1. G. H. Miley, "Direct Nuclear Pumped Lasers - Status and Potential Applications," Laser Interactions and Related Plasma Phenomena, (H. Schwarz and H. Hora, eds.) Plenum Press, Vol. 4A, pp. 181-229, 1977.
2. F. P. Boody, M. A. Prelas, J. H. Anderson, S. J. S. Nagalingam, and G. H. Miley, "Progress in Nuclear Pumped Lasers," Radiation Energy Conversion in Space, edited by Kenneth W. Billman, Vol. 61 of Progress in Astronautics and Aeronautics, AIAA, pp 371-340. 1978.
3. G. H. Miley, S. J. S. Nagalingam, F. P. Boody, and M. A. Prelas, "Production of XeF(B) by Nuclear Pumping," Proc. Int. Conf. on Lasers '78, 1978. pp 5-13.
4. M. A. Prelas, Nuclear Pumping Mechanisms in Atomic Carbon and in Excimers. Nuclear-Pumped Lasers, NASA CP-2107, pp. 23-26. (Paper no. 7 of these proceedings.)

Nuclear Pumping Mechanisms in Atomic Carbon and in Excimers

by

M. A. Prelas
Fusion Studies Laboratory
Nuclear Engineering Program
University of Illinois
Urbana, Illinois 61801

Results from two recent research efforts at the University of Illinois will be discussed: the atomic carbon and XeF* nuclear pumping experiments.

The atomic carbon NPL has three unique features[1]. First, the atomic carbon NPL in mixtures of He + CO_2, Ne + CO, CO_2, and Ar + CO_2 has demonstrated a delay between the laser signal and the excitation pulse, while in He + CO mixtures no delay was observed. Second, the laser threshold is achieved at a lower power deposition than its electrically pumped counterpart (~.5 w/cm^3 vs ~ 90 w/cm^3). Third, the Ar + CO_2 laser has only operated as an NPL.

An experimental and computer modeling program, established at the U. of IL, has shown that in mixtures of He + CO the NPL is populated by a direct mechanism:[2]

$$He(2^3S) + CO \rightarrow C(3p\ ^1P_1) + O + He.$$

The delay observed in He + CO_2 mixtures occurs due to the relative slowness of the various steps required to dissociate CO_2 to form CO:[2]

$$He^* + CO_2 \rightarrow CO_2^+ + e + He$$

$$He^* + CO_2 \rightarrow CO^* + O + He$$

$$CO_2^+ + e \rightarrow CO^* + O$$

$$CO^* + M \rightarrow CO + M + \Delta E.$$

Nuclear pumping of the excimer systems is also under study at Illinois. This potentially offers an important technique for achieving high power lasers due to the possibility of exciting large volumes of gases. Excimer lasers have several features which are important for nuclear pumping. First, they required rare gas metastables and ions, major products in nuclear pumped rare gas plasma, to populate the upper laser level. Second, rare gas-fluorine excimers appear to be kinetically compatible with UF_6; a potential volume pumping source. Third, due to selective channeling into the upper state, excimers offer good fluorescence and lasing efficiency.

Experiments with the XeF excimer at the University of Illinois have shown some promising results[3,4]. First, at lower total pressures the Ar buffer gases are superior to Ne: both Ar and Ne are better than He. Second, in mixtures of $Ar/Xe/NF_3$, using the ^{10}B surface source with peak power deposition ranging from 1 to 37 w/cm^3, a small signal gain of ~ 0.01%/cm (less transients absorption) has been measured. Third, 50% of the energy utilized in Ar metastable production goes into excimer formation. Finally, extrapolation of these results shows that the XeF excimer in $Ar/Xe/NF_3$ mixtures could potentially oscillate with the higher flux obtainable with a fast burst reactor giving a power deposition of ~ 1-5 KW/cm^3.

References

1. M. A. Prelas, et al., "Nuclear Pumping of a Neutral Carbon Laser," Radiation Energy Conversion In Space, edited by K. W. Billman, Vol. 61 of Progress in Astro. and Aero. AIAA, NY, p. 411-418 (1978).

2. M. A. Prelas and G. H. Miley, "Collisional Processes in the Atomic Carbon Nuclear Pumped Laser in He + CO_2 Mixtures," XIV International Conf. on Ionized Gases, Grenoble, France, 1979.

3. G. H. Miley, et al., "Production of XeF(B) by Nuclear Pumping," Lasers '78, Orlando, Florida, Dec. 1-15, 1978.

4. S. J. S. Nagalingham, F. P. Boody and G. H. Miley, "Buffer Effects in Nuclear Pumped XeF*(B)," Lasers '79, Orlando, Florida, Dec. 1979.

LaRC Results on Nuclear Pumped Noble Gas Lasers

R. J. De Young

All the noble gases except He have now lased with nuclear excitation. The noble gas nuclear lasers are the best understood systems thus far and lasing has been achieved with both ^3He and fission fragment pumping. The noble gas nuclear lasing transitions are shown in figure 1. Nuclear pumping of neon (not shown) at 632.8 nm has been achieved by the nuclear laser group of the University of Florida.[1] As shown in figure 1, lasing has occurred for wavelengths of 1.79 μm to 3.65 μm, at pressures from 400 Torr to 4 Atm, and for noble gas concentrations from 0.01% to 30%.[2] It is the purpose of this paper to review the recent experimental and theoretical results obtained for noble gas systems.

In figure 2 the power deposited in ^3He and $^{235}UF_6$ is shown for the $^3He(n,p)^3H$ and $^{235}UF_6(n,ff)FF$ reaction respectively assuming no loss of charged particles to the container walls. From the figure it can be seen that nuclear pumping cannot match the power deposited from typical E-beam machines; thus, potential nuclear laser systems must have

reasonable gain at low power deposition rates. This is exactly the case for the He noble gas mixture lasers.

The gain of a laser medium can be written as:

$$\gamma(\nu) = \frac{\lambda^2}{8\pi\, t_{spon}} [N_2 - N_1(g_2/g_1)]\, g(\nu) \tag{1}$$

$$\text{where} \quad g(\nu) = \frac{(\Delta\nu/2\pi)}{(\nu - \nu_0)^2 + (\Delta\nu/2)^2} \tag{2}$$

is the Lorentzian lineshape function. At line center the gain becomes

$$\gamma_0 = \frac{\lambda^2}{4\pi^2\, t_{spon}} [N_2 - (g_2/g_1)\, N_1] / \Delta\nu \tag{3}$$

where Δ is the full width at half maximum of the laser transition.

By noting eq. 3 we can understand why the noble gas lasers are so easily pumped under nuclear excitation. First, all the lasing wavelengths are in the infrared maximizing the gain by λ^2; second, the inversion density $[N_2 - N_1(g_2/g_1)]$ is easily maintained since for all the transitions the upper laser level lifetime is longer than the lower laser level lifetime and minimal pumping of the lower laser level occurs. Third, $\Delta\nu$ for all noble gas laser transitions is small (as compared to excimer systems for example). Fourth, t_{spon} the radiative lifetime is short but not shorter than the lifetime of the lower laser level. Thus, it is clear why the noble gas systems can be easily pumped with nuclear or electrical excitation.

Noble Gas Laser Excitation Mechanisms

Noting again figure 1, it is observed that the noble gases form a Penning mixture with He metastables. Also, charge transfer from He_2^+ can efficiently ionize the minority Ar, Kr, or Xe lasing species. In either case a high density of noble gas atomic ions is produced. Calculations were undertaken for the ^{3}He-Ar nuclear laser which are summarized in the generalized energy block diagram as shown in figure 3 for ^{3}He-Ar but are equally valid for He-Kr, or He-Xe.[3] Here the efficient production, by charge transfer and Penning ionization, of Ar^+ is shown. Loss of Ar^+ occurs from three body association to form Ar_2^+ or from collisional-radiative recombination which after radiative cascade eventually pumps the upper laser level of the 1.79 μm Ar transition. The lower laser level is pumped predominately by dissociative recombination of Ar_2^+; thus, the minority gas species must be kept low to retard formation of Ar_2^+, Kr_2^+, or Xe_2^+. The favorable lifetimes of the upper and lower laser levels ensure a population inversion if pumping from Ar_2^+ dissociative recombination is kept small.

Figure 4 shows a schematic diagram of the Ar^+ collisional-radiative model used to calculate the flow of energy after recombination. The atomic states within the Saha region are in equilibrium with the free electrons and the states there are assumed to be completely collision dominated. States below the Saha region are assumed to be completely radiative dominated, and

the radiative energy flow into the upper laser level is calculated using the Ar transitions probabilities. Using this model, reasonable gain and power output for the Ar 1.79 μm laser transition were calculated and compared favorably to experimental measurements.

Figure 5 is a comparison between calculated and experimental laser inversion density vs. argon concentration. The results are quite good and should be equally adaptable to the He-Kr and He-Xe systems.

Large Volume Noble Gas Nuclear Pumped Lasers

As noted in figure 2, the pumping power densities for nuclear lasers are small; thus, in order to achieve high power outputs, it is necessary to use large volumes of excited gas. This can be done easily with nuclear pumping since neutrons can penetrate deeply into a high pressure gaseous medium.

Figure 6 shows a nuclear pumped multiple pass box laser presently used for large volume lasing experiments with noble gases.[4] The laser frame is made of stainless steel with aluminum cover plates on which a polyethylene moderator is attached. Gold plane mirrors are aligned internally to reflect the laser beam back and forth through the excited gaseous medium. External dielectric coated mirrors form an optical cavity for laser experiments; alternatively, this configuration could be used as an amplifier by using an external oscillator. Lasing is detected by a multiple element InAs array.

The volume here is 4800 cm^3 as compared to 200 cm^3 for the cylindrical noble gas nuclear lasers. In figure 7 the box laser and cylindrical laser results are compared and show the advantage of the multiple pass large volume systems. Approximately 100 watts peak power has been achieved from box laser II, thus far, from ^{3}He-Ar lasing at 1.79 μm. In figure 8 another plot is shown of the comparison between box and cylindrical laser output as a function of time indicating the progress made with noble gas systems.

Fission Fragment Pumped Ar-Xe Lasing

Experiments were undertaken on the Ar-Xe system with $^{235}UF_6$ fission fragment pumping.[5] This system was found to lase well in the laboratory at 2.65 μm in Xe with up to 5% added UF_6. Since Ar has a stopping distance of 7 cm compared to a He distance of 28 cm for fission fragments, it was thought that the Ar-Xe system would be the most ideal candidate for noble gas fission fragment pumping.

Initial experiments at the reactor used 600 Torr Ar-3% Xe (3% Xe was found to be the optimum concentration for high-pressure electrically pulsed lasing at 2.65 μm) with from 5 to 20% $^{235}UF_6$. No lasing was observed. A pressure transducer was attached to the laser cell with a response time fast enough to detect the gas pressure pulse during the reactor neutron pulse. The output of the pressure transducer is shown in figure 9. Also

shown is the thermal neutron pulse. The pressure pulse is made from shock waves created by the thermal neutron pulse, as shown at the bottom of figure 9. As the $^{235}UF_6$ concentration was lowered in Ar-Xe, it was noted that the pressure pulse did not change. Thus, Ar-Xe was then pulsed with no added $^{235}UF_6$ and lasing was observed from the Ar-Xe mixture at 2.65 μm. The origin of the excitation energy is shown in figure 10. After many $^{235}UF_6$ fillings, UF_5, UF_4, etc., was deposited on the inner laser cell wall, thus creating a source of fission fragments. No more than 1 Torr of $^{235}UF_6$ could be added to the Ar-Xe before laser quenching would result. Since the fissionable coating was not homogeneously deposited on the wall, uneven excitation of the gas medium would result. This was observed as shown in figure 11 where a typical Ar-Xe laser output is compared to the thermal neutron pulse. Also shown is the laser output at 2.027 μm, which was considerably lower than the 2.65 μm laser output. The erratic nature of the excitation source is readily observed.

This is the first laser system to be pumped with fission fragments from $^{235}UF_6$ and with a higher Q optical cavity it may be possible to add sufficient gaseous $^{235}UF_6$ to actually pump Ar-Xe directly.

Conclusions

It has been shown that the noble gas lasers are among the easiest systems to pump by nuclear excitation and as a result all

the noble gases except He have lased under nuclear excitation. The noble gas systems are not ideal for high-power applications but they do give valuable insight into the operation and pumping mechanisms associated with nuclear lasers. At present, the Ar-Xe system is the best noble gas candidate for $^{235}UF_6$ pumping. It appears that the quenching of Ar-Xe lasing is a result of the fluorine and not the uranium or fission fragments themselves. Thus, to achieve lasing with UF_6, a fluorine compatible system must be found.

References

1. R. T. Schneider, Basic Research Relevant to CW-Nuclear Pumped Lasers, NASA CR-158837, 1979.
2. R. J. DeYoung, N. W. Jalufka, and F. Hohl, AIAA J., 16, 991 (1978).
3. J. W. Wilson, R. J. DeYoung, and W. L. Harries, J. Appl. Phys., 50, 1226 (1979).
4. R. J. DeYoung and F. Hohl, First Int. Sym. on Fission Induced Plasmas and Nuclear Pumped Lasers, Orsay, France, May 23-25, 1978.
5. L. A. Newman and T. A. De Temple, Appl. Phys. Let., 27, 678 (1975).

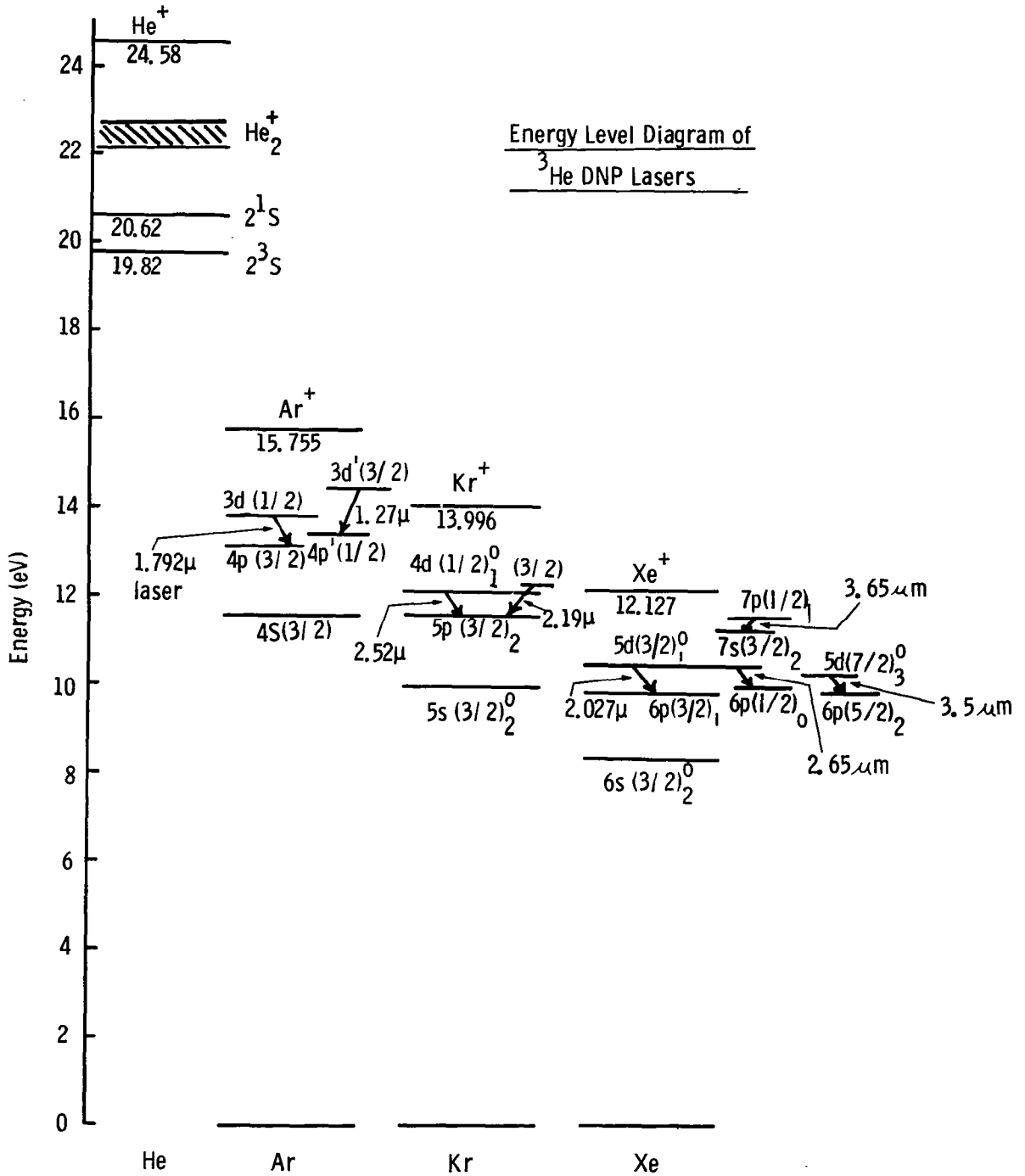
Energy Level Diagram of
3He DNP Lasers
Energy (eV)
He+
24.58
He2+
2 1S
20.62
2 3S
19.82
Ar+
15.755
3d'(3/2)
3d (1/2)
1.27μ
Kr+
13.996
1.792μ
laser
4p (3/2)
4p'(1/2)
4d (1/2)0 1 (3/2)
Xe+
12.127
7p(1/2)1
3.65μm
4S(3/2)
2.52μ
5p (3/2)2
2.19μ
5d(3/2)0 1
7s(3/2)2
5d(7/2)0 3
5s (3/2)0 2
2.027μ
6p(3/2)1
6p(1/2)0
6p(5/2)2
3.5μm
2.65μm
6s (3/2)0 2
He
Ar
Kr
Xe

Figure 1

POWER DEPOSITED vs. NUCLEAR AND E— BEAM EXCITATION

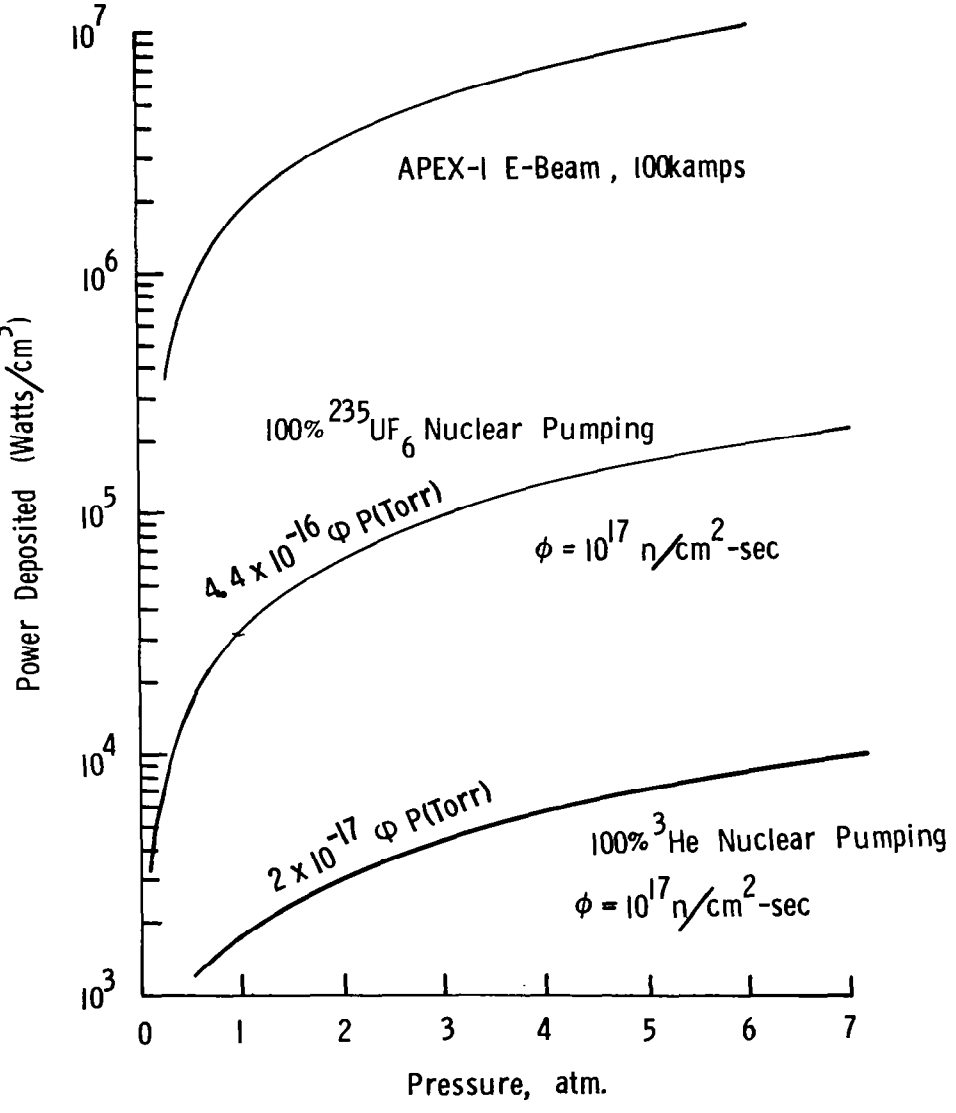

Figure 2

Collisional Processes in ^{3}He-Ar DNP Laser

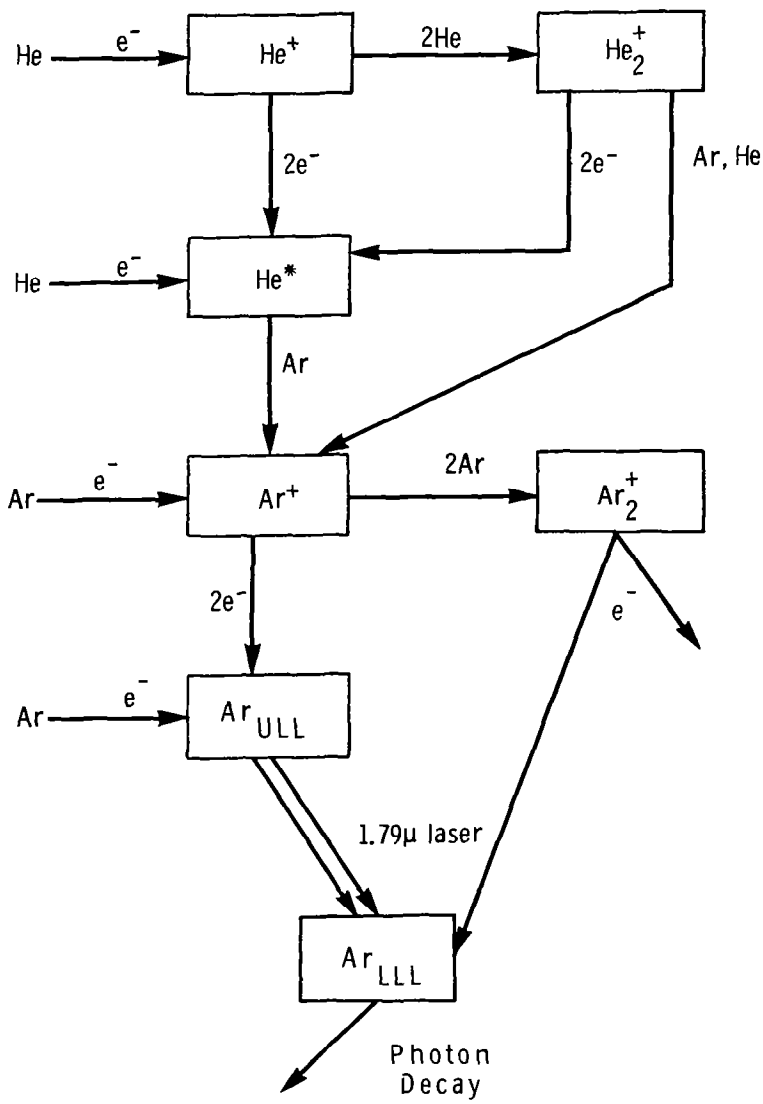

Figure 3

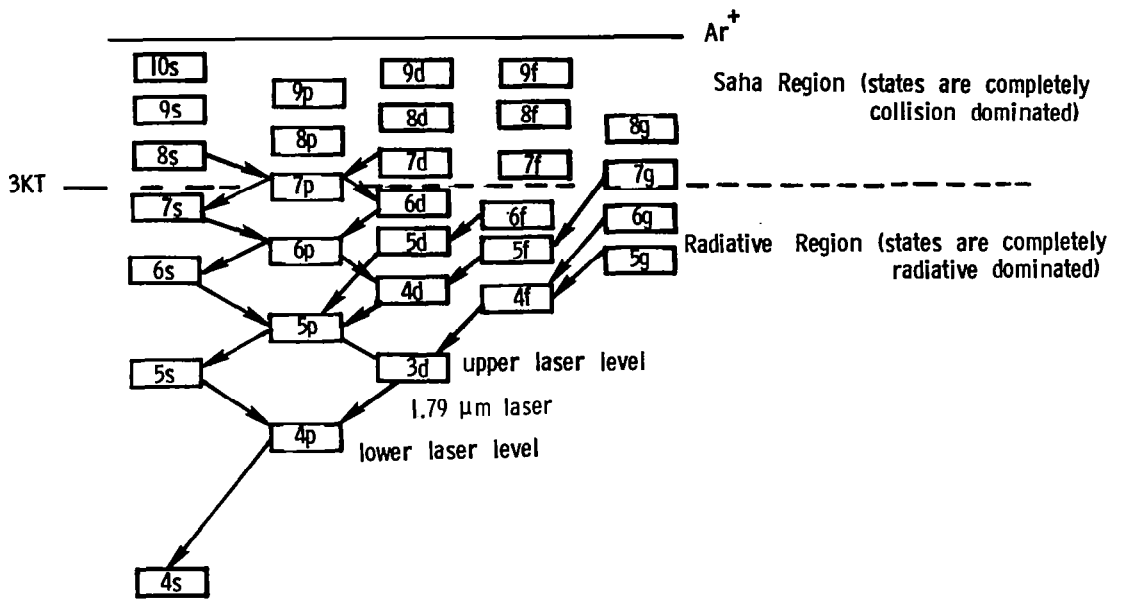

Figure 4

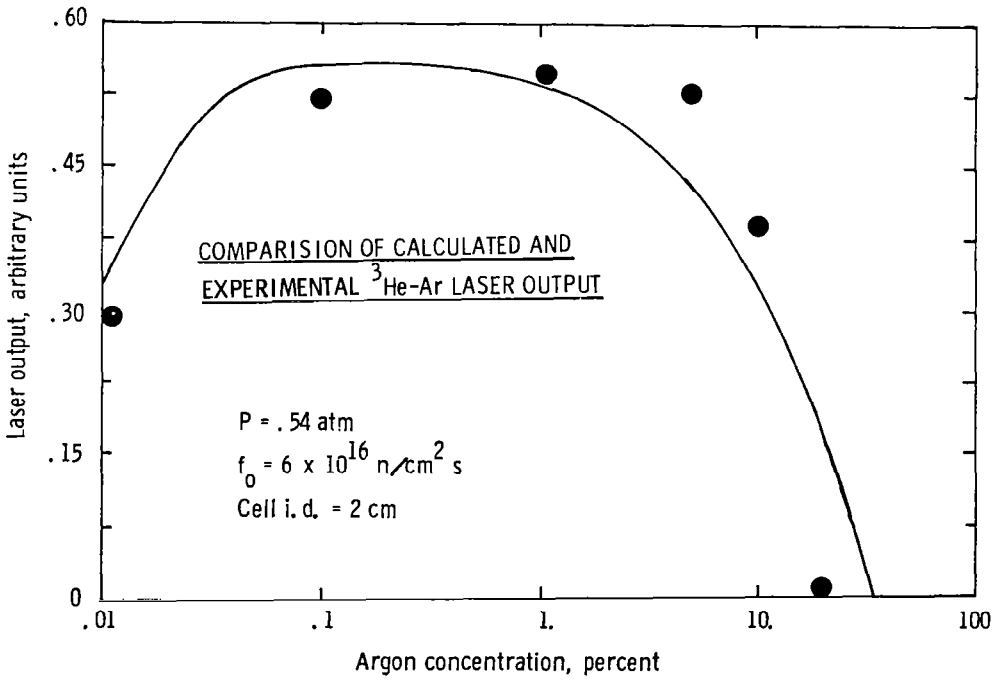

Figure 5

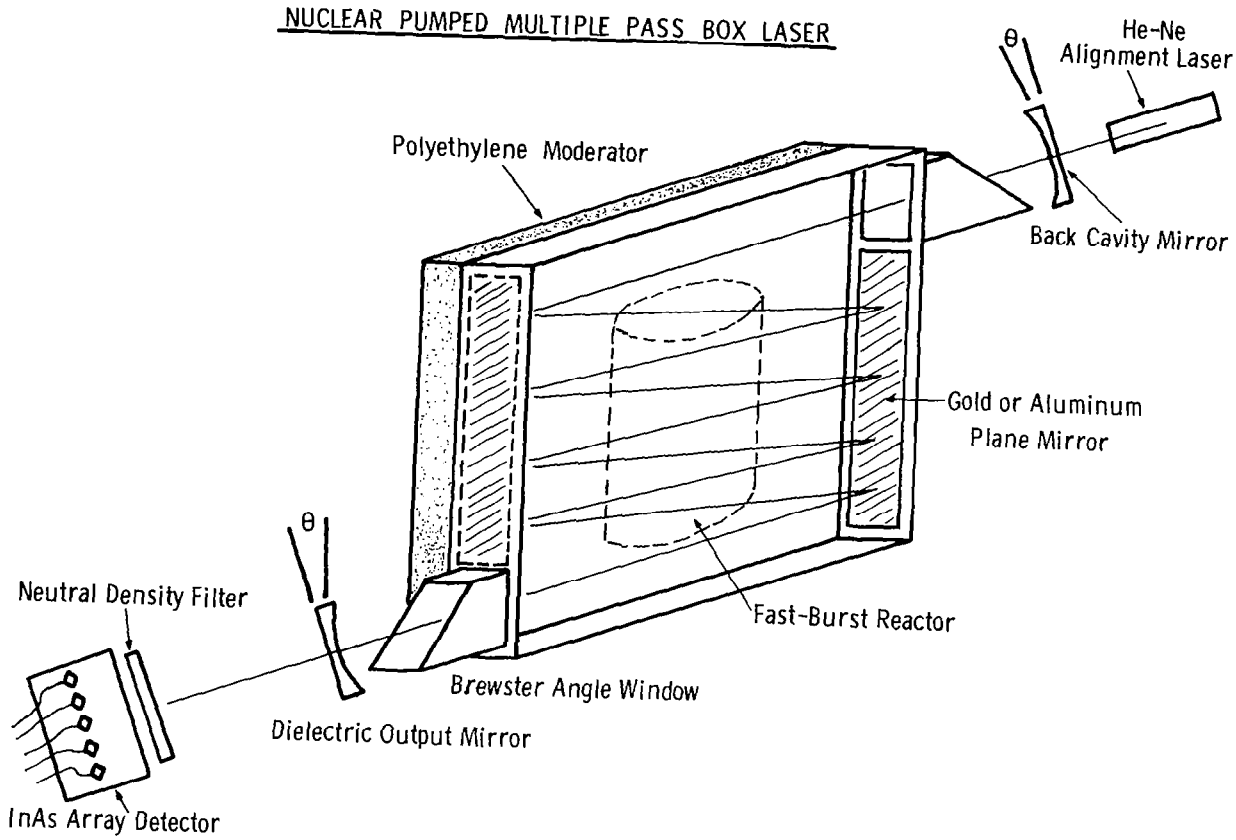
NUCLEAR PUMPED MULTIPLE PASS BOX LASER
θ
He-Ne
Alignment Laser
Polyethylene Moderator
Back Cavity Mirror
Gold or Aluminum
Plane Mirror
θ
Neutral Density Filter
Fast-Burst Reactor
Brewster Angle Window
Dielectric Output Mirror
InAs Array Detector

Figure 6

PEAK LASER OUTPUT FROM CYLINDRICAL AND BOX LASERS

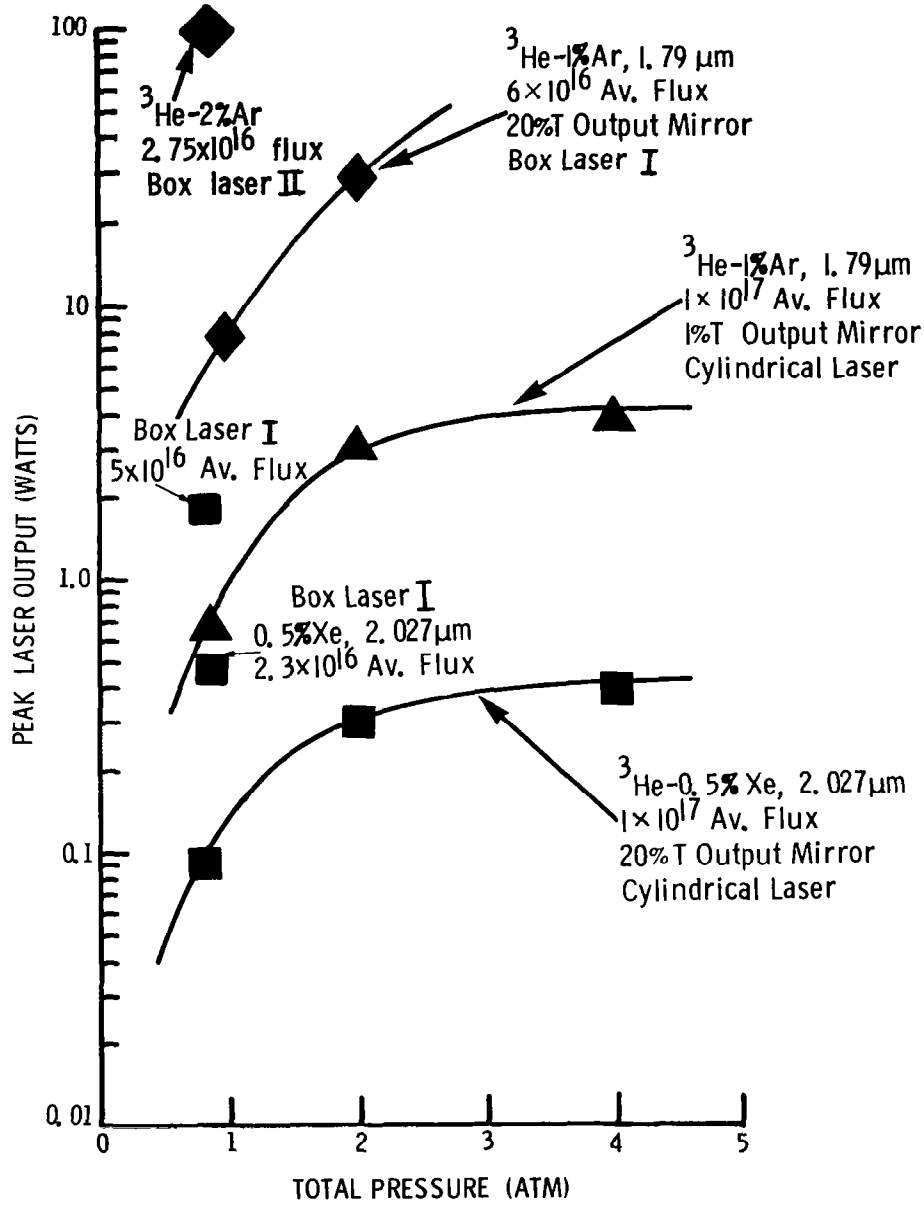

Figure 7

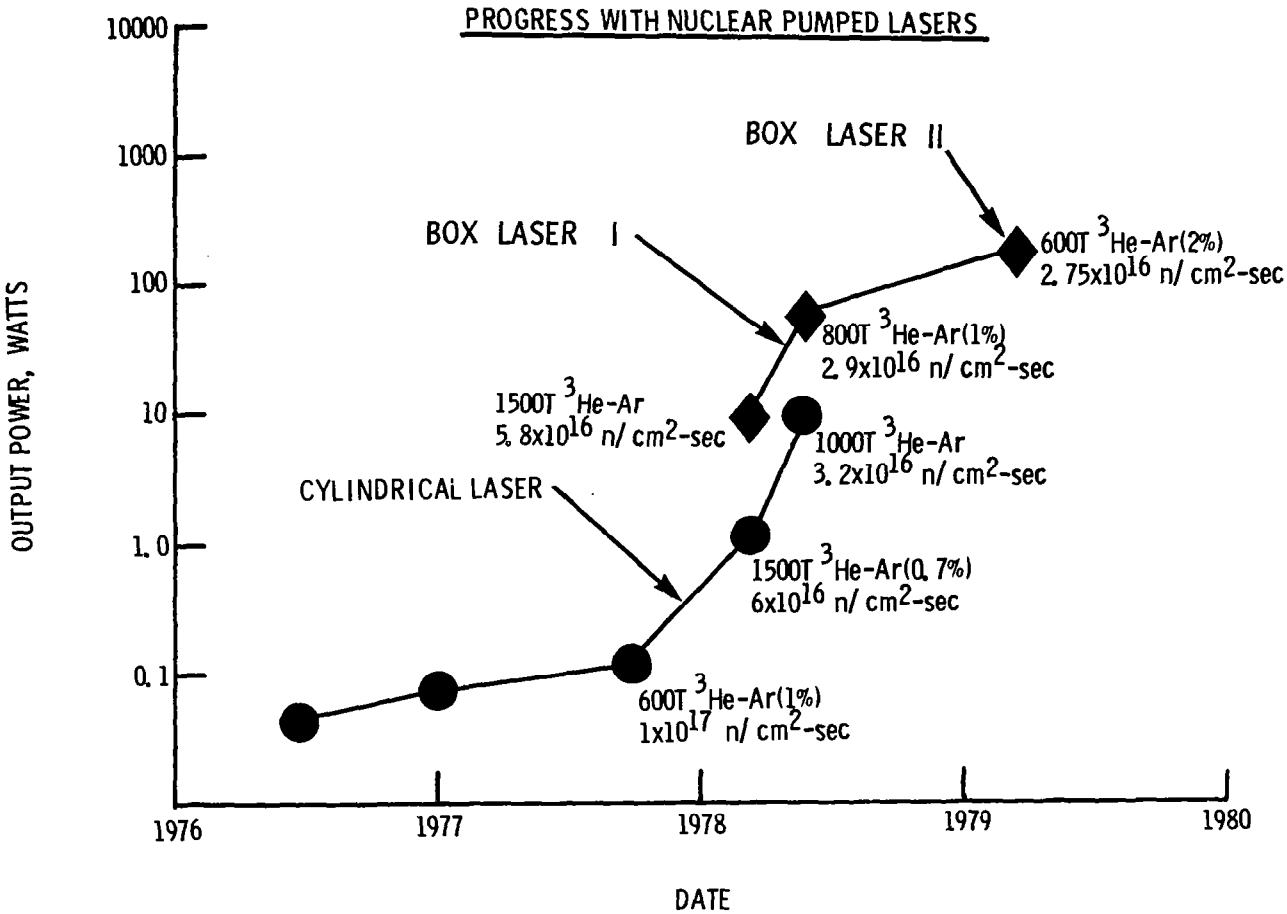
PROGRESS WITH NUCLEAR PUMPED LASERS
OUTPUT POWER, WATTS
10000
1000
100
10
1.0
0.1
1976
1977
1978
1979
1980
DATE
BOX LASER II
BOX LASER I
CYLINDRICAL LASER
600T 3He-Ar(2%)
2.75x10^16 n/cm^2-sec
800T 3He-Ar(1%)
2.9x10^16 n/cm^2-sec
1500T 3He-Ar
5.8x10^16 n/cm^2-sec
1000T 3He-Ar
3.2x10^16 n/cm^2-sec
1500T 3He-Ar(0.7%)
6x10^16 n/cm^2-sec
600T 3He-Ar(1%)
1x10^17 n/cm^2-sec

Figure 8

FISSION FRAGMENT PUMPED Ar-Xe PRESSURE PULSE

- 600Torr, Ar-3% Xe

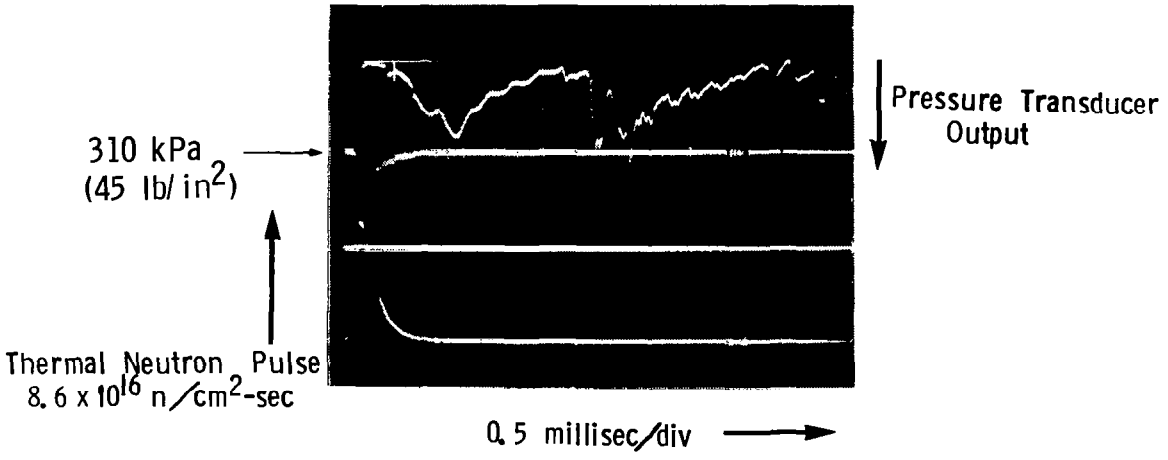

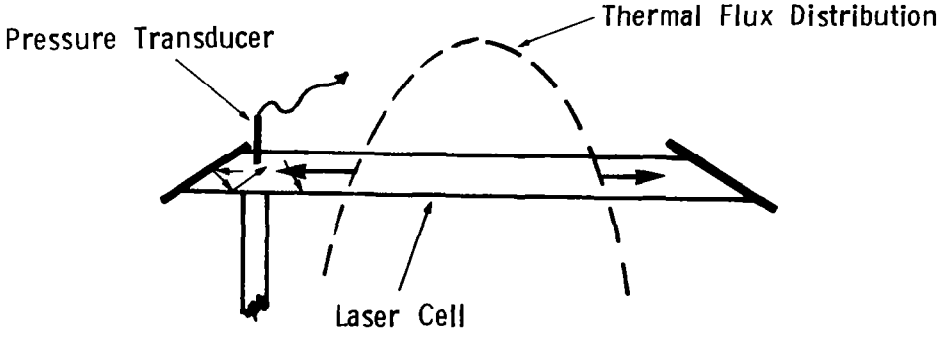

Figure 9

Ar-Xe "ALMOST" $^{235}UF_6$ PUMPED NUCLEAR LASER

- 600 Torr, Ar-3% Xe
- 8×10^{16} n/cm^2-sec

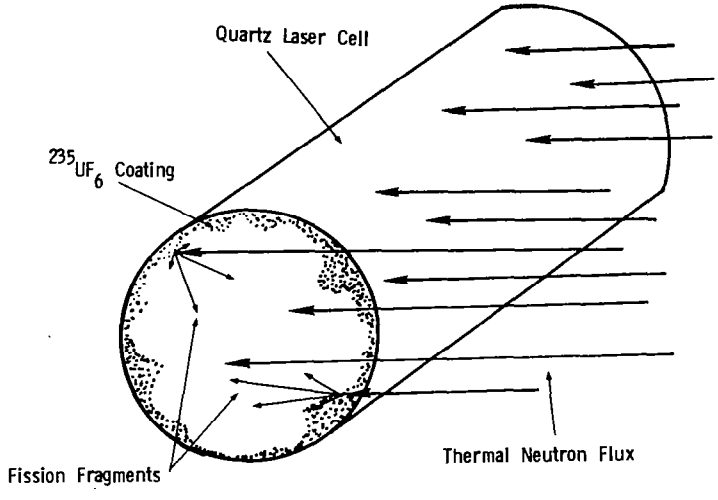

Figure 10

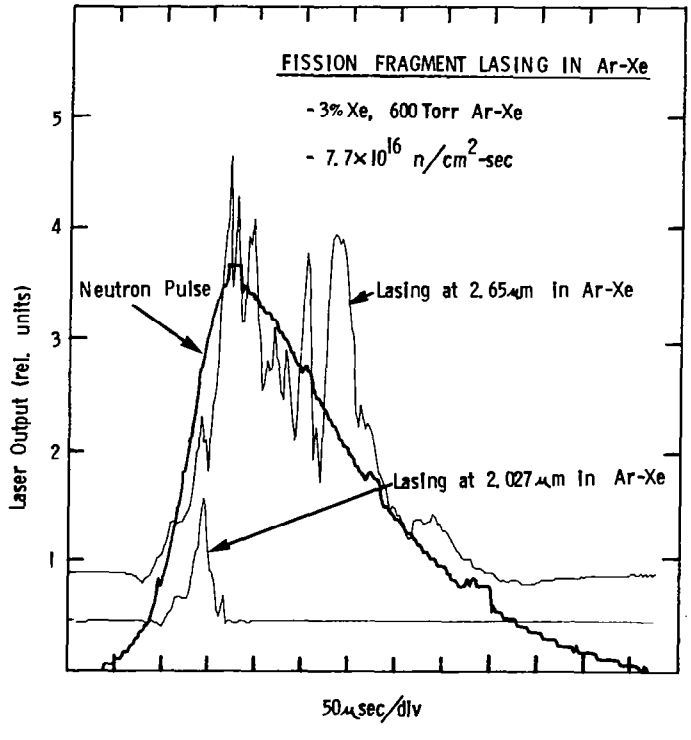

Figure 11

Nuclear Excitation of CO_2 and CO

N. W. Jalufka
NASA, Langley Recearch Center
Hampton, Virginia 23665

The CO_2 laser with its high efficiency and high power output (in both CW and pulsed modes) has been of considerable interest to researchers in the direct nuclear pumped laser field. So far, direct nuclear pumped lasing of the CO_2 laser has not been achieved and the results obtained are limited. The first nuclear pumped CO_2 laser experiments were carried out by DeShong at the Argonne National Laboratory[1]. DeShong used B-10 coatings and electrical pumping to observe a decrease in laser threshold up to a thermal flux of 5×10^8 n cm^{-2} sec^{-1}. At higher flux (up to a peak of 2×10^{10} n cm^{-2} sec^{-1}) he observed an increase in laser threshold but obtained insufficient data to explain this result. Allario and Schneider[2] observed enhancement of the output of a ^3He-N_2-CO_2 laser when the laser was placed in a pulsed thermal neutron field of $< 10^8$ n cm^{-2} sec^{-1}. Experiments by Ganley, Verdeyen and Miley[3] showed an increase in the power and efficiency of a CO_2 laser when the discharge was irradiated with energetic α and Li ions produced by the (n, α) reaction in B-10. Andriyakhin et al.[4] have also carried out experiments with nuclear enhancement of CO_2 lasers. McArthur, Miller and Tollefsrud[5] measured a small signal gain of ≈ 0.04 cm^{-1} in an electrically pulsed CO_2 system using a fast burst reactor as a preionizer.

The nuclear pumped laser research group at the NASA Langley Research Center has made several attempts to obtain lasing in CO_2 using the U. S. Army's fastburst reactor at the Aberdeen Proving Ground, MD.

High power output is achieved in the electrical discharge CO_2 laser by the addition of N_2. Vibrational energy is transferred from the v=1 meta-stable level of N_2 to the 001 level of CO_2 which is the upper laser level (Figure 1). However, it is not clear that this mechanism would be the primary means of exciting the upper laser level in a nuclear excited discharge as these discharges, due to high densities and low temperatures, tend to be dominated by collisional-radiative recombination. Consequently, mixtures of CO_2-^3He were tried as well as CO_2-N_2-^3He.

The nuclear excited laser experiments were carried out using a 2.5 cm OD quartz tube 80 cm long. The ends were cut at Brewsters' Angle and were fitted with KCℓ windows. The tube was placed inside a 60 cm long by 15 cm OD C_2H_2 moderator and was connected to a gas handling and vacuum pumping system. The cavity consisted of 2.5 cm diameter mirrors either Ge or gold coated. Both mirror sets employed consisted of a flat back mirror and a 10 meter radius of curvature output mirror with a 1.5- to 2-mm diameter hole for output coupling. The detector was an AuGe operated at 77°K and was placed such that it was well shielded against radiation. Table 1 lists the various conditions of gas mixture, total pressure and neutron flux used in these experiments. In no case was any indication of lasing observed.

Futher study of the CO_2 system was directed to an experiment to measure gain in a nuclear pumped CO_2 amplifier system. The experimental set up is shown in Figure 2 and consisted of a C.W. CO_2 laser, which served as a probe laser, a 2.5 cm ID by 70 cm long quartz cell with flat NaCℓ windows and an AuGe detector operated at 77°K. The quartz cell was placed inside a 60 cm long by 15 cm OD C_2H_2 moderator and was connected to the gas handling and vacuum system. The beam from the probe laser was directed through the amplifier cell and was focussed onto the AuGe detector with a BaF_2 lens. The probe laser was operated at a power level of 100 mW which produced a 50 mV signal from the AuGe detector. The power output of the probe laser was monitored during the reactor pulse by observing the DC power output of the AuGe detector. The nuclear pumped amplifier tube was filled to 1 atmosphere pressure with a gas mixture consisting of equal parts CO_2 and N_2 (up to 20%) and the balance ^3He.

No gain (increase in probe laser signal) was observed for any of the reactor pulses. Absorption did occur during the reactor pulse and lasted for several milliseconds into the afterglow reaching 100% absorption at 20% CO_2. These results are shown in Figure 3. These results suggest that it is the lower laser level which is strongly pumped by the nuclear discharge. Figure 4 is a plot of the Maxwellian part of the electron energy distribution for temperatures of 300, 600, and 900°K. Cross sections for electron impact excitation of several vibrational levels (including the upper laser level) are also shown on the figure. The 010 is the first excited vibrational level and is coupled to both the 020 level (lower laser level of the 9.4 μm band)

and the 100 level (lower laser level of the 10.6 μm band). The cross section for the 020 level is plotted and this level is also representative of the 100 level since both are Σ_g^+ states and differ by only 0.013 eV in energy. The 001 level is the upper laser level. Collisional excitation rates into these levels are proportional to the convolution of the electron distribution curve with the cross section. From figure 4 it is apparent that for electron temperatures below 900°K, population of the lower levels will dominate over the upper level. This agrees with our experimental results as the 100 level was responsible for the absorption which was measured. Therefore, it appears that at the temperatures and electron energy distribution encountered in direct nuclear pumped lasers, electron collisons (at least in the Maxwellian part of the distribution) are detrimental to a population inversion.

We are also carrying out experiments on a ^{3}He-CO system. The laser tube is cooled by a closely wrapped coil of P.V.C. tubing through which liquid N_2 flows. We have been able to maintain a tube wall temperature of 100 °K in this way and the system lases readily in the laboratory with peak power output of several Watts.

References

1. DeShong, J. A., Argonne National Laboratory Report, ANL-7310, 1967.
2. Allario, F. and Schneider, R. T.; NASA SP-236, 1971.
3. Ganley, T., Verdeyen, J. T., and Miley, G. H., App. Phys. Letts. 18, 568, 1971.
4. Andriyakhin, V. M., Velikhov, E. P., Vasil'tsov, V. V., Krasil'nikov, S. V., Pis'mennyi, V. D., Novobrantsev, I. V., Rakhimov, A. T., Starostin, A. N., and Khvostionov, V. E., JETP Letts. 15, 451, 1972.
5. McArthur, D. A., Miller, G. H., and Tollefsrud, P. B., Appl. Phys., Letts. 23, 303, 1973.

TABLE I
CO_2 NPL EXPERIMENTS

Pulse No.	$\%CO_2$	$\%N_2$	$\%^3He$	Total Press.	Neutron Yield	Results
1	20	--	80	400 Torr	7.6×10^{16}	No Lasing
2	20	--	80	400 Torr	7.6×10^{16}	Back Mirror/ Blocked
3	20	--	80	400 Torr	7.3×10^{16}	No Lasing
4	2.5	--	97.5	200 Torr	4.2×10^{16}	No Lasing
5	2.5	--	97.5	200 Torr	2.4×10^{16}	No Lasing
259	10	20	70	600 Torr	7.7×10^{16}	No Lasing
260	10	20	70	300 Torr	7.7×10^{16}	No Lasing
329	.5	9.5	90	600 Torr	9.85×10^{16}	No Lasing
330	.5	9.5	90	600 Torr	9.24×10^{16}	No Lasing Tube Cooled with liq. N_2 Vapor

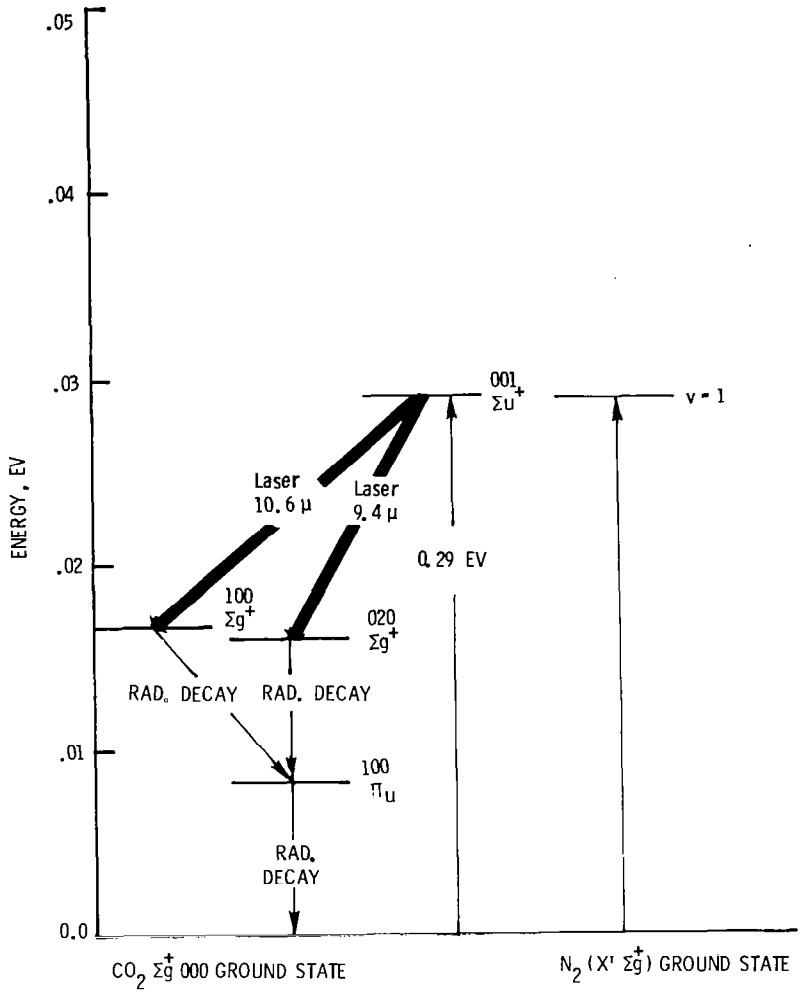

Figure 1.- Energy level diagram for CO_2.

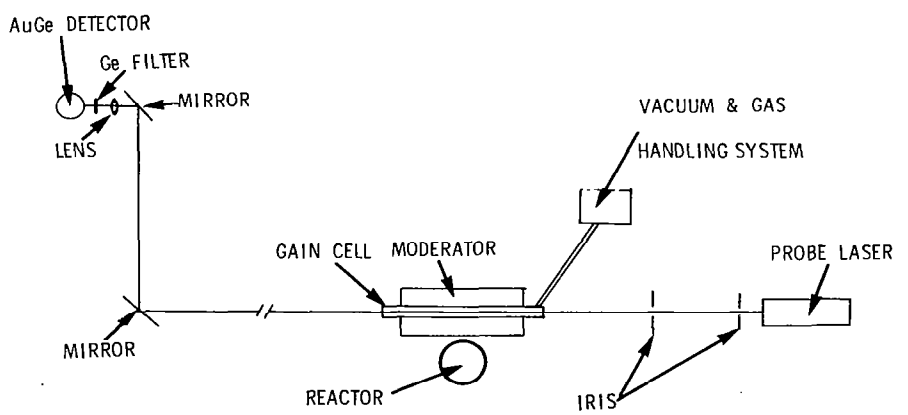

Figure 2.- CO_2 gain measurements.

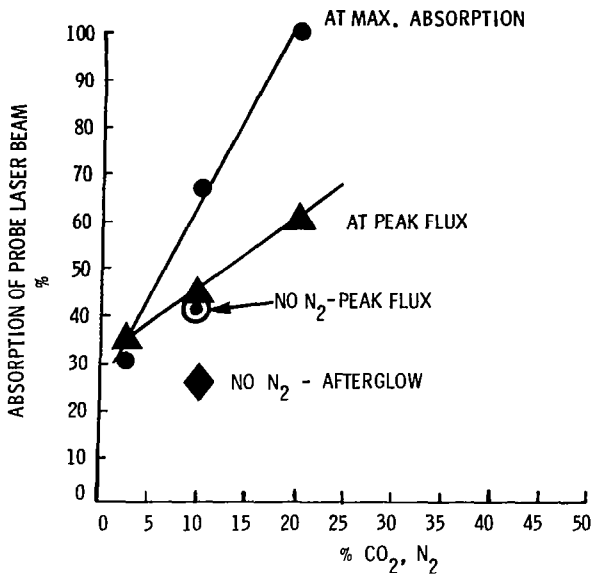

Figure 3.- Probe beam absorption versus CO_2 concentration.

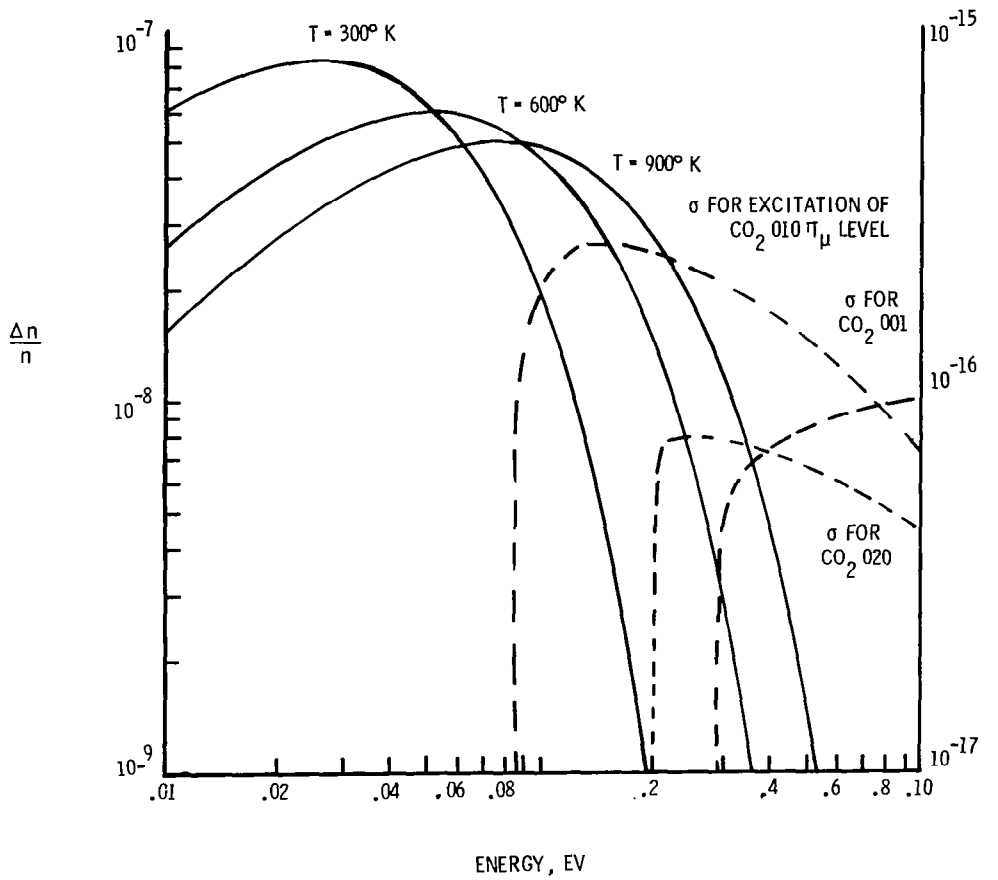

Figure 4.- Maxwellian electron energy distributions and excitation cross sections for CO_2 vibration levels.

Nuclear Pumped Laser Modeling

J. W. Wilson and A. Shapiro
Langley Research Center
Hampton, VA 23665

We developed a model for an indirectly nuclear pumped laser experiment. The apparatus consists of the usual cylindrical neutron moderator enclosing a gas filled quartz cell. The quartz cell in this case has two concentric compartments; the larger outer compartment is filled with ^3He and fluorescent gases which are coupled radiatively to the inner compartment which is filled with a lasing gas for efficient optical pumping. A cross section of the system is shown in figure 1. The fluorescent gas in this study is taken as a mixture of Ar, Kr and F_2. The perfluoro-alkyliodide is chosen as the lasant material of the inner compartment.

The alkyliodide is photodissociated to form atomic iodine in the ^2p state which slowly radiates to the ground atomic state. Collisional de-excitation is slow for alkyliodide, except for the methyliodide, so that energy storage is greatly facilitated. The photoabsorption cross section is shown in figure 2 for two different iodides for which good absorption is achieved between 250 and 320 nm depending on the choice of material.

Some candidate excimer fluorescent systems are given in figure 3. The maximum fluorescent efficiency (n_{rad}) and maximum laser efficiency (n_{laser}) for the 1.315 μm atomic iodine line are given. Important kinetic factors are not included in these efficiencies.

We have calculated with a simple model the degree of photoabsorption in the lasant gas of the KrF* and Ar_2F^* excimer fluorescence by assuming the quartz cell to be surrounded by a polished aluminum reflector. The dimensions used are those given in figure 1 and absorption in the fluorescent gas was neglected. The fractional absorption is shown in figure 4 as a function of C_3F_7I pressure in the inner compartment. Nearly complete absorption is achieved above about 60 torr.

The emphasis of the present work is to evaluate the kinetic efficiencies of various gas combinations in the outer fluorescence tube with intent to maximize the fluorescence output in the iodine pump band. The kinetic processes in the model are listed in figure 5. Most reaction rates have been found in the literature although a few are taken to be "typical" values.

The main kinetic sequence is shown in figure 6. Energy is supplied to the gas from kinetic energy of reaction products formed in the ^3He gas by thermal neutrons. This kinetic energy is transferred to the gas through impact in which positive ions and free electrons are formed and various atomic and molecular states are excited. This impact energy is handed over to the dominant gas species in the tube which we will show to be ^3He and Ar at the peak fluorescence output. The reactions labeled in figure 6 are those which appear dominant according to a detailed kinetics model.

Results of the kinetics model are shown in figure 7. The total gas pressure was taken as 1 atmosphere with 0.5 torr of F_2 added. Larger amounts of F_2 shows serious quenching. A

parametric study was made to determine the best mixture of gases for peak KrF* output. High ^3He concentrations result in excessive leakage of the ^3He reaction products to the cell walls because of the small ^3He ionization cross section. Too little ^3He reduces the input power level and about 75 percent appears to be about the best ^3He concentration. The remaining 25 percent of the gas is to be divided between Ar and Kr. If too little Kr is used then ArF* becomes the dominant fluorescence. If too much Kr is used the KrF* is lost to the formation of the trimolecular excimer Kr_2F^*.

Similar results are obtained at 2 and 3 atmospheres of total pressure in figures 8 and 9. The optimum Kr concentration is reduced at higher pressure due to the increased importance of Kr_2F^* formation.

The effects of varying the F_2 concentration are shown in figure 10 from which it is seen that the optimum is between 0.15 and 0.2 torr. The radiative power output at 1 atm is

$$\zeta_o = 1.1 \times 10^{21} \text{ eV/cm}^3 \text{ sec}$$

The input power is

$$\eta_i = 7.75 \times 10^{21} \text{eV/cm}^3 \text{ sec}$$

for an overall radiative efficiency of

$$\eta_{rad} = 14.25\%$$

and kinetic efficiency of

$$\eta_k = 42\%$$

This high kinetic efficiency is achieved only if the F_2 concentrations are kept sufficiently low so as to minimize quenching. Thus, the dominant negative particles in the plasma

are free electrons with the result that positive ion losses arise through recombination and excimer formation is through the metastables as follows:

$$Ar_2^+ + Kr \longrightarrow Kr^+ + 2\ Ar$$

$$Kr^+ + e + M \longrightarrow Kr^* + M$$

$$Kr^* + F_2 \longrightarrow KrF^* + F$$

We consider now the use of a $^3He/Ar/F_2$ mixture to generate Ar_2F^* fluorescence at 284 nm. Figure 11 shows the fluorescence output for various ^3He concentrations. The efficient conversion into Ar_2F^* requires high Ar concentration as indicated in the figure.

Figure 12 shows the fluorescence output for 0.5 atm of ^3He as a function of Ar pressure. Again efficient conversion occurs for high Ar pressure. Similar results are shown in figures 13 and 14. The total radiant output at 1 atm of ^3He is

$$\zeta_o = 1.5 \times 10^{21}\ eV/cm^3\text{-sec}$$

with the corresponding input of

$$\zeta_i = 1.02 \times 10^{22}\ eV/cm^3\text{-sec}.$$

The overall radiative efficiency is

$$\eta_{rad} = 14.7\%$$

with a corresponding kinetic efficiency of

$$\eta_k = 66\%$$

This high kinetic efficiency is possible only if the F_2 concentration is kept sufficiently small to prevent quenching. As a result, the dominant negative particles in the plasma are free electrons with the result that positive ion losses are

through electronic recombination and excimer formation is through the action of metastables as follows:

$$Ar_2^+ + e \longrightarrow Ar^* + Ar$$

$$Ar^* + Ar + M \longrightarrow Ar_2^* + M$$

$$Ar_2^* + F_2 \longrightarrow Ar_2F^* + F$$

as the main kinetic sequence and an important secondary sequence as follows:

$$Ar^* + F_2 \longrightarrow ArF^* + F$$

$$ArF^* + Ar + M \longrightarrow Ar_2F^* + M$$

The Ar_2F^* radiative output is shown as a function of F_2 concentration in figure 15.

Replacement of the F_2 by NF_3 in the KrF system reduces the output due to the reduced excimer formation rate

$$Kr^* + NF_3 \longrightarrow KrF^* + NF_2$$

as compared to the

$$Kr^* + F_2 \longrightarrow KrF^* + F$$

In addition, the rate

$$Kr^* + NF_3 \longrightarrow Kr + NF_3$$

is very competitive with excimer formation whereas

$$Kr^* + F_2 \longrightarrow Kr + F_2$$

does not occur. Insufficient data is presently available to judge the effect of replacing NF_3 with F_2 in the Ar_2F system. Indications are, however, that F_2 is probably the more efficient fluorine donor.

INDIRECT NUCLEAR PUMPED IODINE LASER

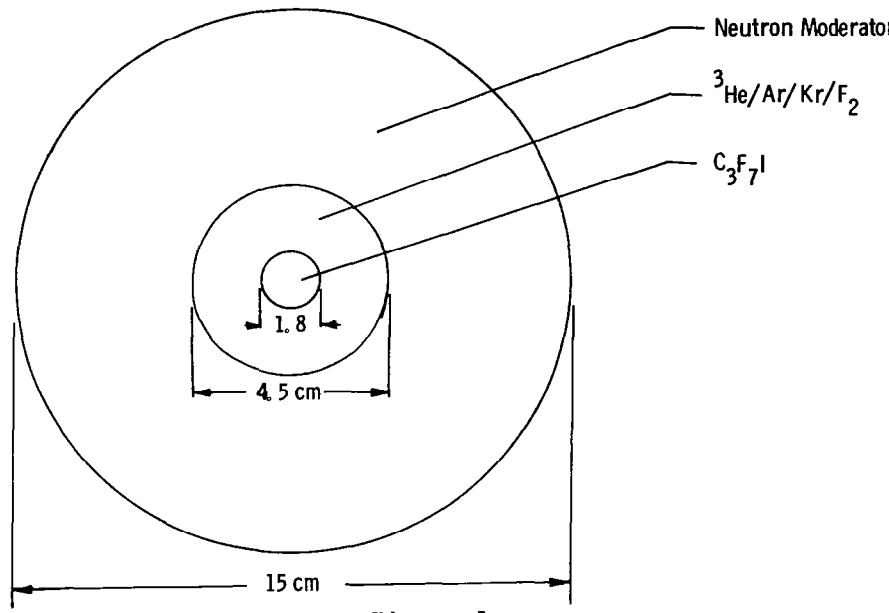

Figure 1

ALKYLIODIDE PHOTODISSOCIATION CROSS SECTION

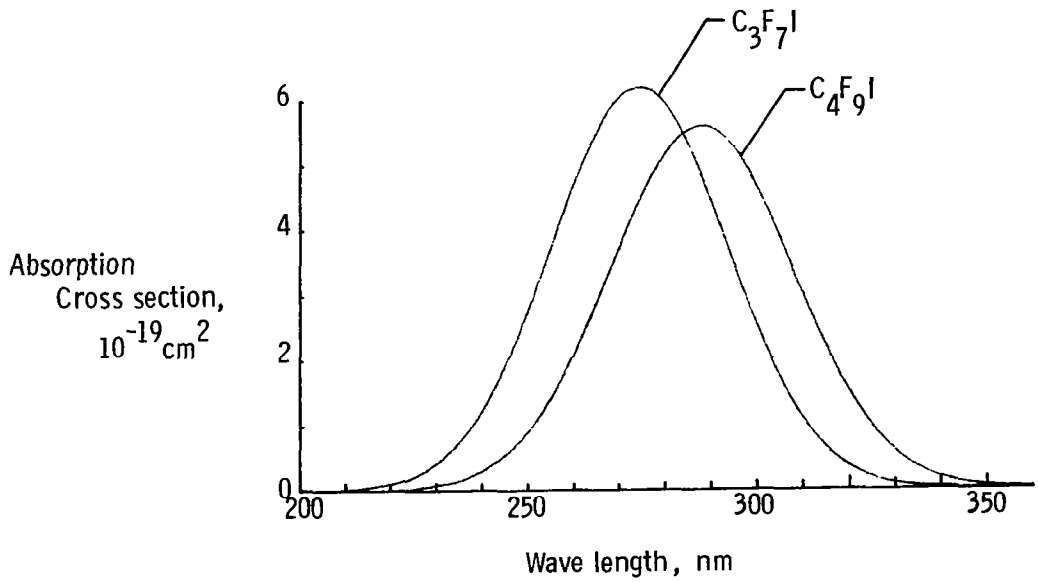

Figure 2

RARE GAS UV FLUORESCENCE

	λ_0, nm	ε_γ, eV	W, eV	η_{rad}, %	η_{laser}, %
Ar_2	126	9.86	27.3	50.5	--
ArF	193	6.44	27.3	33.0	--
Ar_2F	284	4.37	27.3	22.4	3.5
Kr_2	147	8.45	24.9	47.5	--
KrF	249	4.99	24.9	34.0	3.8
Kr_2F	415	2.99	24.9	16.8	--
Xe_2	172	7.22	21.2	47.7	--
XeF	346	3.59	21.2	23.7	--
XeBr	282	4.41	21.2	29.1	4.4
XeI	252	5.65	21.2	37.2	4.4

Figure 3

UV ABSORPTION IN ISOPROPYLIODIDE

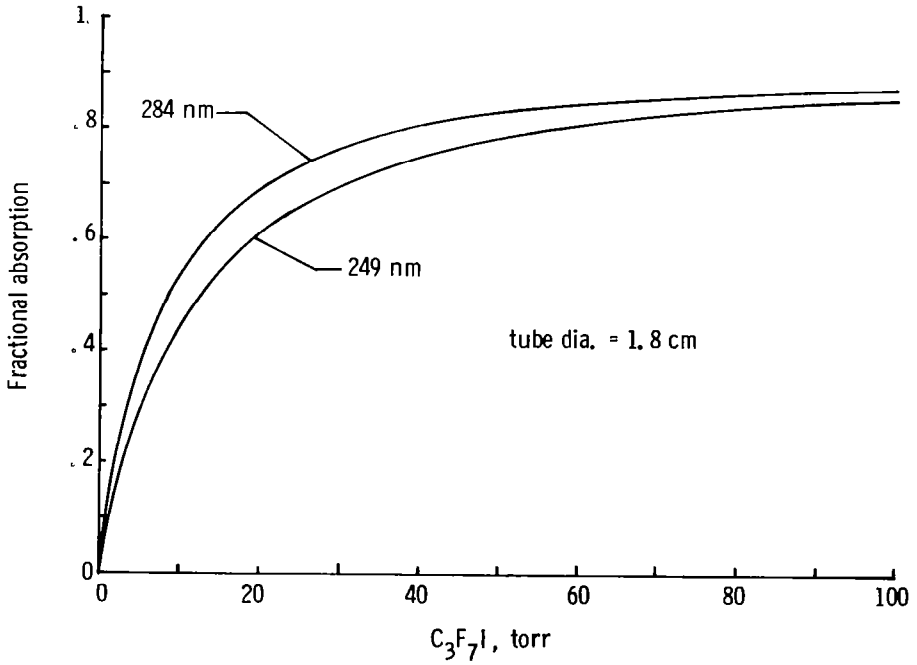

Figure 4

KINETIC PROCESSES

Excitation and Ionization

$$p + X \longrightarrow X^+ + e + p$$
$$\longrightarrow X^* + p$$

Charge Transfer, Penning Ionization, Electron Attachment

$$X^+ + Y \longrightarrow X + Y^+$$
$$X^* + Y \longrightarrow X + Y^+ + e$$
$$e + F_2 \longrightarrow F^- + F$$

Ionic Neutralization

$$Y^+ + F^- \longrightarrow YF^*$$
$$F_2^+ + F^- \longrightarrow 3F$$

Electronic Recombination

$$Y_2^+ + e + M \rightarrow Y^* + M$$
$$Y_2^+ + e + e \rightarrow Y^* + e$$
$$F_2^+ + e \rightarrow 2F$$

Dimerization, Excimer Formation

$$X^+ + Y + M \rightarrow (XY)^+ + M$$
$$X^* + Y + M \rightarrow (XY)^* + M$$

Excitation Transfer

$$X^* + Y \longrightarrow X + Y^*$$

Quenching

$$(XY)^* + M \rightarrow X + Y + M$$

Harpoon

$$ArF^* + Kr \rightarrow KrF^* + Ar$$

Radiative Decay

$$(XF)^* \longrightarrow X + F + h\nu$$

Figure 5

BASIC KINETIC SEQUENCE OF NUCLEAR PUMPED EXCIMERS

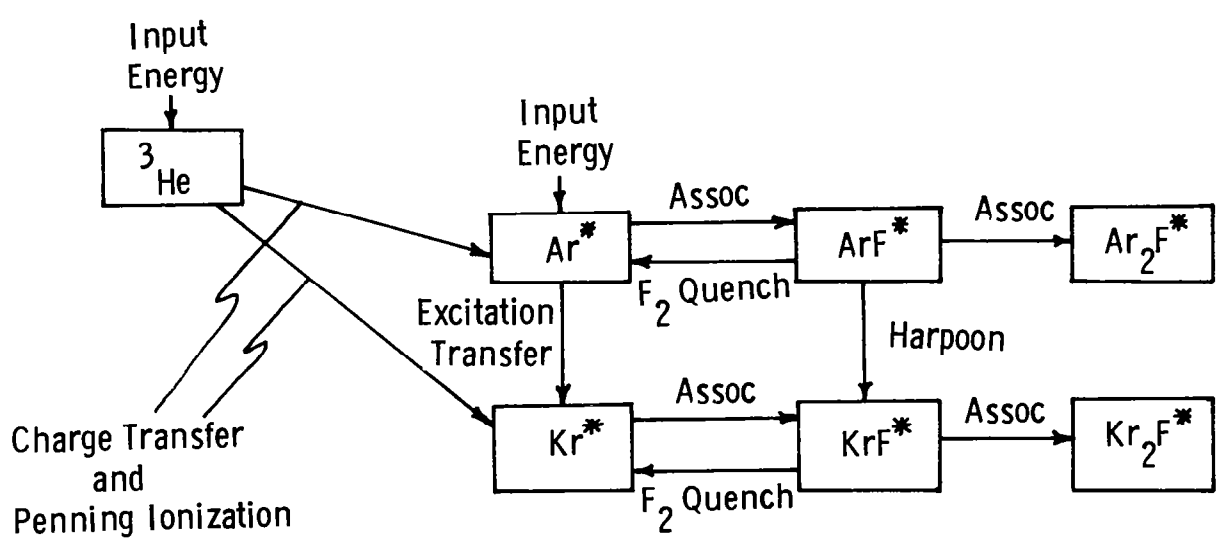

Figure 6

KrF FLUORESCENCE

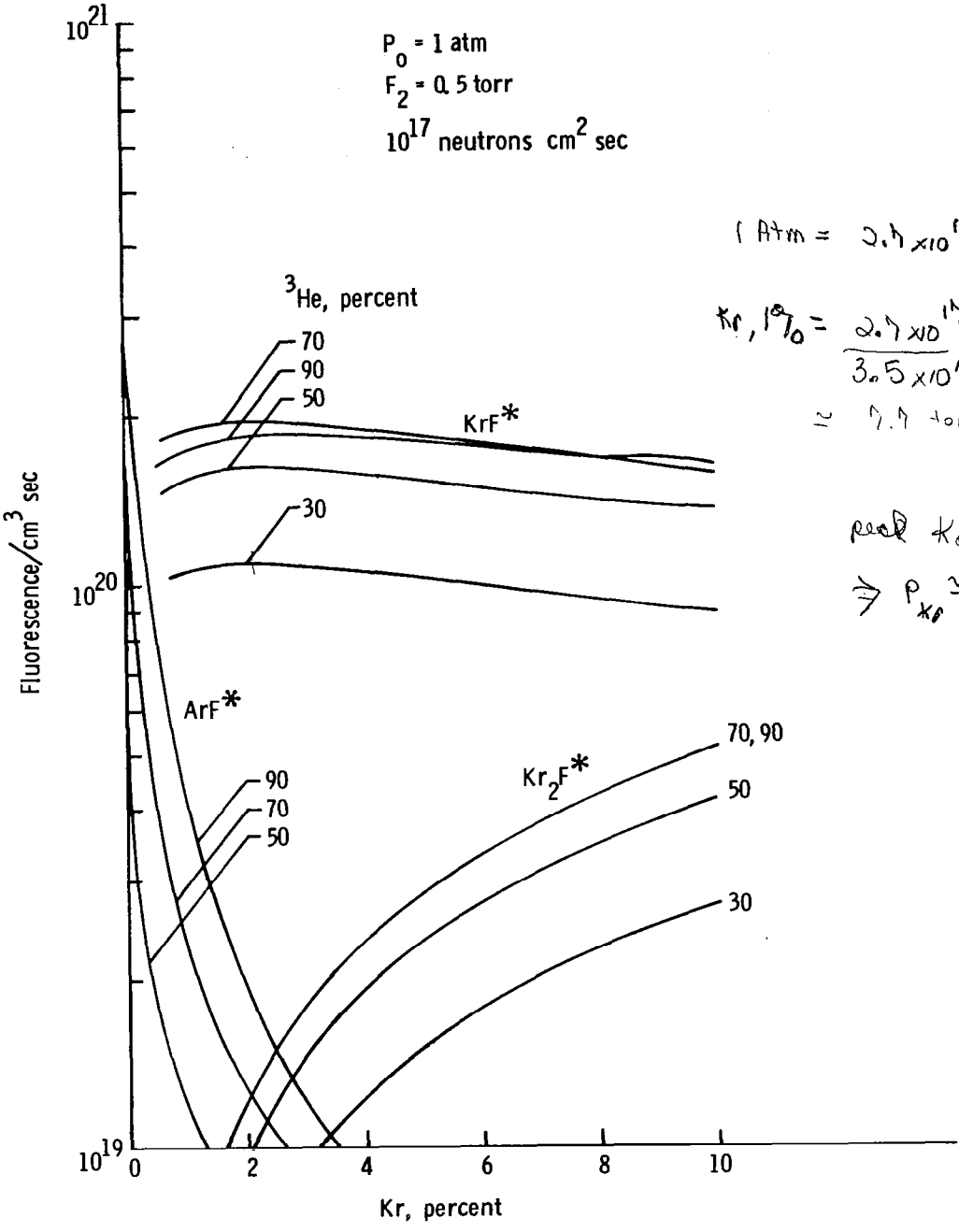

Figure 7

KrF FLUORESCENCE

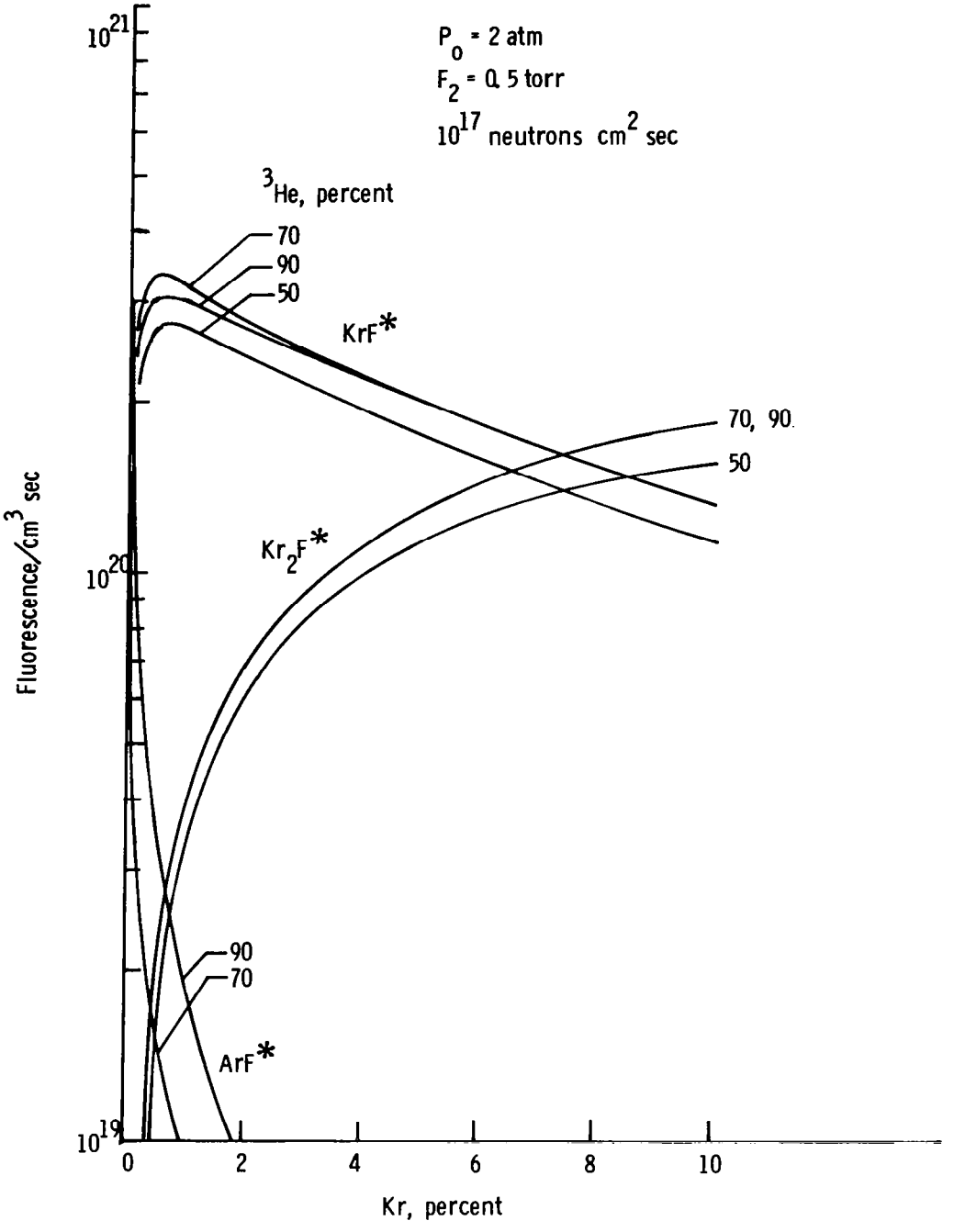

Figure 8

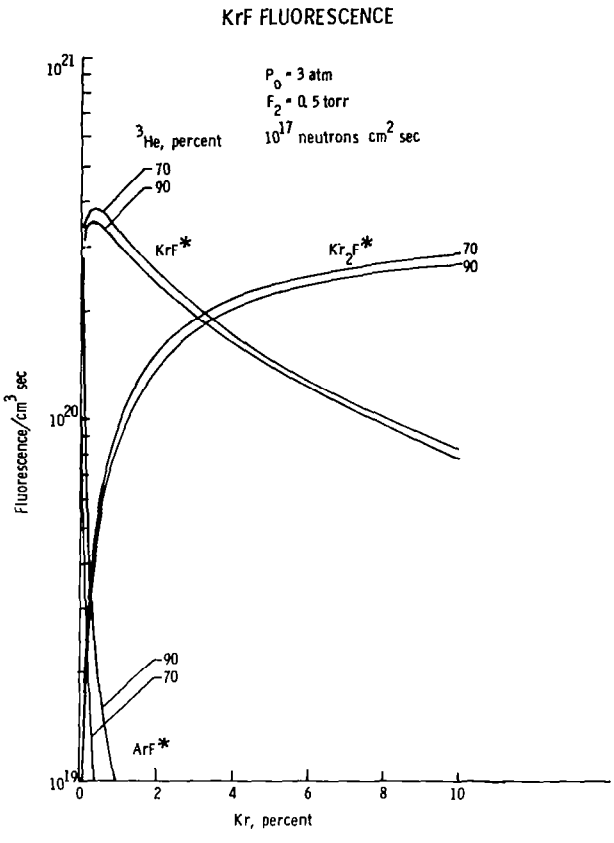

Figure 9

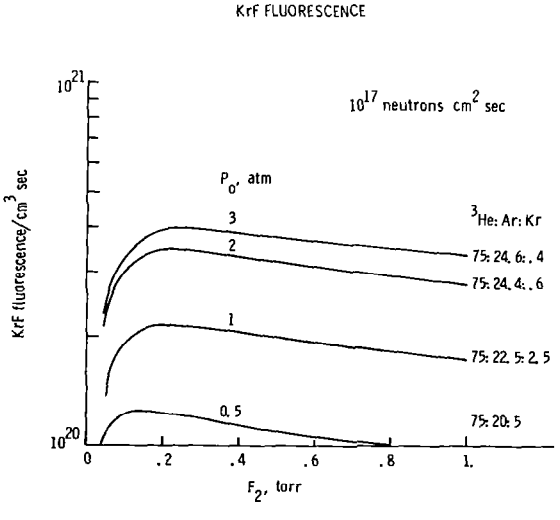

Figure 10

Ar_2F FLUORESCENCE

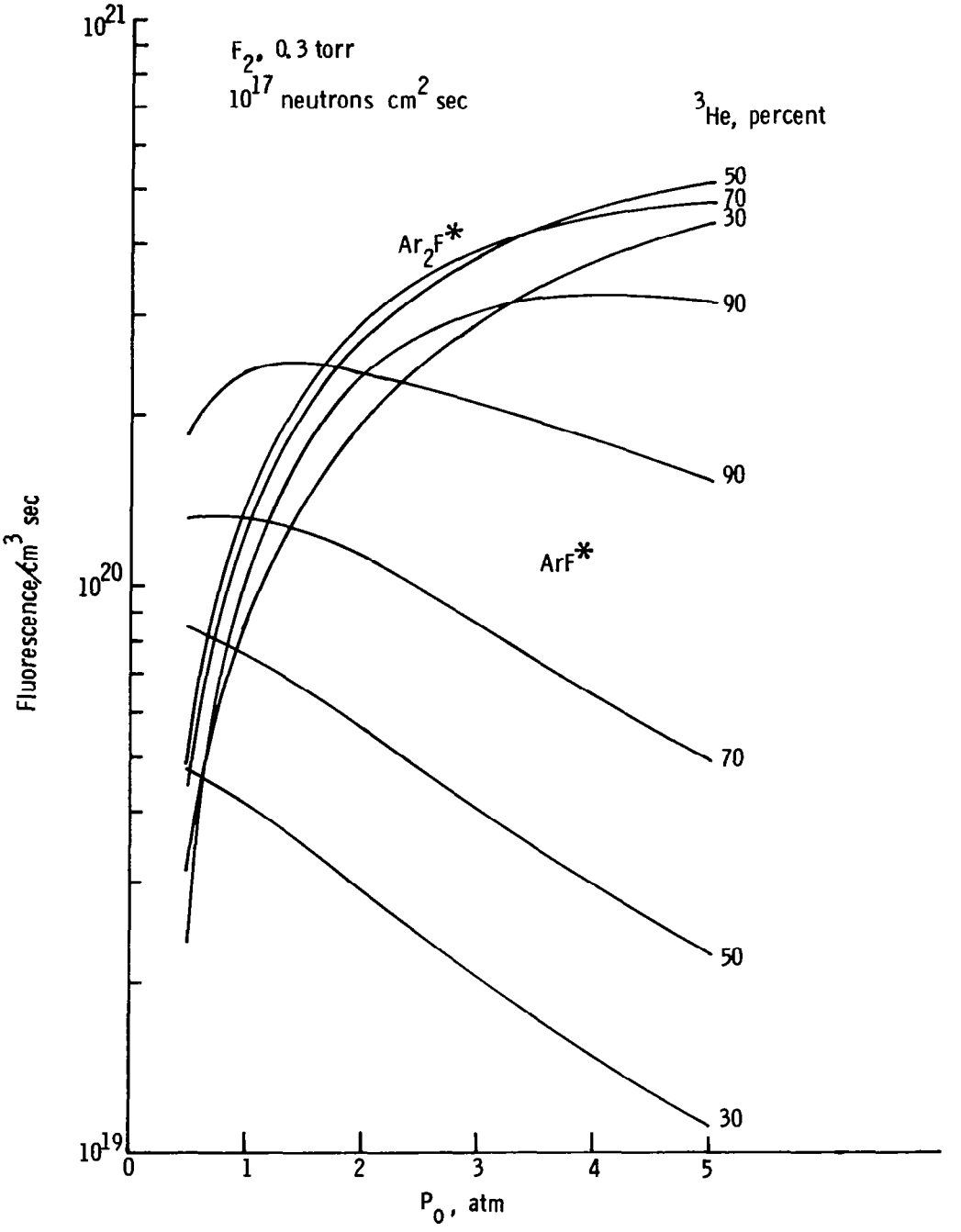

Figure 11

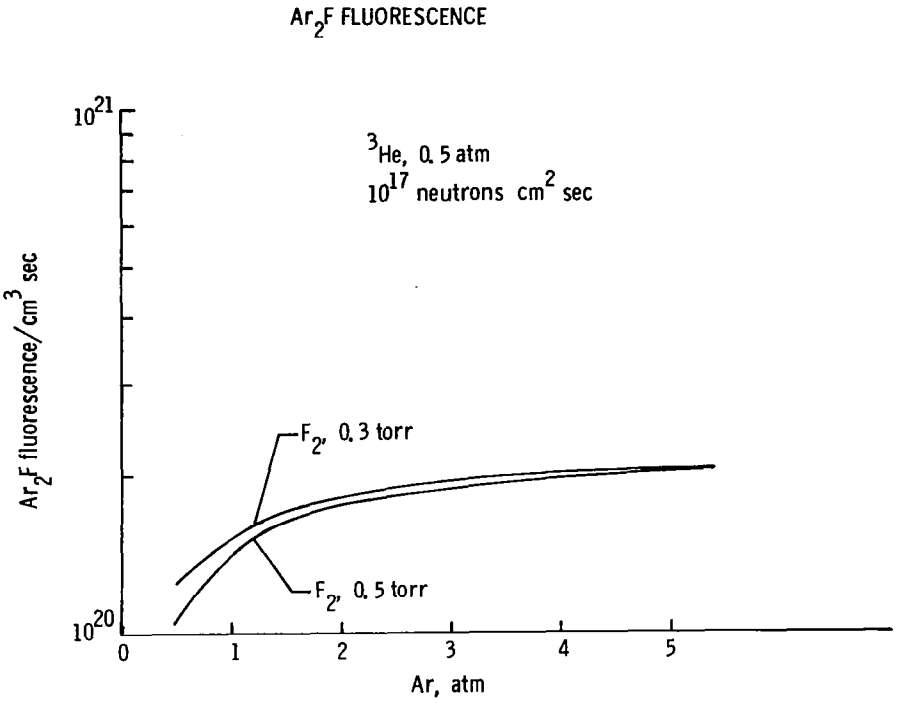

Figure 12

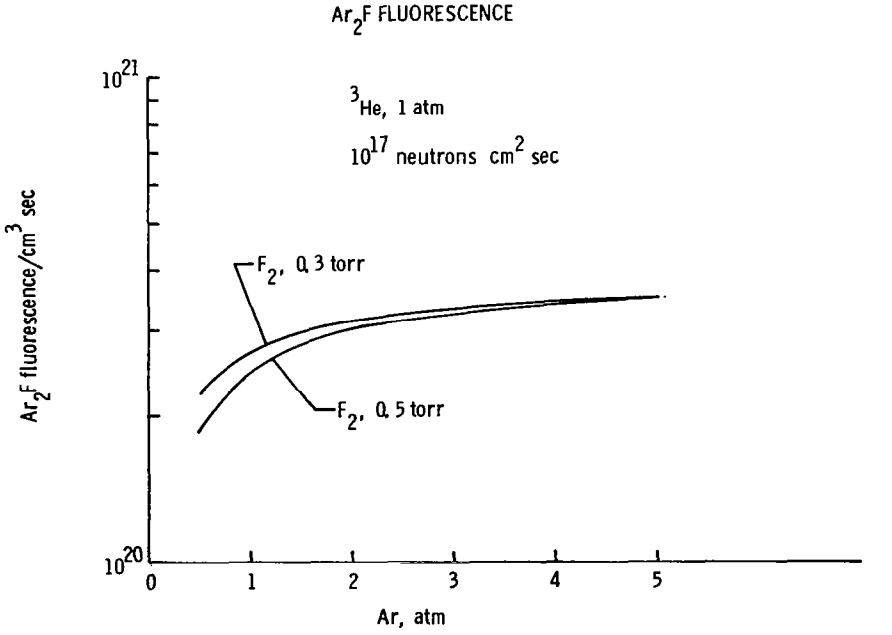

Figure 13

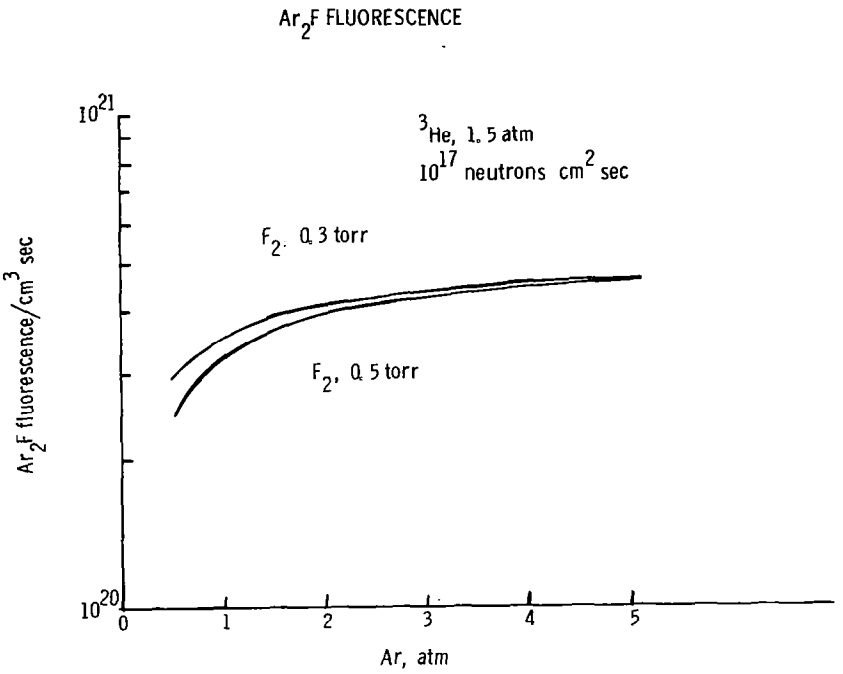

Figure 14

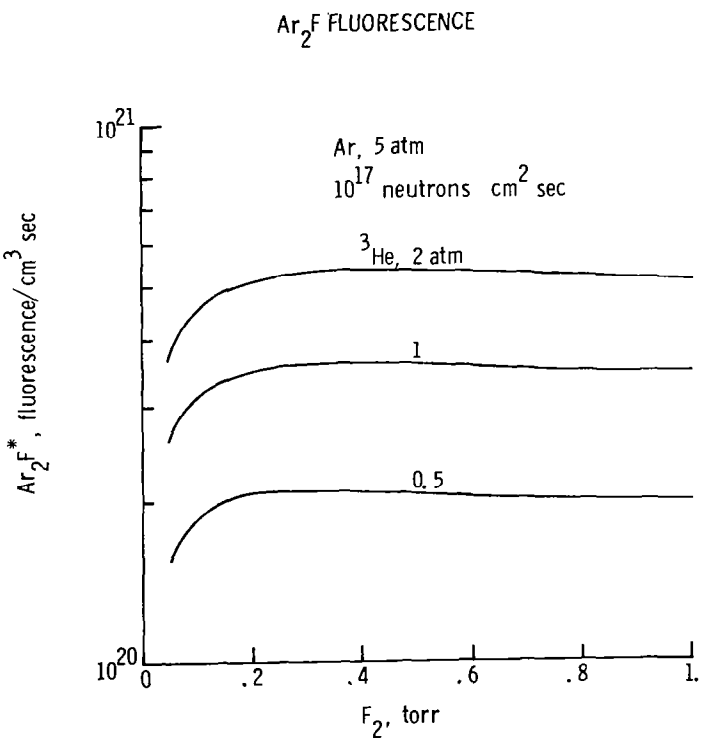

Figure 15

KINETICS OF A CO_2 NUCLEAR PUMPED LASER*

H. A. Hassan**
Mechanical and Aerospace Engineering Department
North Carolina State University, Raleigh, North Carolina 27650

Abstract

A detailed kinetic model is presented for the analysis of a nuclear pumped CO_2-N_2-He laser system. The model assumes that collisional recombination is the dominant pumping mechanism. The results show that, for mixtures typical of those employed in electric discharge systems, the gain coefficients are such that lasing is not expected to take place. On the other hand, concentrations of CO_2 in the range 1/2%-3% are optimal for direct nuclear pumping.

Introduction

Direct nuclear pumping (DNP) was demonstrated in 1975 using a wall source of fission fragments[1,2] and in 1976 using a volume source of fission fragments[3]. Since these developments, such pumping was demonstrated at a number of laboratories using molecular and atomic systems with one notable exception, namely, CO_2. The situation was further complicated by a study[4] of a direct nuclear pumped CO_2 system in which the authors concluded that such a system was not feasible. Upon careful examination of this work it became evident that the authors ignored the dominant pumping mechanism, which is collisional recombination[5,6] and, as such, their conclusions cannot be considered valid.

In principle, there is no obvious reason for such a behavior especially because such a system has been highly successful as an electric discharge laser. Therefore, this work is undertaken with the objective of explaining the mystery surrounding the direct nuclear pumping of CO_2 lasers. To achieve this objective a detailed kinetic model which incorporates all important reactions in a ^3He-N_2-CO_2 mixture is presented. The choice of a volume source of fission fragments, resulting from the $^3He(n,p)^3H$ reaction, ensures more efficient energy utilization. Because the dominant component of the system is ^3He, it is assumed that the energy of the fission fragments, which are protons and tritons, is deposited first into He in the form of ionization and excitation and then is transferred to the excited states of CO_2 by charge transfer, Penning ionization and recombination. This mechanism of nuclear pumping has been substantiated by theory[6] and experiment[5] for a ^3He - Xe system. Because they are essentially thermal[7,8], direct electron excitation is not taken into consideration in this study.

Based on the above model, it is shown that for mixtures representative of electric discharge systems, the gain coefficients are such that lasing is not expected to take place. On the other hand, for a pressure of the order of one atmosphere, and neutron flux of the order of 3×10^{16} n/cm^2 sec, concentrations of CO_2 in the range 1/2% - 3% are optimal for direct nuclear pumping.

* Supported, in part, by NASA Grant NSG 1058.
**Professor, Associate Fellow AIAA.

Analytical Formulation

1. General Considerations

The experimental setup representative of a nuclear pumped laser by a volume source of fission fragments consists of a tube filled with fissionable material and a lasing medium surrounded by a moderator and placed in a fast-burst reactor, Fig. 1. When the thermalized neutrons interact with the fissionable material, high-energy fission fragments are formed and these, together with the primary and secondary electrons, ionize and excite the background gas. When ^3He is used, the fission fragments are protons and tritons with average initial energies of 0.57 Mev and 0.19 Mev, respectively. The electrons are essentially thermal but non-Maxwellian[7,8] and thus the resulting plasma is recombination dominated. This implies that the dominant pumping mechanism is collisional recombination and not electron excitation.

By treating particles in the various excited states as different species, the multifluid conservation equations may be used to describe the plasma generated by the $^3He(n,p)^3H$ reaction. The experimental arrangements of current DNP lasers are such that the steady state approximation, i.e., where the effects of gradients are negligible, is appropriate. As may be seen from Ref. 9, the pressures and temperatures for such experiments are essentially constant and the composition is obtained from the relation

$$R_s = 0 \qquad (1)$$

where R_s is the production rate of species 's' resulting from both nuclear and kinetic processes. To determine R_s one needs to estimate the rates of ionization and excitation of He atoms and the important kinetic processes in the CO_2-N_2-He system. For representative tube diameters (2-3 cm) and pressures of the order of one atmosphere, Wilson and DeYoung derived the following expression for the power density, P_d, released by $^3He(n,p)^3H$ reaction[10]

$$P_d = 9.3 \times 10^{-18}\ p\ f_o\ x_{He}\ (kw/cm^3) \qquad (2)$$

where p is the pressure in atmospheres, f_o is the flux (n/cm^2 sec) of thermal electrons and x_{He} is the ^3He fraction. If one assumes that N_2 and CO_2 concentrations are small, then the energy required to create an excited or ionized state, i.e., the 'w' values, may be approximated by those appropriate for He. Thus, the production rates of He^+ and He* from nuclear sources are obtained by dividing P_d by the appropriate 'w' value.

With the production rates of He^+ and He* from nuclear sources known, the next step is to present the important kinetic processes in the system. Such processes must include pertinent charge transfer, Penning ionization, recombination and V-V and V-T energy transfer.

2. Important Kinetic Processes

In a CO_2-N_2-He nuclear pumped system, there are probably hundreds of kinetic processes that can take place. Because the objective of this work is to determine the range of operating conditions under which nuclear pumping of CO_2 may become possible, no attempt has been made to include all possible products or all known reactions. Thus, the analysis considers twenty-five species and fifty-three simultaneous reactions. It should be noted that the model can be easily expanded to allow for more reaction products and more reactions.

At the high pressures of interest He_2^+ is formed. Rate of the reaction[11]

$$He^+ + 2He \rightarrow He_2^+ + He \qquad (3)$$

ranges from 6.78×10^{-32} to 10.7×10^{-32} cm^6/sec. Because of reaction (3), the reactions included will consist of those of He_2^+, He^+ and He^* with CO_2, N_2 and some of their reaction products together with some mixed reactions.

Charge transfer reactions involving ions with large recombination energies, such as He^+, and polyatomic molecules tend to produce mainly dissociative ion products. Dimer ions, such as He_2^+, have somewhat lower recombination energies and therefore do not cause as much dissociative ionization. Although rates involving charge transfer reactions are known, in most cases the reaction products are not. Thus, certain uncertainties will exist in the kinetic model. On the other hand, Penning ionization tends to populate all the energetically accessible electronic molecular energy levels and consequently, generates emission from a variety of electronic states and vibrational rotational sublevels within a given state[12].

The recent work of Anicich et al.[13] shows that the $He^+ - N_2$ reaction yields 69% atomic ions and 31% molecular ions at a rate of 1.2×10^{-9} cm^3/sec. Thus

$$He^+ + N_2 \rightarrow \begin{cases} N_2^+ + He & (4) \\ N^+ + N + He & (5) \end{cases}$$

On the other hand, flowing after-glow methods[14] give a rate of 1.5×10^{-9} for N_2^+ formation and 1.7×10^{-9} for N^+ formation. The N_2^+ in reaction (4) is currently a subject of some controversy[12]; some believe it is $N_2^+(C^2\Sigma_u^+)$ while others believe it is $N_2^+(B^2\Sigma_u^+)$.

For the sake of simplicity, He^* is identified with the metastable state $He(2^3S)$. Collisions of He_2^+ and $He(2^3S)$ with N_2 yield[15-17]

$$He_2^+ + N_2 \rightarrow N_2^+(B^2\Sigma_u^+) + 2He, \quad [1.1 \times 10^{-9}] \qquad (6)$$

$$He_2^+ + N_2 + He \rightarrow N_2^+(B^2\Sigma_u^+) + 3He, \quad [1.8 \times 10^{-29}] \qquad (7)$$

$$He(2^3S) + N_2 \rightarrow N_2^+(B^2\Sigma_u^+) + He + e, \quad [6.96 \times 10^{-11}] \qquad (8)$$

with the quantities in the square bracket indicating the rates. The ions $N_2^+(C^2\Sigma_u^+)$ and $N_2^+(B^2\Sigma_u^+)$ are converted to their ground states by stimulated and spontaneous emissions and by collisions. Because we are not interested in the nitrogen laser, the N_2^+ ions in the above reactions are treated as ions in their ground state.

A large number of possible states appear when N_2^+ recombines. The literature is very sketchy as to the results of such a recombination. Therefore, it will be assumed that such a process will eventually lead to $N_2^* = N_2(v = 1)$ and to the ground state. The important N_2^+ recombination reactions and their rates are summerized as follows[18-20]:

$$N_2^+ + e \rightarrow N^* + N, \quad [2.2 \times 10^{-7}] \qquad (9)$$

$$N_2^+ + M + e \rightarrow N_2 + M, \quad [10^{-26}] \qquad (10)$$

with M being a third body,

$$N^* + N^* \rightarrow N_2^* + h\nu, \quad [1.6 \times 10^{-19}] \qquad (11)$$

$$N^* + N^* + N_2 \rightarrow N_2^* + N_2, \quad [2.4 \times 10^{-33}] \qquad (12)$$

At high pressures N_4^+ is formed according to the reactions[21]

$$N_2^+ + 2N_2 \rightarrow N_4^+ + N_2, \quad [5.0 \times 10^{-29}] \qquad (13)$$

$$N_2^+ + N_2 + He \rightarrow N_4^+ + He, \quad [1.9 \times 10^{-29}] \qquad (14)$$

and recombines according to the reaction[19]

$$N_4^+ + e \rightarrow N_2 + N_2, \quad [2 \times 10^{-6}] \qquad (15)$$

Again, using the results of Ref. 5, one finds that the major products of $He^+ + CO_2$ are

$$He^+ + CO_2 \rightarrow \begin{cases} CO^+ + O + He, & 77\% \\ O^+ + CO + He, & 18\% \\ C^+ + O_2 + He, & 4\% \end{cases} \qquad (16)$$

with a rate of 1.2×10^{-9} cm^3/sec. Similarly, reactions involving $He_2^+ + CO_2$ yield[15,16]

$$He_2^+ + CO_2 \rightarrow \begin{cases} CO_2^+ + 2He \\ O^+ + CO + 2He, \quad [1.6 \times 10^{-9}] \\ CO^+ + O + 2He \end{cases} \qquad (17)$$

$$He_2^+ + CO_2 + He \rightarrow \begin{cases} CO_2^+ + 3He \\ O^+ + CO + 3He, \quad [6.7 \times 10^{-29}] \\ CO^+ + O + 3He \end{cases} \qquad (18)$$

Parker et al.[22] indicate that the fragment ion produced in highest abundance is expected to be the one whose appearance potential (AP) is nearest to the recombination energy (RE) of the bombarding ion.

In other words, a process for which the energy defect $\Delta E = RE - AP$ is nearest to zero should predominate. For He_2^+ the recombination energy varies over the range 18.3 - 20.3 ev. The appearance potentials of $CO_2^+(A^2\pi_u)$, $(B^2\Sigma_u^+)$, $(C^2\Sigma_g^+)$ are 17.32, 18.08 and 19.40 ev., respectively, while the appearance potential of $O^+(4S_{3/2})$ is 19.39 ev. Similarly, the appearance potential of $CO^+(^2\Sigma_g^+) + O(^3P)$ is 19.56 ev. Thus, all of the products indicated in reactions (17) and (18) are characterized by small ΔE and, therefore, it is difficult to tell which product is dominant.

Penning ionization of CO_2 yields[23]

$$He(2\ ^3S) + CO_2 \rightarrow He + CO_2^+ + e, \quad [8.2 \times 10^{-10}] \qquad (19)$$

Two mechanisms for CO_2^+ recombination will be considered[19]:

dissociative,

$$CO_2^+ + e \rightarrow CO^* + O, \quad [3.8 \times 10^{-7}] \qquad (20)$$

and neutral stabilized,

$$CO_2^+ + e + M \rightarrow CO_2^* + M, \quad [10^{-26}] \qquad (21)$$

It will be assumed that CO_2^* in reaction (21) is $CO_2(10\mathring{0})$ which is the lower laser level. This assumption is prompted by the observation that transitions in CO_2^+ involved mostly symmetric and bending modes[22,24]. It is further assumed that excited N_2 and CO will deposit their energy in the antisymmetric mode of CO_2 which is the upper laser level. All rates involving the vibrational states of CO_2 have the general representation[25]

$$\ln K = A + BT^{-1/3} + CT^{-2/3} \qquad (22)$$

The reactions considered are

$$CO_2(0\mathring{1}0) + M \rightarrow CO_2 + M, \quad M = CO_2,\ N_2, CO,\ He \qquad (23)$$

$$CO_2(02\mathring{0}, 10\mathring{0}) + M \rightarrow CO_2(0\mathring{1}0) + M, \quad M = CO_2,\ N_2,\ CO \qquad (24)$$

$$CO_2(00\mathring{1}) + M \rightarrow CO_2(02\mathring{0}, 10\mathring{0}) + M, \quad M = CO_2,\ N_2, CO \qquad (25)$$

$$CO_2(00\mathring{1}) + CO_2 \rightarrow CO_2(02\mathring{0}, 10\mathring{0}) + CO_2(0\mathring{1}0) \qquad (26)$$

$$CO_2(00\mathring{1}) + N_2 \rightleftarrows CO_2 + N_2(v = 1) \qquad (27)$$

$$CO_2(00\mathring{1}) + CO \rightleftarrows CO_2 + CO(v = 1) \qquad (28)$$

Other reactions employed in the kinetic model and their respective rates are as follows[14,19]:

$$He^+ + O_2 \rightarrow He + O^+ + O, \quad [1.5 \times 10^{-9}] \qquad (29)$$

$$O^+ + CO_2 \rightarrow O_2^+ + CO, \quad [1.2 \times 10^{-9}] \qquad (30)$$

$$C^+ + CO_2 \rightarrow CO^+ + CO, \quad [1.9 \times 10^{-9}] \qquad (31)$$

$$CO^+ + CO_2 \rightarrow CO_2^+ + CO, \quad [1.1 \times 10^{-9}] \qquad (32)$$

$$N_2^+ + CO \rightarrow CO^+ + N_2, \quad [0.7 \times 10^{-10}] \qquad (33)$$

$$N_2^+ + CO_2 \rightarrow CO_2^+ + N_2, \quad [9 \times 10^{-10}] \qquad (34)$$

$$N^+ + CO \rightarrow CO^+ + N, \quad [5 \times 10^{-10}] \qquad (35)$$

$$N^+ + CO_2 \rightarrow CO_2^+ + N, \quad [1.3 \times 10^{-9}] \qquad (36)$$

$$O_2^+ + e \rightarrow O + O, \quad [2.1 \times 10^{-7}] \qquad (37)$$

$$O_2^+ + e + M \rightarrow O_2 + M, \quad [10^{-26}] \qquad (38)$$

$$CO^+ + e + M \rightarrow CO^* + M, \quad [10^{-26}] \qquad (39)$$

$$O + O + M \rightarrow O_2 + M, \quad [3 \times 10^{-33}] \qquad (40)$$

$$O + CO + M \rightarrow CO_2 + M, \quad [10^{-31}] \qquad (41)$$

The rate quoted for reaction (41) is that appropriate for NO. A value of 10^{-32} was also employed in the calculations with minor effects on the gain coefficients for CO_2 concentrations $\geq$ 1%.

3. Gain and Power Calculations

If the rotational levels are in equilibrium at a temperature T, the gain coefficient for a single P-branch transition J of the $CO_2(00\mathring{1}) - CO_2(10\mathring{0})$ band can be written as[26]

$$\gamma = \frac{\lambda^2}{4\pi} \frac{hc}{kT} (2J - 1) A_{u\ell} (s_u n_u - s_\ell n_\ell) g(0) \qquad (42)$$

where

$$s_u = B' \exp[-h_c B' J(J - 1)/kT] \qquad (43)$$

$$s_\ell = B \exp[-h_c BJ(J + 1)/kT] \qquad (44)$$

λ is the wave length, h is Planck's constant, k is Boltzmann's constant, c is the speed of light, $A_{u\ell}$ is Einstein coefficient for spontaneous emission from the upper to the lower laser level, n_u and n_ℓ are the number densities and B' and B are the rotational constants[27] of the upper and lower levels. The quantity g(0) is the shape factor. For the pressures required for DNP, homogeneous broadening is dominant and thus

$$g(0) = 2/\pi\Delta\nu \qquad (45)$$

where

$$\Delta\nu = \frac{1}{\pi} \Sigma\, n_i \sigma_i \left[\frac{8kT}{\pi}\left(\frac{1}{m_{CO_2}} + \frac{1}{m_i}\right)\right]^{1/2} \qquad (46)$$

n_i is the number density, σ_i is the collision cross section and m_i is the particle mass of species i.

The gain coefficient can be calculated after a solution of the governing equations, i.e., Eqs. (1), is achieved. On the other hand, the power output depends on the cavity employed. Moreover, the

kinetic model has to be supplemented by the reaction

$$CO_2(00^01) + h\nu \rightarrow CO_2(10^00) + 2h\nu, \quad \nu = c/\lambda \qquad (47)$$

The above reaction contributes - $\gamma I/h\nu$ and $\gamma I/h\nu$, respectively, to the production rates of $CO_2(00^01)$ and $CO_2(10^00)$ where I is the intensity. To calculate I an additional relationship is required and this is provided by the threshold condition

$$\gamma = - \ell n(r_1 r_2)/2L \qquad (48)$$

where r_1 and r_2 are the reflectivities of the mirror and L is the length of the cavity.

The calculation of I requires the simultaneous solutions of Eqs. (1), (42) and (48). To calculate the total power output, one needs to determine the manner in which the intensity varies with area. If the beam is Gaussian, then, for all practical purposes, an area whose diameter is three times the spot size will pass all beam power. Thus

$$P = \pi(3w_s/2)^2 I_t \qquad (49)$$

where P is the power output, I_t is the transmitted intensity and w_s is the spot size

$$w_s = (b\lambda/\pi)^{1/2} \qquad (50)$$

where b is the equivalent confocal radius. Of course, if the beam is not Gaussian, a different area will have to be employed.

Results and Discussion

Calculations were carried out for various mixtures, pressures and fluxes for a single cavity of length 60 cm and mirror reflectivities of 1.0 and 0.99. The radii of curvature were assumed equal to two meters. It is also assumed that for the $He_2^+ + CO_2$ reaction 90% of the ions are CO_2^+, 5% O^+ and 5% CO^+. Unless indicated otherwise, the pressure is one atmosphere and the neutron flux is 3×10^{16} n/cm^2 sec.

One of the most important assumptions made in the kinetic model is that the neutral stabilized recombination of CO_2^+, reaction (21), yields the lower laser level $CO_2(10^00)$. It turned out that, for all the CO_2 concentrations considered, $\geq$ 1/2%, CO_2^+ was the dominant ion. Thus, this assumption yields conservative estimates of the gain coefficient and power output.

Figures 2 and 3 show the effects of CO_2 concentration on gain and power output. It is seen that in both cases there is an optimum concentration where the gain or power output is optimum. This can be traced to the fact that the upper laser level increases with CO_2 concentration and with $N_2(v = 1)$. Because the total fraction of CO_2 and N_2 is fixed for this calculation, an optimum mix must exist. The effect of N_2 on gain and power output is indicated in Figs. 4 and 5 for a fixed CO_2 fraction. In spite of the fact that the power deposition is decreased with increasing N_2 fraction, $N_2(v = 1)$ increases and this would suggest more pumping for the upper laser level. However, because of the pressure employed, reaction (27) is, in effect, in equilibrium. Thus, the decrease in both the gain coefficient and power output is a result of reaction (25) which indicates increased depletion of $CO_2(00^01)$ with increased N_2.

Figures 6 and 7 show the effects of pressure on the gain coefficient and power output. For pressures of about 1.8 atmosphere and higher, the power output is zero because the gain coefficient is less than the threshold gain for the cavity and operating conditions considered. As is seen in Figs. 8 and 9 both the gain coefficient and power output increase with neutron flux. The power deposition is proportional to the pressure and neutron flux; thus, both parameters have similar effects on power deposition. However, their individual effects on the gain coefficient and the power output are quite different. Increasing the power deposition will result in increased ionization and excitation and this will result in increasing the upper laser level. Thus, if this is achieved by increasing the neutron flux, then this will result in increased gain coefficient and power output. On the other hand, if this is achieved by increasing the pressure, then increased frequency of collisions will depopulate the upper level. Also, neutral stabilized recombination of CO_2^+, which increases with pressure, will result in increased population of the lower laser level. Thus, for a given mixture, there is an optimum pressure at which the gain is optimum and a different pressure at which the power output is optimum. Evidently, the peak gain for the case indicated in Fig. 6 takes place at a pressure lower than half of an atmosphere.

Concluding Remarks

The results presented here indicate that mixtures for optimum gain and power output are quite different from those employed in electric discharge lasers. This is expected because the excitation mechanisms in both cases are quite different. The gain coefficients and laser power outputs are in general lower than corresponding quantities for electric discharge lasers. One of the attractive features of direct nuclear pumping is that one can excite large (of the order of a neutron mean free path) high pressure volumes. When cavities of such dimensions are employed increased power output will result.

References

[1] McArthur, D. A. and Tollefsrud, P. B., "Observation of Laser Action in CO Gas Excited Only by Fission Fragments," Applied Physics Letters, Vol. 26, Feb. 1975, pp. 187-190.

[2] Helmick, H. H., Fuller, J. L. and Schneider, R. T., "Direct Nuclear Pumping of a Helium-Xenon Laser," Applied Physics Letters, Vol. 26, March 1975, pp. 327-328.

[3] Jalufka, N. W., DeYoung, R. J., Hohl, F. and Williams, M. D., "A Nuclear Pumped $^3He - A_r$ Laser Excited by the $^3He(n,p)^3H$ Reaction," Applied Physics Letters, Vol. 29, Aug. 1976, pp. 188-190.

[4] Andriyakhin, V. M., Vasil'tsov, V. V., Krasil'nikov, S. S. and Pis'mennyi, V. D., "Nuclear Pumping in Molecular Gas Lasers," Soviet Physics JETP, Vol. 36, No. 5, May, 1973, pp. 865-869.

[5]DeYoung, R. J., Jalufka, N. W. and Hohl, F., "Direct Nuclear-Pumped Lasers Using the $^3He(n,p)^3H$ Reaction," AIAA Journal, Vol. 16, No. 9, Sept. 1978, pp. 991-998.

[6]Deese, J. E. and Hassan, H. A., "Direct Nuclear Pumping by a Volume Source of Fission Fragments," AIAA Journal, Vol. 16, No. 10, Oct. 1978, pp. 1030-1034.

[7]Hassan, H. A. and Deese, J. E., "Electron Distribution Function in a Plasma Generated by Fission Fragments," The Physics of Fluids, Vol. 11, No. 12, Dec. 1976, pp. 2005-2011.

[8]Deese, J. E. and Hassan, H. A., "Distribution functions in Plasmas Generated by a Volume Source of Fission Fragments," The Physics of Fluids, Vol. 22, No. 2, Feb. 1979, pp. 257-262.

[9]Deese, J. E. and Hassan, H. A., "Analysis of Nuclear Induced Plasmas," AIAA Journal, Vol. 14, No. 11, Nov. 1976, pp. 1589-1597.

[10]Wilson, J. W. and DeYoung, R. J., "Power Density in Direct Nuclear-Pumped ^3He Lasers," Journal of Applied Physics, Vol. 49, No. 3, March, 1978, pp. 980-988.

[11]Chen, C. H., Judish, J. P. and Payne, M. G., "Charge Transfer and Penning Ionization of N_2, CO, CO_2, and H_2S in Proton Excited Helium Mixtures," The Journal of Chemical Physics, Vol. 67, No. 7, Oct. 1977, pp. 3376-3381.

[12]Bowers, M. T. and Laundenslager, J. B., "Thermal Energy Ion-Molecule Interactions," in Principles of Laser Plasmas, Edited by G. Bekefi, Wiley-Interscience, New York, 1976, pp. 89-124.

[13]Anicich, V. G., Laudenslager, J. B. and Huntress, W. T., Jr., "Product Distributions for Some Thermal Energy Charge Transfer Reactions of Rare Gas Ions," The Journal of Chemical Physics, Vol. 67, No. 10, Nov. 1977, pp. 4340-4350.

[14]Massey, H. S. W., Electronic and Ionic Impact Phenomena, Vol. 3, Oxford, London, 1971, pp. 2061-2063.

[15]Lee, F. W., Collins, C. B. and Waller, R. A., "Measurement of the Rate Coefficients for the Bimolecular and Termolecular Charge Transfer Reactions of He_2^+ with Ne, A_r, N_2, CO, CO_2 and CH_4," The Journal of Chemical Physics, Vol. 65, No. 5, Sept. 1976, pp. 1605-1615.

[16]Bohme, D. K., Adams, N. G., Mosesman, M., Dunkin, D. B. and Ferguson, E. E., "Flowing Afterglow Studies of the Reactions of the Rare-Gas Molecular Ions He_2^+, Ne_2^+ and $A_{r_2}^+$ with Molecules and Rare-Gas Atoms," The Journal of Chemical Physics, Vol. 52, No. 10, May 1970, pp. 5094-5101.

[17]Schmeltekopf, A. L. and Fehsenfeld, F. C., "De-excitation Rate Constants for Helium Metastable Atoms With Several Atoms and Molecules," The Journal of Chemical Physics, Vol. 53, No. 8, Oct. 1970, pp. 3173-3177.

[18]Kasner, W. H. and Biondi, M. A., "Electron-Ion Recombination in Nitrogen," The Physical Review, Vol. 137, No. 2A, Jan. 1965, pp. A317-A329.

[19]Bartner, M. H. and Baurer, T., (Eds.), Defense Nuclear Agency Reaction Rate Handbook Series, Dept. of Defense Information and Analysis Center, General Electric Co., Santa Barbara, California, 1972. Chapters 16 and 18.

[20]Delcroix, J. L., Ferreira, C. M. and Ricard, A., "Metastable Atoms and Molecules in Ionized Gases," in Principles of Laser Plasmas, Edited by G. Bekefi, Wiley-Interscience, New York, 1976, pp. 159-233.

[21]Bohme, D. K., Dunkin, D. B., Fehsenfeld, F. C. and Ferguson, E. E., "Flowing Afterglow Studies of Ion-Molecule Association Reactions," The Journal of Chemical Physics, Vol. 51, No. 3, Aug. 1969, pp. 863-872.

[22]Parker, J. E., Milner, R. G. and Robertson, A. M., "Energy Transfer and Primary Product Ion Excitation in He^+/CO_2 and H_2^+/CO_2 Charge-Transfer Collisions," International Journal of Mass Spectrometry and Ion Physics, Vol. 24, 1977, pp. 429-445.

[23]Riola, J. P., Howard, J. S., Rundel, R. D. and Stebbings, R. F., "Chemionization Reactions Involving Metastable Helium Atoms," Journal of Physics B: Atomic and Molecular Physics, Vol. 7, Feb. 1974, pp. 376-385.

[24]Ajello, J. M., Emission Cross Sections of CO_2 by Electron Impact in the Interval 1260-4500A°, II," The Journal of Chemical Physics, Vol. 55, No. 7, Oct 1971, pp. 3169-3177.

[25]Blauer, J. A. and Nickerson, G. R., "A Survey of Vibrational Relaxation Rate Data for Processes Important to CO_2-N_2-H_2O Infrared Plume Radiation," AIAA Paper No. 74-536, June 1974.

[26]Cool, T. A., "Power and Gain Characteristics of High Speed Flow Lasers," Journal of Applied Physics, Vol. 40, No. 9, Aug. 1969, pp. 3563-3573.

[27]Herzberg, G., Molecular Spectra and Molecular Structure, II. Infrared and Raman Spectra of Polyatomic Molecules, 1st ed., Van Nostrand, New York, 1945, p. 395.

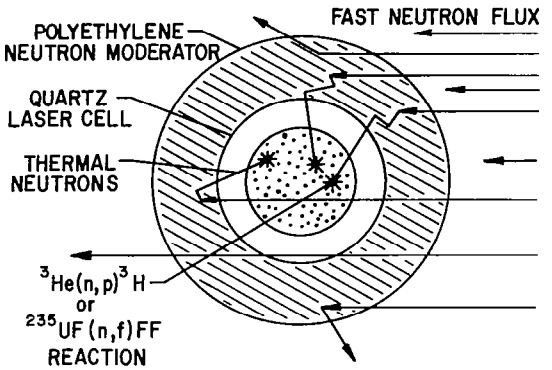

Fig. 1. Schematic of a Nuclear Pumped Laser

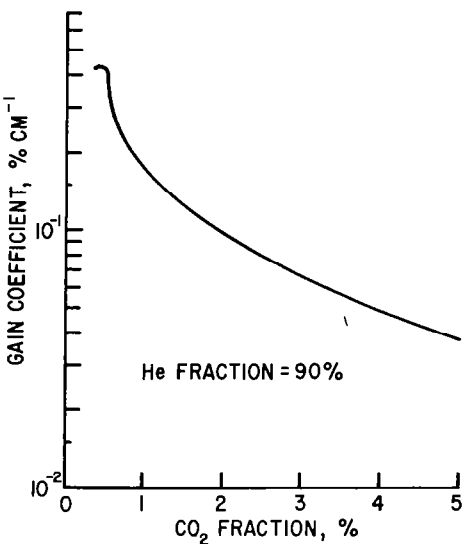

Fig. 2. Effect of CO_2 Fraction on Gain Coefficient

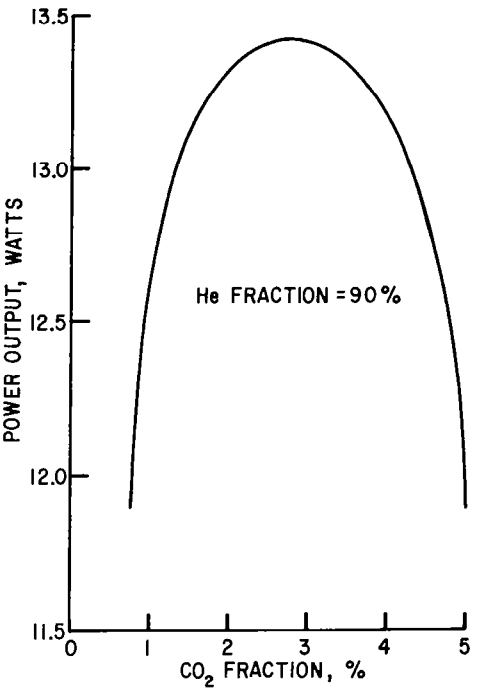

Fig. 3. Effect of CO_2 Fraction on Power Output

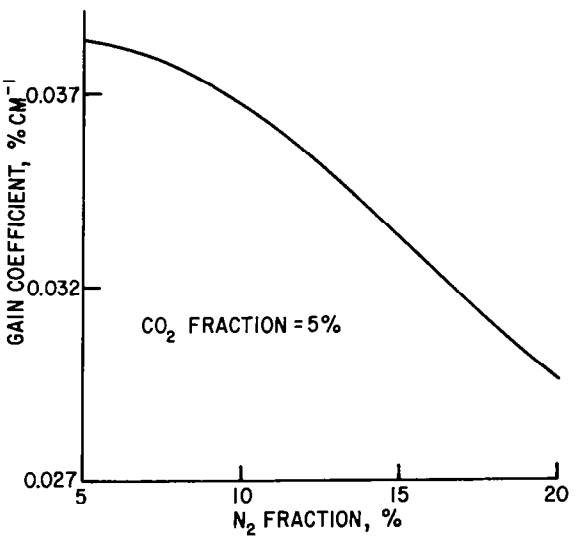

Fig. 4. Influence of Nitrogen on Gain Coefficient

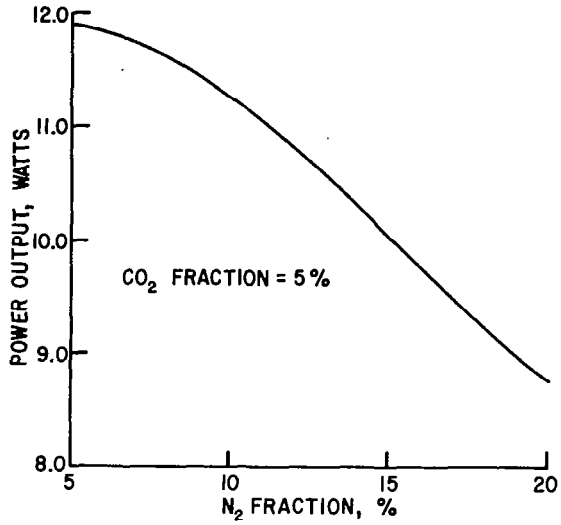

Fig. 5. Influence of Nitrogen on Power Output

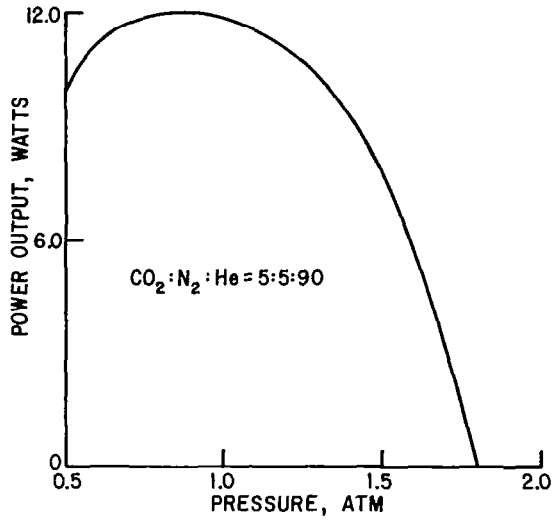

Fig. 7. Influence of Pressure on Power Output

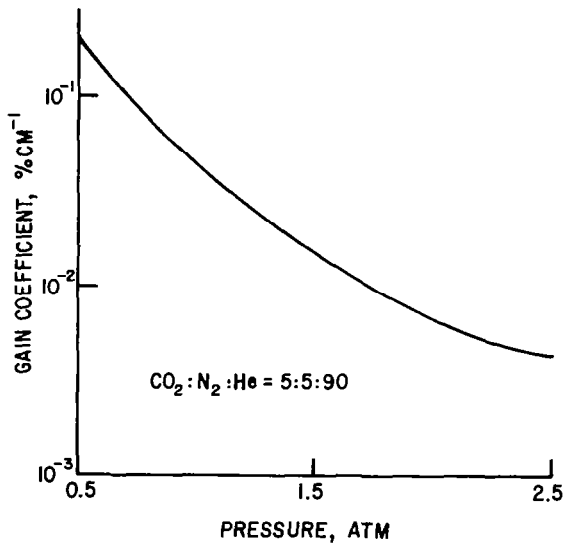

Fig. 6. Influence of Pressure on Gain Coefficient

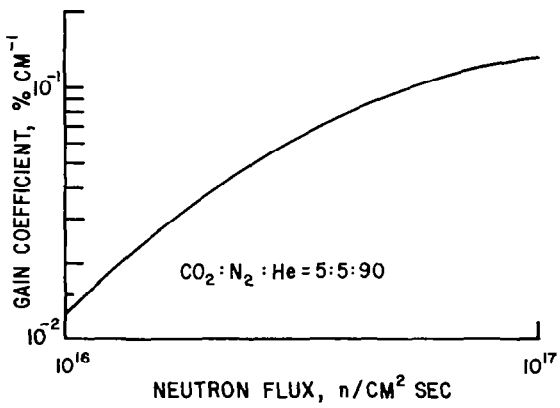

Fig. 8. Influence of Neutron Flux on Gain Coefficient

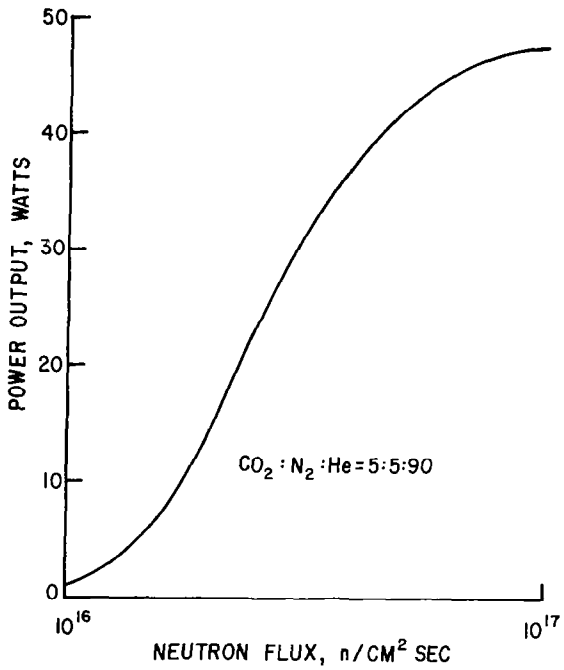

Fig. 9. Influence of Neutron Flux on Power Output

Reprint of AIAA Paper 79-1566.

NUCLEAR PUMPED LASER RESEARCH AT THE JET PROPULSION LABORATORY

by

Gary R. Russell
Jet Propulsion Laboratory
Pasadena, CA 91103

A. Nuclear-Electric Iodine Laser

Data have been obtained using a partially nuclear excited xenon flashlamp to pump an iodine laser. The laser consists of an inner quartz tube 2.7 cm in diameter and 30 cm in length filled with CF_3I circumscribed by a coaxial xenon flashtube 4.9 cm in diameter, also 30 cm in length. Strips of uranium (^{235}U), spot welded to stainless steel foil, are placed around the inner circumference of the outer quartz tube with a separation, in the axial direction, between strips of 1.3 cm to allow an axial electrical discharge in the outer annular region of the flashtube. The laser assembly is surrounded by a polyethylene moderator. Laser energy at 1.315 μ is coupled out of the central laser tube through a 1% transmitting MLD mirror through a notch filter (1.3 ± .05 μ) and detected by a germanium detector. Thermal neutron pulses of about 200 μs (FWHM) duration are obtained from the LASL Godiva IV fast burst reactor.

The laser was operated at a CF_3I lasant pressure and xenon flashtube pressure of 50 and 725 torr respectively. The Godiva (ΔT) was varied between 175 and 284°C. The flashlamp electrical power supply capacitance and voltage were held constant at 15 μF and 3.5 kV respectively. Both CF_3I and xenon were supplied to the laser test section by a remote controlled gas handling system that was positioned adjacent to the Godiva reactor and laser during test operations. The electrical discharge

was triggered by the increase in electrical conductivity in the xenon flashtube, and generally occurred about 100 μs after the peak of the thermal neutron pulse. Analysis of the laser pulse shapes, with and without nuclear flashlamp augmentation, indicated that the deposition of nuclear energy is equally as effective as electrical energy deposition in producing laser pulse energy output.

Future work will consist of tests of direct nuclear and electrical pumping of lasants containing a mixture of CF_3I, Xe, and ^3He. No external flashlamp will be used. Nuclear pumping will be attained with the use of ^3He instead of uranium foils because of possible contamination of the foils by the CF_3I.

B. E-beam Pumping of High Pressure CF_3I

An experiment has been initiated to measure amplification at 1.315 μ of E-beam pumped CF_3I at pressures of several atmospheres. The experimental set-up consists of a Febetron 706 E-beam machine operating at 500 keV having a pulse width of 3 ns, an E-beam laser test section, and a coaxial photodissociation iodine laser which is used for amplification measurements.

The iodine laser is 30 cm in length and 1 cm in diameter with an output mirror transmission of 5%. The coaxial flashlamp is operated with argon at a pressure of 200 torr, and power supply capacitance and voltage of 60 μF and 3 kV respectively. The iodine laser pulse width varies from 50 to 100 μs.

The E-beam is triggered to fire at the beginning of the iodine laser pulse. The laser signal is transmitted through a beam splitter where a part of the signal is transmitted through the E-beam laser test section. The remaining laser signal and the amplified signal are recorded simultaneously on an oscilloscope.

Preliminary data taken at a CF_3I pressure of one atmosphere show that, for a part of the iodine laser pulse, amplification of almost a factor of two is measured. Since the gain length in the E-beam laser test section is about 1-2 cm

and the coaxial laser gain length is 30 cm, the measurements indicate that the gain in the E-beam pumped CF_3I is an order of magnitude greater than in the coaxial laser tube.

Future research will consist of tests conducted at CF_3I pressures ranging from pressures of 0.1 to several atmospheres. In addition, data will be obtained varying the CF_3I partial pressure in a background buffer gas consisting of helium-xenon mixtures to simulate future nuclear pumped laser tests where ^3He will be used as a source of nuclear energy.

DETERMINATION OF THE EFFICIENCY OF PRODUCTION OF EXCITED ELECTRONIC STATES USING γ-RAY AND FISSION FRAGMENT PUMPING

by

W. M. Hughes, J. F. Davis, W. B. Maier,
R. F. Holland and W. L. Talbert, Jr.

We are conducting experiments to determine two of the key issues of a high energy nuclear pumped laser which utilizes fission of volumetrically dispersed ^{235}U to excite the medium. The two key issues are: (1) the efficiency of conversion of fission fragment kinetic energy to visible light output, and (2) the optical quality of the excited media.

Initial considerations of laser systems that might meet these requirements indicated that "typical" gaseous excimer laser systems have serious limitations. For example, a self-critical XeF^* laser using volumetrically dispersed UF_6 is virtually impossible because of optical absorption and short radiative lifetime (even when no collisional relaxation is invoked).

The recent demonstration of the solubility of UF_6 in liquified rare gases and the determination of many of the properties of the rare gas halide trimers and rare gas group VI dimers allow for the possibility of attaining a true high energy high efficiency nuclear pumped laser system. Liquid rare gas media offer a number of advantages including high heat capacity, reduced collisional relaxation of electronic excited states (because of inhibited motion), increased vibrational and rotational relaxation, collisional enhancement of some metastable electronic states and enhancement of preferred kinetic pathways (compared to gas phase). Kinetic considerations indicate that net efficiencies on the order of 10% are possible for production of visible light output.

Experiments have been conducted in gaseous and liquified xenon using both γ-ray and fission fragment pumping. Light output from the xenon excimer has been monitored in the VUV at ∿173 nm by an absolutely calibrated photon detection system. The xenon emission is being monitored in order to determine the efficiency of production of the rare gas excited states (all of the rare gases are predicted to act similarly) since these states are the direct precursors to the visible emitting systems proposed. The energy input was determined using γ-ray and fission fragment calorimeters. The efficiency thus determined is on an energy output divided by an energy input basis and utilizes no kinetic model to interpret the data. The preliminary efficiency results thus determined were found to be ∿50% for γ-ray pumping in gaseous and liquified xenon and >20% for fission fragment pumping of gaseous xenon. Fission fragment pumping of liquified xenon is being investigated at present. Spectral data taken for both gaseous and liquified xenon indicate that the spectral emission is only from Xe_2^*.

Calculations indicate that the proposed systems can reach laser threshold using either the GODIVA IV or SKUA burst facilities. If the theoretical treatment proves to be correct one can anticipate kilojoule operation using the SKUA burst facility which will be operational late this calendar year.

EXPERIMENTAL NUCLEAR PUMPED LASER SIMULATIONS*

W. E. Wells
Department of Physics
Miami University
Oxford, Ohio 45056

At Miami University the problems of Nuclear Pumped Lasers are being investigated by studies in four areas:

Electron-Ion Recombination,
NPL Plasma Simulations,
Excited State-UF_6 reactions (flowing afterglow),
and New Lasers and Laser Processes.

Electron-Ion Recombination

Almost all, if not all, of the NPL's discovered to date depend on recombination as a principal means of population. Electron-Ion recombination for molecules is generally of the form

$$M_2 + e \rightarrow M^* + M$$

This type of reaction has been well studied.

For atomic ions and some molecules e.g. He_2^+ the recombination scheme is more complicated, and is due to a large number of processes acting simultaneously. This is generally termed Collisional-Radiative Recombination. We have calculated the effects[1] of neutral collisions on this process when the neutral is of the same species as the Ion, figure 1, and when the neutral is different from the Ion, for the rare gases, figure 2. It can be noted that the recombination of Ar^+ for example is a factor of 10 higher in Helium than in Argon.

NPL Plasma Simulations

A long pulse electron beam-generated plasma can be utilized to simulate an NPL plasma. At Miami we are just starting to utilize an electron beam with the following characteristics

>250 keV electrons,
@ 10 A/cm^2,
a repetition rate of 2/sec.,
and a pulse length of 1 μsec.

---

*This research supported by NASA and BMDATC.

The plasma is evaluated with the following diagnostics

Optical Spectra,
Dye Laser Probes,
and Ion mass spectra.

With this system, quasi-steady state plasma can be produced and has the same energy densities as NPL's.

Excited State - UF_6 Reactions

A flowing afterglow will be utilized by Michel Touzeau and R.A. Tilton to measure the interactions of excited states with neutral UF_6 at the University of Paris . A flowing afterglow is being constructed at Miami to incorporate a mass spectrometer with a flowing afterglow system to provide molecule and ion formation rates.

New Lasers and Laser Processes

Collisions induced by stimulated absorption of photons have recently been discovered[2]. Theory indicates that the inverse process should also exist. This process, the stimulated emission of photons creating collisions, could be ideally suited for UF_6 based NPL's. Experiments are planned to investigate this possibility.

REFERENCES

[1]B.L. Whitten, L.W. Downes, W.E. Wells, "Collisional Radiative Recombination in High Pressure Noble Gas Mixtures", 1st. Int. Sym. on NPL, Paris (1978).

[2]D.B. Lidow, R.W. Falcone, J.F. Young and S.E. Hairris, Phys. Rev. Lett., 37E, 1590 (1976).

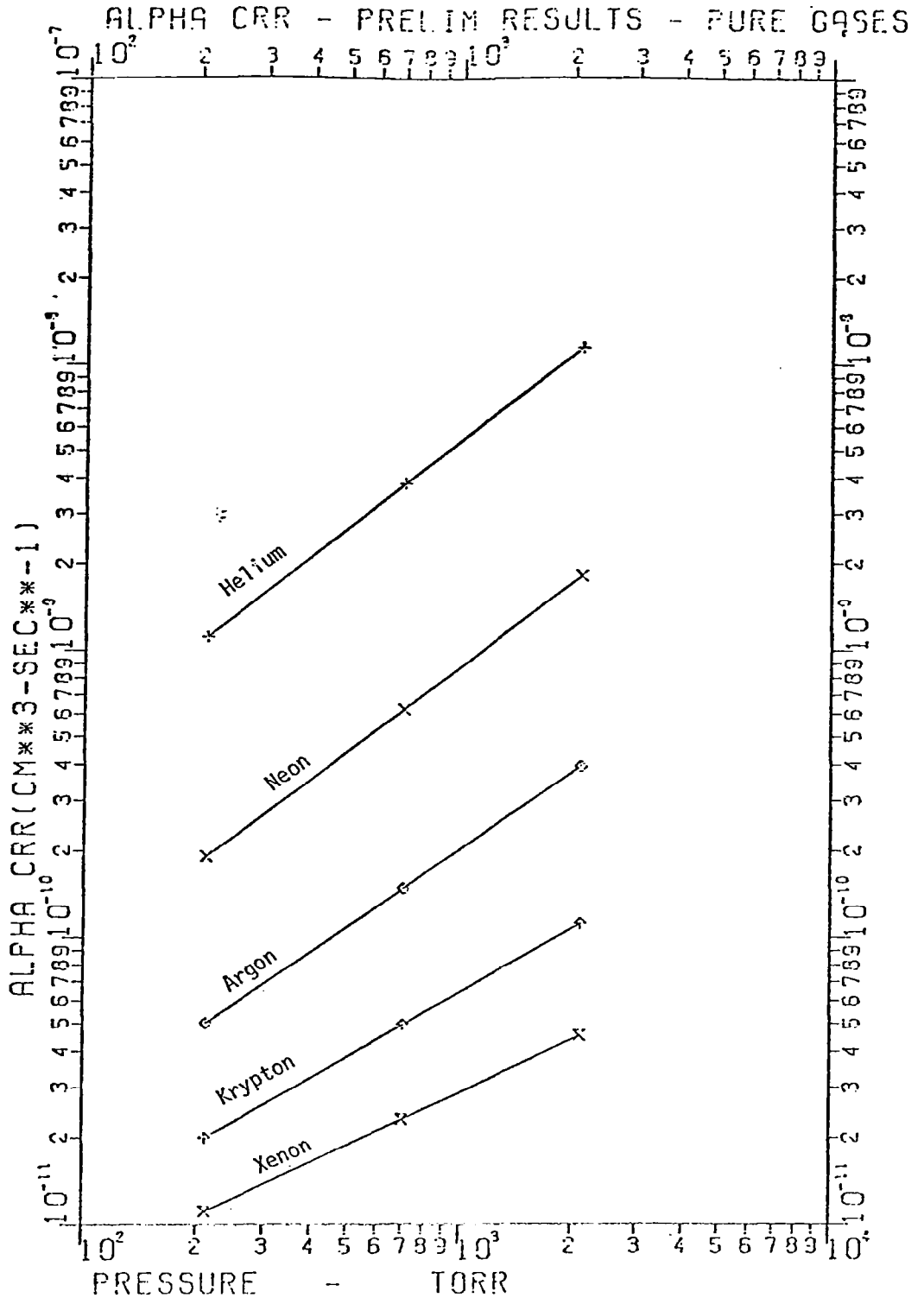

Figure 1.- Effects of neutral collisions on electron-ion recombination when neutral is of same species as ion.

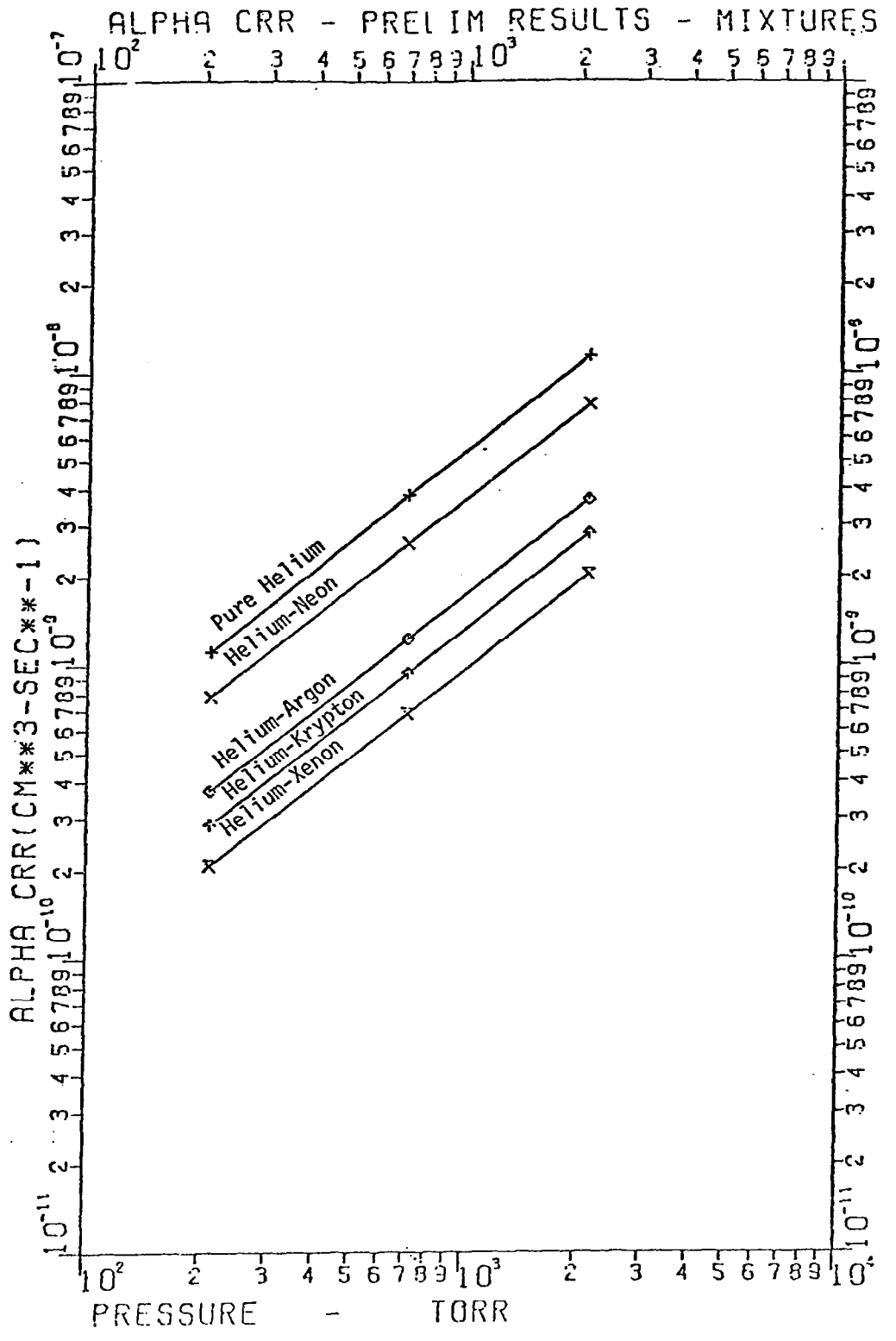

Figure 2.- Effects of neutral collisions on electron-ion recombination when neutral is of different species from ion.

E-Beam Simulation of Nuclear Induced Plasmas

J.T. Verdeyen and J. Gary Eden*
Gaseous Electronics Laboratory
Department of Electrical Engineering
University of Illinois at Urbana-Champaign
Urbana, IL 61801

Summary:

The Gaseous Electronics Laboratory has just started the research effort on this topic. Consequently, this brief discussion presented here will concentrate on the future plans rather than preliminary results. However, some definite results of the work carried out by Dr. Eden and his co-workers at the Naval Research Laboratory on Proton beam excitation will be discussed in detail since this is germane to the topic of this meeting.

*Dr. J. Gary Eden is presently at the Naval Research Laboratory but will be joining the Department of Electrical Engineering at Illinois in August 1979.

Discussion:

After an exceedingly painful and slow start, nuclear pumping has now reached the stage where reasonable optical power levels have been achieved. It is logical therefore that we stand back and ask some rather fundamental questions about the pumping schemes to ascertain whether there is an optimum coupling between the source of energy - the reactor - and the lasing medium.

Although any source of energy can and has been used to excite a laser, usually one scheme has an overwhelming advantage in terms of efficiency over the other competitive methods. For instance, optical pumping of a gas laser was successful quite early, but lost in the competition with the more convenient and efficient discharge pumping. By the same token, nuclear pumping has had to take a back seat to the more readily available E-beam excitation even though the physics of the two schemes would appear to be similar.

For instance, surface and volumetric sources have been used in conjunction with reactors to pump various gases. While the details of the nuclear reactions differ, it is generally agreed that the electrons resulting from passage of the fission fragments through gas are the ultimate source of the excitation of the laser levels, either by direct impact excitation of ground state atoms (from below) or by recombination (thereby populating the states from the top).

From that viewpoint then, E-beam excitation is an excellent simulation of a fissioning plasma environment without the attendant difficulties of a reactor. This is the purpose of our research at the Gaseous Electronics Laboratory.

Of course, the ultimate goal of all working in nuclear pumping is to achieve lasing in a UF_6 plasma. Because of the multitude of energy states in this molecule, we can anticipate that it will tend to deactivate many of the usual laser levels. This, in turn, requires a higher pumping rate to achieve threshold - a most unfavorable direction for any scheme but especially so for nuclear pumping. The reason is that the available power densities in a reactor tend to be considerably lower than in an E-beam or in a discharge. Thus our first goal is to study the kinetics of various excited states in the presence of UF_6.

Although lasing in a predominantly UF_6 plasma is assumed to be the most convenient and straightforward approach, it is possible to conceive of utilizing the spontaneous radiation from this system to excite another gas isolated from this primary energy source. For instance, the efficiency of producing UV photons from the Xenon excimer Xe_2 is high and furthermore its spontaneous decay rate is also fast. The latter fact precludes Xe_2 as being a candidate for lasing in the fissioning plasma, but this does not preclude it from being the photon source for another system such as the mercury halides. From this standpoint, the Ar^+ UF_6 seems to be a natural for producing 193 nm $(ArF)^*$ photon for the HgX_2 system. Fortunately, this will be a natural fallout of the planned study discussed in the preceding paragraph.

One final issue should be noted in closing. Even though the physics of excitation of the laser levels in a nuclear pumped system might appear to be similar to E-beam exication, some evidence has

appeared which suggests that there are measurable differences. For instance, the group at NRL has succeeded in pumping lasers by protons and apparently has achieved higher efficiencies than with E-Beams. In other words, the laser energy out, divided by the proton energy deposited in the gas, is greater with the heavy particle excitation than with the electron. This is, of course, most encouraging for nuclear pumping. The details of this experiment will be discussed by Dr. Eden.

Efficient XeF laser excited by a proton beam[a)]

J.G. Eden, J. Golden, R.A. Mahaffey,[b)] J.A. Pasour,[b)] and R.W. Waynant

Naval Research Laboratory, Washington, D.C. 20375

The efficient generation of stimulated emission from XeF at 351 and 353 nm has been achieved by pumping $RG/Xe/NF_3$ gas mixtures (RG = argon, neon, or helium) with an intense (~ 10 A cm^{-2}) beam of ~200-keV protons. For an active medium ($T = 300$°K) consisting of Ar, Xe, and NF_3 at a total pressure of 1 atm and 30% cavity output coupling, the volumetric output, efficiency, and threshold pump power for the laser were determined to be 5–10 J/liter amagat, 1.7 ± 0.7%, and 1.5 MW cm^{-3}, respectively. Much lower efficiencies were obtained for neon and helium diluent mixtures.

In 1978, the first demonstration of a gas laser pumped by an intense proton beam was reported.[1] This new means of laser excitation was made possible by the development during the last four years of several sources capable of efficiently generating intense p-beams ($> 10^{12}$ protons/cm^2 pulse).[2–5]

Weak proton beams ($\sim 10^7$ protons/pulse) have been employed for some time in studies of the kinetic behavior of excited rare gases[6] and various molecules of laser interest (Cl_2, OH, etc.).[7] Also, near-infrared laser transitions in Ar, Kr, Xe and Cl have been pumped[8,9] by the volumetric nuclear reaction $^3He(n,p)^3H$, which liberates a 560 keV proton and a 190 keV tritium ion. *Both* of these particles ionize the background gases and lasing results.

The extension of p-beam pumping to the rare-gas–halide (RGH) lasers is attractive due to the large efficiencies (1–9%) that have been reported for these lasers[10] using discharge or e-beam excitation. In this paper, the characteristics of a p-beam-pumped XeF laser are reported.[11] For $Ar/Xe/NF_3$ gas mixtures at 1 atm and cavity output coupling of 30%, efficiencies of 1.7 ± 0.7% and volumetric laser outputs in the range 5–10 J/l-amagat have been obtained.

A reflex tetrode[2] powered by the NRL Seven Ohm Line generator produced the p beams for these experiments. Typical beam parameters were proton energies of ~450 keV, a current density of ~ 10 A cm^{-2}, and a pulse duration of ~50 ns FWHM. The generator and tetrode were the same as described in Ref. 1 except that the tetrode was operated with a first anode (A_1)–cathode (K) gap of ≈ 1.7 cm.

The laser cell, however, was redesigned for these studies. Figure 1 is a cross-sectional diagram of the cell and the foil support assembly. All of the cell parts except the polyvinyl chloride window mounts (not shown) were fabricated from aluminum which was chosen for its mechanical strength and electrical conductivity. Support for the p beam window (3-μm thick Mylar foil) was provided by resting the foil against a plate with a honeycomb array of holes and a geometrical transmission of 60%.

Demountable Brewster-angle windows made of Suprasil grade quartz were installed on the cell. Since the penetration depth of 200-keV protons (roughly the energy remaining after emerging from the Mylar foil) in 1 atm of argon is ~5 mm, the laser axis was situated ~1–2 mm from the proton window and was oriented perpendicular to the incoming beam. Research-grade rare gases and technical-grade NF_3 were used in these experiments and before each firing, the laser cell was filled with a fresh gas mixture.

The optical cavity consisted of two dielectric-coated mirrors of 5-m radius of curvature separated by 70 cm. One of the mirrors was a total reflector ($R \sim 98\%$, $T \sim 0.3\%$) at 350 nm, while the output coupler transmitted either 0.3, 6,

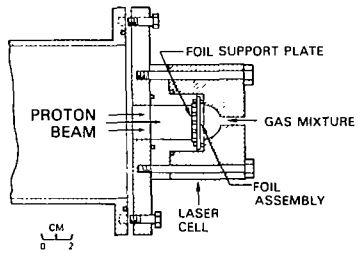

FIG. 1. Cross-sectional view of the proton-beam laser cell and foil support assembly. With this arrangement, laser cell pressures in excess of 1 atm could be accommodated. The proton-beam aperture was 18.2 cm^2.

[a)]Work supported by ONR and DOE.

[b)]Sachs-Freeman Associates, Bladensburg, Md.

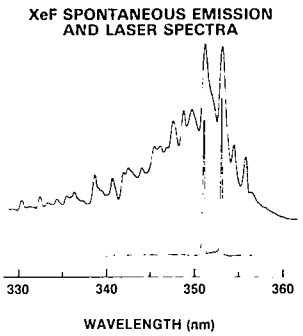

FIG. 2. XeF spontaneous emission (top trace) and laser spectra obtained from 750 Torr Ar/20 Torr Xe/4 Torr NF_3 gas mixtures. The spectrograph resolution was 0.02 nm for laser emission and 0.16 nm for fluorescence. The vertical scales for both spectra are logarithmic.

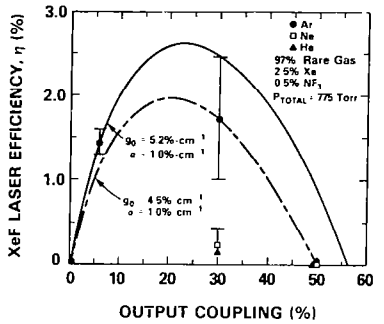

FIG. 3. Efficiency of the XeF laser as a function of output coupling of the optical cavity for various rare-gas diluents. The curves are solutions of Rigrod's equation fitted to the argon data. The dashed and solid curves are normalized to $\eta = 1.7\%$ and $T = 30\%$, and $\eta = 2.4\%$ and $T = 30\%$, respectively. The $T = 30\%$ argon point represents the statistical average of five trials and the $T = 6\%$ point, two trials.

30, or 50% at the lasing wavelengths. The laser and axial spontaneous emission were monitored either by a 1-m spectrograph and photographic film or by a Hamamatsu S-20 photodiode and neutral density filters. For laser energy measurements, the photodiode and filters were calibrated against an XeCl discharge laser (308 nm) using a Gen-Tec calorimeter. The XeCl laser was used as the calibration source due to the small standard deviation (11%) in the output energy of the device from shot to shot.

The efficiency of the p-beam-pumped XeF laser for a given pulse was determined by measuring both the laser output energy (E_o) and the number of protons entering the laser cell. This procedure was necessary due to the variability in the proton dose per pulse. The number of protons incident on the gas was inferred using nuclear activation techniques.[1,12] First, with the laser cell evacuated, thick boron nitride targets were placed around the p-beam aperture of the laser cell as well as in the cell itself. With this arrangement, the ratio R_i of the number of protons entering the cell, N_i, to the number striking the target surrounding the aperture, N_0, was determined by comparison of the residual radioactivity induced in the targets by the nuclear reaction $^{14}N(p,\gamma)^{15}O$. Subsequently, for each shot, N_0 was measured so that N_i could be inferred from $R_i N_0$. The energy of a proton emerging from the Mylar window was assumed to be equal to the peak inductively corrected voltage applied to the anode of the tetrode minus the energy lost in the window. The energy deposited in the Mylar was calculated using the range-energy data of Northcliffe and Schilling.[13] For these experiments, the proton-beam energy entering the laser cell (E_p) was found to range from ~ 0.3 to 2.3 J, all of which was assumed to be absorbed by the gas mixture.

The fraction of the beam delivered to the laser gas (as determined by the method outlined above) was consistent with an estimate that accounted for the divergence of the p-beam. Bleachable blue cellophane and damage of the Mylar proton window were used to estimate the beam's divergence. Typically, the beam cross section at the laser cell aperture was roughly circular with a diameter of ~ 7.5 cm. Also, the beam filled ~ 11 cm^2 (or $\sim 60\%$) of the cell's 18.2-cm^2 (9.6×1.9 cm) rectangular aperture.

Figure 2 shows microdensitometer tracings of the XeF laser and spontaneous emission spectra obtained with p-beam excitation of 97% Ar, 2.5% Xe, and 0.5% NF_3 gas mixtures at a total pressure of ~ 1 atm. The spectra are typical of those obtained from e-beam experiments, and lasing occurs on the $v' = 1 \rightarrow v'' = 4$, $v' = 0 \rightarrow v'' = 2$ (351 nm), and $v' = 0 \rightarrow v'' = 3$ (353 nm) vibrational transitions[14] of the $B \rightarrow X$ band of XeF. Although not shown, laser pulse lengths were observed to vary from 10 to 20 ns FWHM.

Several experiments were conducted to study the dependence of the XeF laser output power and efficiency η ($\equiv E_o/E_p$) on: (1) the output coupling T of the laser cavity and (2) the rare-gas diluent used for the laser mixture. Figure 3 presents the results of these experiments for various output couplings ($0.3 \leqslant T \leqslant 50\%$) and for He, Ne, and Ar as the mixture diluent. The highest laser efficiencies were obtained for $T = 30\%$ and Ar diluent. Averaged over five shots, η was found to be $1.7 \pm 0.7\%$ where the error is one standard deviation in the data. The best efficiency observed was $2.7^{+1.1}_{-0.5}\%$. The errors shown are due to noise on the photodiode waveform and uncertainty in E_p.

To determine the small signal gain g_0 and loss α coefficients for the XeF laser, the efficiency-vs-coupling data were

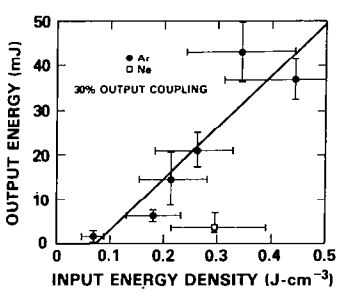

FIG. 4. Dependence of the XeF laser output energy on the input (p-beam) energy density. The solid line represents the linear least-squares fit of the argon data points, and its zero-energy density intercept is 74 mJ/cm^3. The laser threshold for neon diluent is roughly three to four times greater than that for argon.

fit to an equation given by Champagne and co-workers [15] which is based on Rigrod's analysis [16] of high-gain lasers. The dashed curve in Fig. 3 represents the best fit of Eq. (1), Ref. 15, to the Ar data with the constraint that the line pass through the $T = 30\%$, $\eta = 1.7\%$ point. For this solution, $g_0 = 4.5\%\ \text{cm}^{-1}$ and $\alpha = 1.0\%\ \text{cm}^{-1}$. However, the greatest uncertainty in the Ar data is at $T = 50\%$. Although weak lasing was obtained for this output coupling, large variations in the proton energy/pulse made the assignment of error limits difficult. For this reason, a second fit of Rigrod's equation to the Ar data is shown in Fig. 3 (solid curve). Again, the curve was normalized at $T = 30\%$ but this time at the upper limit of the error bar at $\eta = 2.4\%$. This solution yields $g_0 = 5.2\%\ \text{cm}^{-1}$ and $\alpha = 1.0\%\ \text{cm}^{-1}$ and agrees well with the $T = 6\%$ data. A third curve, normalized to the lower bound of the $T = 30\%$ point at $\eta = 1.0\%$, was not included since it would deviate greatly from the $T = 6$ and 50% data. From the curves of Fig. 3, the maximum efficiency obtainable for the *p*-beam-excited XeF laser for these gas mixtures appears to lie between 2.0 and 2.7% for $20 \leqslant T \leqslant 25\%$. No attempt has yet been made to optimize the gas mixture other than to study different diluents.

Clearly, the *p*-beam-pumped XeF laser is considerably less efficient for He and Ne diluents than it is for Ar at 1 atm despite comparable energy inputs to the three gases. This comparison between the performance of Ar and Ne diluents is similar to that reported[17] for the e-beam-pumped XeF laser at atmospheric pressure. The poor efficiency of Ne diluent mixtures at low pressures (< 1.5 atm) is possibly due to Penning ionization of Xe by Ne_2^* excimers, where the formation rate of Ne_2^* varies as p_{Ne}^2.

The *p*-beam laser efficiencies reported above compare quite favorably with those obtained using much longer (0.5–2.0 μs) e-beam pulses. Although Hsia *et al.* [18] have obtained efficiencies up to 5.5% by heating the gas to ~ 450 °K, the best room-temperature results are currently $\eta \sim 2$–2.5%. [19] For e-beam excitation pulses < 100 ns, the best previously reported value was 0.5% obtained by Ault and co-workers. [20] Since the RGH lasers perform more efficiently for pump pulses > 100 ns, the use of microsecond proton beams [4] may improve the efficiencies reported here. Also, the volumetric laser outputs obtained in these experiments were typically 5–10 J/l-amagat which equal or exceed those obtained using e-beam pumping. [10,17–19] The largest value observed was 9.9 ± 1.5 J/l-amagat which corresponds to 43 ± 7 mJ output ($T = 30\%$, argon) from 4.6 cm^3 of excited gas at a density of 0.93 amagat.

Figure 4 shows the variation of the laser output energy with the input energy density. The solid line represents the linear least-squares fit of the Ar data. Input energy *density*, rather than input energy, was plotted on the abscissa because fluctuations in the tetrode voltage change the proton energy and range which vary the excited-gas volume. Therefore, it is necessary to normalize the input energy to the excited volume. The zero-input energy density intercept of the line gives a threshold energy density for the *p*-beam-pumped XeF laser of 74 mJ cm^{-3}, or for a 50-ns FWHM pump beam, 1.5 MW cm^{-3}. Again, this threshold value is comparable to those observed for pure e-beam pumping but is considerably larger than the power thresholds obtained for e-beam sustained discharge operation (< 300 kW cm^{-3}). [21]

In summary, the first demonstration of a rare-gas–halide laser pumped by a proton beam has been reported. Laser efficiencies up to 2.7%, volumetric laser outputs up to 9.9 J/l-amagat, and a threshold power density of 1.5 MW cm^{-3} have been observed for $T = 30\%$ and using Ar diluent at a total gas mixture pressure of ~ 1 atm. These values compare favorably with state-of-the-art e-beam experiments, and optimization of the gas-mixture composition will likely improve these results. Also, operation of the XeF laser in He diluent has been reported which, to date, has not been achieved with electron-beam pumping. Proton-beam excitation of the RGH lasers offers the possibility of operating these devices at gas pressures $\lesssim 1$ atm, where acoustics and excited-specie absorption problems are minimized.

It appears that the most attractive laser candidates for future proton-beam pumping studies are those atomic or molecular lasers, such as Cl_2 at 258 nm, [22] which require the lighter rare gases as diluents but the upper laser level formation kinetics do not demand high pressures.

The authors are grateful to D. Epp for excellent technical assistance throughout the course of these experiments. The authors also thank Drs. C.A. Kapetanakos and A.W. Ali for many valuable discussions and suggestions, and L.F. Champagne for reviewing the manuscript.

[1] J. Golden, J.G. Eden, R.A. Mahaffey, J.A. Pasour, A.W. Ali, and C.A. Kapetanakos, Appl. Phys. Lett. 33, 143 (1978).
[2] J.A. Pasour, R.A. Mahaffey, J. Golden, and C.A. Kapetanakos, Phys. Rev. Lett. 40, 448 (1979) and references cited therein.
[3] M. Greenspan, S. Humphries, J. Maenchen, and R.N. Sudan, Phys. Rev. Lett. 39, 24 (1977).
[4] S.C. Luckhardt and H.H. Fleischmann, Appl. Phys. Lett. 30, 182 (1977).
[5] S.J. Stephanakis, D. Mosher, G. Cooperstein, J.R. Boller, J. Golden, and S.A. Goldstein, Phys. Rev. Lett. 37, 1543 (1976).
[6] T.E. Stewart, G.S. Hurst, T.E. Bortner, J.E. Parks, F.W. Martin, and H.L. Weidner, J. Opt. Soc. Am. 60, 1290 (1970).
[7] C.H. Chen and M.G. Payne, Appl. Phys. Lett. 28, 219 (1976); ibid., Opt. Commun. 18, 476 (1976).
[8] N.W. Jalufka, R.J. DeYoung, F. Hohl, and M.D. Williams, Appl. Phys. Lett. 29, 188 (1976).
[9] R.J. DeYoung, N.W. Jalufka, and F. Hohl, paper presented at the 16th AIAA Aerospace Sciences Meeting, Huntsville, Ala., 1978 (unpublished).
[10] See, for example, the review paper of M. Rokni, J.A. Mangano, J.H. Jacob, and J.C. Hsia, IEEE J. Quantum Electron. QE-14, 464 (1978).
[11] Preliminary results for the work described here were reported previously: J.G. Eden and J. Golden, Paper TUA3, 1978 Annual Mtg. of the Optical Society of America, San Francisco, 1978 (unpublished); J. Golden, J.G. Eden, R.A. Mahaffey, J.A. Pasour, and R.W. Waynant, Proc. of the Int. Conf. on Lasers '78, Orlando, Fla., 1978 (unpublished).
[12] F.C. Young, J. Golden, and C.A. Kapetanakos, Rev. Sci. Instrum. 48, 432 (1977).
[13] L.C. Northcliffe and R.F. Schilling, Nucl. Data Tables A 7, 233 (1970).
[14] J. Tellinghuisen, J. Chem. Phys. 64, 4796 (1976).
[15] L.F. Champagne, J.G. Eden, N.W. Harris, N. Djeu, and S.K. Searles, Appl. Phys. Lett. 30, 160 (1977).
[16] W.W. Rigrod, J. Appl. Phys. 36, 2487 (1965).
[17] L.F. Champagne and N.W. Harris, Appl. Phys. Lett. 31, 513 (1977).
[18] J.C. Hsia, J.A. Mangano, J.H. Jacob, and M. Rokni, Appl. Phys. Lett. 34, 208 (1979).

[19]J.C. Hsia and J.A. Mangano, 8th Winter Colloquium on Quantum Electronics, Snowbird, Utah, 1978 (unpublished); L.F. Champagne (private communication).
[20]E.R. Ault, R.S. Bradford, Jr., and M.L. Bhaumik, Appl. Phys. Lett. **27**, 413 (1975).
[21]C.H. Fisher and R.E. Center, Appl. Phys. Lett. **31**, 106 (1977).
[22]A.K. Hays, Paper TUA5, 1978 Annual Mtg. of the Optical Society of America, San Francisco, 1978 (unpublished).

Reprinted from Applied Physics Letters, vol. 35, no. 2, July 15, 1979, pp. 133-135.

Nuclear Pumped Lasers - Advantages of O_2 (1Δ)

J. J. Taylor
Air Force Weapons Laboratory
Kirtland Air Force Base

POTENTIAL

The HEL community sees the primary weapon advantages potentially available from NPL as high average power coupled with long shot time (less than 100 sec).

SYSTEM ISSUES

The Air Force Weapons Laboratory (AFWL) sees the NPL as a very young technology with major issues to be addressed before being seriously considered as an HEL weapon contender. Problems of shielding, heat dissipation, high efficiency FF pumping, good beam quality, and thermal blooming all need engineering level solutions prior to gaining support from the HEL weapons community.

For AF airborne applications, development of lightweight shielding and cooling is necessary. For ground base applications, integration of the nuclear pumping source and the laser cavity is a major unknown.

To take full advantage of high power and long shot times for airborne operation, the heat dissipation problem must be solved while keeping system weight as low as possible. For ground based systems, the high weight problem becomes unimportant, but the integration of a reactor cooling system and a laser cavity is still a far term prospect. Efficient pump rates must be achieved since only small percentage losses in a very high power pumping source will cause tremendous waste heat buildups.

Good beam quality is an absolute necessity to maintain a compact beam. Poor beam quality quickly offsets gains made by a very high power pumping source.

Thermal blooming is an extremely critical issue for high power laser systems. If higher power causes thermal blooming to continually worsen, then this phenomenon will put a cap on the utility of very high power lasers within the atmosphere.

$O_2(1\Delta)$

O_2 is strongly recommended as a laser gas for NP for a ground based system. Some of its characteristics are an excited lifetime of 45 min, continuous wave (CW) operation, and efficient energy transfer to iodine (I).

The long lifetime of the O_2 excited state avoids the cooling/laser cavity integration problem. The O_2 can be excited in the reactor core, then pumped away from the reactor to be mixed with I and lased.

ADVANTAGES

CW operation is required to get high power through the atmosphere without air breakdown.

The long lifetime of the excited O_2 state allows for separation of the laser and the pumping reactor. This feature bypasses the worries of FF's disturbing the laser cavity medium and the concern of FF damage to resonator mirrors.

Separation of the laser and the nuclear reactor eliminates the need to design cooling systems and laser resonators around each other. Conventional reactor design with the addition of O_2 flow tubes should suffice.

The weapons laboratory is currently working with the O_2-I laser. That limits the feasibility and critical design issues to only several nuclear pumping questions since AFWL will work the I laser details such as mirror coatings, resonator design, cavity shapes, closed or open cycle laser, window materials, etc.

O_2 ISSUES

The three most critical NP issues for O_2 appear to be the following:

(1) Can we achieve greater than 15 percent excitation of O_2? Fifteen percent minimum excitation is required to transfer energy to I.

(2) Do fission fragments pump O_2 into the singlet delta state efficiently? Note that extremely high efficiencies are not required since current reactor cooling does not depend on O_2 molecules to absorb fission fragment energy.

(3) What is the maximum pressure that the O_2 system can operate at during the transfer from the reactor to the laser? Too high a pressure will cause O_2 deactivation from wall collisions; too low a pressure will make high energy transfer difficult.

PROPOSALS

(1) Propose that NPL physicists calculate the theoretical FF pumping efficiency of O_2.

(2) If the theoretical efficiency looks reasonable, then perform experimental verification.

(3) Experimentally determine the collisional deactivation time of O_2 versus pressure.

(4) Propose that AFWL/NPL community jointly work on a systems feasibility study to determine the amount of excited O_2 that can be generated and delivered to an I laser.

(5) Propose that AFWL study thermal blooming of very high power laser beams to determine their transmission characteristics through the atmosphere.

CONCLUSIONS

- To achieve lasing in a reactor core requires a scientific breakthrough
- The use of a O_2 transfer medium should lead to a near-term ground-based high energy laser
- Development of airborne nuclear powered lasers requires a scientific breakthrough

SIMULATION STUDIES FOR A NUCLEAR PHOTON PUMPED EXCIMER LASER

THOMAS G. MILLER
U.S. Army Missile Command
Redstone Arsenal, AL 35809

and

JOHN E. HAGEFSTRATION
Ballistic Missile Defense
Advanced Technology Center
Huntsville, AL 35807

Simulation studies are underway to determine the feasibility of a nuclear photon pumped excimer laser. Recent experiments at Auburn University underline the difficulty of using UF_6 mixed with various gases to produce a nuclear pumped laser. These experiments indicate at least three basic problems that will hinder the development of nuclear pumped lasers that use homogeneous mixtures of UF_6 and various gases:

(1) the large optical absorption of UF_6

(2) the large quenching rates of UF_6 for most gases

(3) the difficulty involved in handling UF_6 and the subsequent clean-up problems

Because of the above, coupled to the fact that charged particle energy can be efficiently converted to radiant energy at 1720 Angstrons by allowing the charged particles to impinge on high pressure xenon, has led us to consider nuclear photon pumped lasers.

Fig 1 shows a sketch of how such a laser might be constructed. A neutron source is placed in the center of a cylinder made of a material that has a large neutron inelastic scattering cross section such as iron. The purpose of the iron is to serve as a containment device and to convert neutron kinetic energy to gamma and x-ray energy. Surrounding the iron cylinder is a cylinder of moderator such as graphite. The purpose of the moderator is to further slow down the neutrons that have been inelastically scattered by the iron. The moderating cylinder is surrounded by another cylinder filled with a mixture of high pressure xenon. In this large cylinder several tubes are placed which contain the lasing gas, say XeF_2. Photons are produced in the high pressure xenon by both the gamma and x-rays that enter the cylinder. If a gas that has a large fission cross section such as ^3He is mixed with the xenon gas, additional energy will be developed to produce additional photons, which should make the process more efficient.

Such a system has recently been developed using high energy electrons to produce photons from high pressure xenon.[1,2] In both cases the lasing gas was XeF_2.

We are in the process of performing simulation studies using such a system where high pressure Xe is bombarded with electrons and protons to form 1720 Angstrons. These photons are in turn used to photodissociate XeF_2 to produce XeF^*. Fig 2 shows a view of the experimental set-up. Electrons or protons from a 2 MeV Febetron are used to produce 1720 Angstron radiation from Xe_2 states, as previously described. These photons are used to photodissociate XeF_2 according to the following:

$$XeF_2 + h\gamma(1720\ A^o) \rightarrow XeF^* + F$$

The photons enter into the quartz tube containing the XeF_2. A cavity is formed via the two cavity mirrors. Primary measurements are overall conversion efficiency measurements and gain vs time measurements.

1- "A New Blue-Green Excimer Laser in XeF".
W.K. Bischel, H.H. Nakano,
D.J. Eckstrom, R.M. Hill, D.L. Huestis
and D.C. Lovents
Appl. Phys. Lett. 34(9) 1 May 79

2- "XeF(B→X) Laser Optically Excited by Incoherent Xe_2^* (172-nm) Radiation"
J. Gary Eden
Optics Letters, Vol 3. No 3, Sept 78

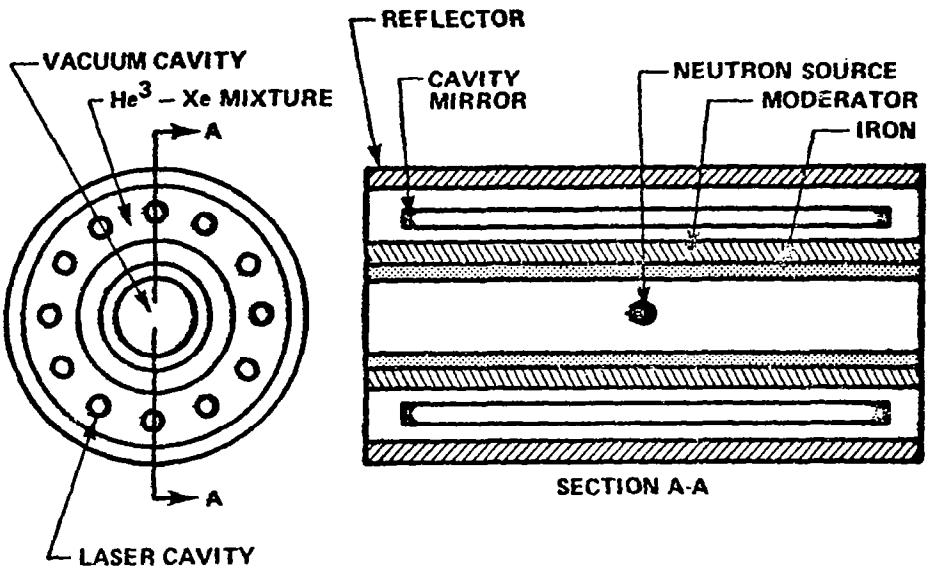

A NUCLEAR PHOTON PUMPED EXCIMER LASER

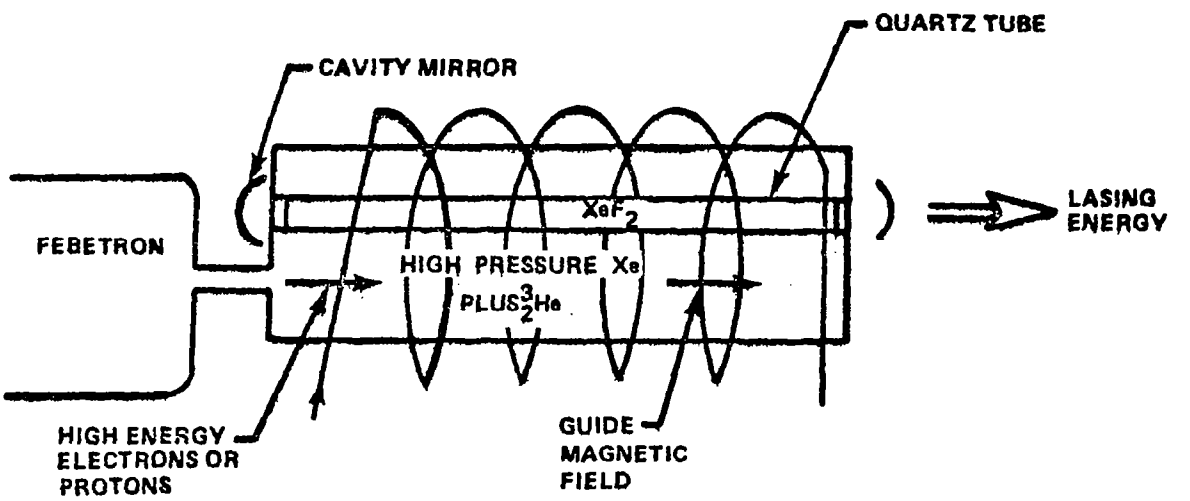

NUCLEAR PHOTON PUMPED EXCIMER LASER SIMULATION EXPERIMENT

Concept for UF_6-Fueled Self-Critical DNPL Reactor System

R. J. Rodgers
Fluid Dynamics Laboratory
United Technologies Research Center
E. Htfd., CT. 06108

ABSTRACT

An analytical study of a self-critical nuclear pumped laser system concept was performed. The primary emphasis was on a reactor concept which would use gaseous uranium hexafluoride (UF_6) as the fissioning material. A reference configuration was selected which has a 3.2 m^3 lasing volume as the reactor core. The core is composed of a series of hexagonal graphite tubes which are surrounded by a reflector-moderator composed either of heavy water or beryllium. Results of neutronics calculation predict a critical mass of 4.9 kg of U^{235} in the form of $^{235}UF_6$. The configuration would operate in a continuous steady-state mode. The average gas temperature in the core is 600 K and the UF_6 partial pressure within the lasing volume is 0.34 atm.

Laser transitions requiring average fission power densities less than approximately 1 kW/cm^3 for excitation are most attractive. Operation at wavelengths greater than approximately 400 nm may be required because of limitations imposed by the opacity of gaseous UF_6. Further research directed toward identification of UF_6 compatible lasing transitions is required for further evaluation.

INTRODUCTION

Self-critical nuclear pumped lasers are one of several possible nuclear pumped laser types currently being studied. This type of laser if proven feasible offers the possibility of very high power operation in a continuous steady-state mode. Possible applications for such lasers include space power generation, space power transmission, and space propulsion. Recent investigations of lasers using gaseous UF_6 as the fissionable material are described in Refs. 1 and 2. Gaseous systems provide a means for deposition of fission energy directly in the lasing medium. Volumetric excitation of the lasing medium thus should be more efficient in gaseous systems than in systems employing coatings or foils.

In self-critical gaseous systems it is necessary to select a reactor geometry which meets both the nuclear criticality requirements and the laser optical configuration requirements of the system. A description of a self-critical UF_6 fueled reactor system has been described in Ref. 3 and is briefly outlined herein. In general, cavity reactor configurations are designed having approximately spherical geometry or cylindrical geometry with length-to-diameter ratio of approximately one. This generally results in good neutron economy and leads to systems having low critical mass. High power lasers have been designed in many configurations, some of which are highly two-dimensional and thus unattractive for self-critical nuclear pumping.

SELF-CRITICAL DNPL REACTOR DESIGN CHARACTERISTICS

A self-critical direct nuclear pumped laser (DNPL) reactor concept requires that the reactor configuration be designed such that parasitic neutron capture of reactor component materials is small. This will permit a low critical mass of nuclear fuel, which enhances the potential performance of the system. For this study, emphasis was placed on use of enriched gaseous UF_6 (93.5% U-235) fuel which is mixed with a gaseous lasing medium in the reactor. The fissioning of the nuclear fuel provides a mechanism to continuously deposit energy in a large lasing volume through fission fragment interaction.

The self-critical UF_6 gaseous core laser reactor has a fuel mixture which is typically composed of three distinct components with unique functions to perform. First, UF_6 must be present in sufficient quantity to produce a sustained fission reaction and thereby to provide the energy source to pump a large volume of the lasing gas mixture. Second, a host gas such as He, Ne, or Ar is present as the dominant energy storage member. The host gas possesses high excitation and ionization energy levels which are populated in the host gas by interaction with high energy fission products. Third, a lasing gas is needed, such as Xe, which is present in small quantities. Energy is transferred by collisions between the excited and ionized host species and lasing gas with the creation of excited and/or ionized states of the lasing gas. Lasing then occurs as the lasing gas radiatively relaxes between energy levels corresponding to its characteristic wavelengths.

An important parameter relative to the lasing system is the neutron flux level required to induce efficient laser action. The flux level required determines the overall reactor power level of a self-critical system. The characteristics of several DNPL laser experiments (Refs. 4 through 11) are listed in TABLE I. The full advantage of high power nuclear pumped laser systems occurs when fission energy is volumetrically created within the lasing medium and the neutron source is not external to the laser cell. This is a characteristic of a self-critical DNPL reactor system and it increases the "useful thickness" and, hence, volume of the pumped lasing region. The data in TABLE I indicate that the lasing threshold neutron flux level is in the range of 10^{15} to 10^{17} n/cm^2-s with the lowest threshold to date being 4×10^{14} n/cm^2-s for mixtures of He-CO and He-CO_2 (Ref. 7). Research is in progress to identify DNPL systems with lower threshold flux levels. Such systems would be highly attractive for use in a self-critical UF_6-fueled reactor with the lasing medium intimately combined in the nuclear core because the total power level could be reduced.

Neutronics Considerations

To determine a set of operating conditions for the self-critical DNPL reactor for sizing purposes, parametric relationships were derived between several reactor variables. Included were relationships between total reactor power, power density, neutron flux level, U-235 mass, U-235 density, and U-235 pressure. Use of these relationships allowed rapid assessment of the effect on reactor design characteristics of changes in parameter values.

Parametric results are shown in Fig. 1, for a reactor which has a U-235 critical mass of 6.0 kg and gas temperature of 600 K. Figure 1 illustrates the inter-relationship among the power density, neutron flux, and total power, with U-235 density and pressure. The probable operating region of interest is indicated in Fig. 1 as having a neutron flux level between 10^{14} and 10^{16} n/cm^2-s. This flux range is within that where laser action has been produced in several recent experiments (see TABLE I and Refs. 4 through 11). A possible extended operating region is indicated for a maximum uranium (U) species partial pressure less than 10 atm, with a more probable operating region limited to U partial pressure less than 1 atm and a minimum U pressure of 0.01 atm.

At the assumed critical mass of 6 kg and temperature of 600 K, the range in U-fuel partial pressure between 0.01 and 10 atm corresponds to fuel volumes and, hence, maximum lasing volumes between approximately 120 and 0.12 m^3, respectively. For the flux range between 10^{14} and 10^{16} n/cm^2-s, the power density ranges between 0.001 and 1.0 kW/cm^3. Results for a different critical mass at the given power and power density can be determined by scaling the pressure and density directly and by scaling the flux inversely with the U-235 mass ratio, $M_{crit}/6.0$ kg. The 6 kg U-235 critical mass is considered typical of that which could be obtained in a gas core reactor system. For this mass of U-235, the range for reactor total power level is between approximately 20 MW and 2000 MW for steady-state systems. The ability to operate efficiently at high pressure depends on the specific lasing medium used in the reactor and upon the optical absorption coefficient of UF_6 at the specific laser wavelength.

Optical Considerations

In examining potential lasing gas candidates, it is necessary to assess the effect of the UF_6 relative to quenching of laser action at a particular wavelength. The spectral absorption cross section of UF_6 (Ref. 12) is shown in Fig. 2 between 200 and 400 nm. Also indicated are the wavelengths at which potential lasers (KrF, XeBr, I_2, XeF, and N_2) would operate.

Three laser candidate media which operate at wavelengths for which UF_6 absorption is known to be relatively low are the I_2 (342 nm), Xe (351, 353 nm), and N_2 (358 nm) lasers. The KrF and XeBr lasers would appear to suffer from too large a UF_6 quenching effect due to the UF_6 optical absorption loss in a self-critical UF_6 DNPL system. Estimates for the maximum efficiency have been made for the I_2 laser (13 percent, Ref. 13) and Xe laser (7 percent, Ref. 14). With a knowledge of the gain characteristics for selected transitions, the optical absorption cross section of UF_6 can be used to define a varying U density criteria as a function of wavelength. Wavelengths at which the density is above the nuclear criticality density may be considered candidates for potential self-critical DNPL systems.

REFERENCE REACTOR CONFIGURATION

A conceptual DNPL reference reactor which is shown in Fig. 3 was selected based on the results of the parametric analyses. The core is a matrix of fuel cells. A length-to-diameter (L/D) ratio of approximately one is used for the core. This geometry has a small surface area to volume ratio which reduces neutron leakage from the core. Above and below the fuel cell matrix are regions which contain the laser optics components such as mirrors, beam splitters, etc. A tank of heavy water (0.9975 D_2O) reflector-moderator surrounds the matrix and optics regions. At the top of the D_2O tank, there is a laser power extraction channel with optical windows on the ends. The channel is filled with high pressure deuterium gas to reduce neutron leakage from the core and to provide a transparent light path through the D_2O reflector-moderator.

The core of the reference design consists of a series of modular unit cells in a hexagonal matrix. The central unit fuel cell operates as a master oscillator. The output of the master oscillator is optically coupled to the other fuel cells which act as single-stage amplifiers connected in parallel. The geometry of the unit cell module is shown in Fig. 4. The module is a hexagonally shaped rod of graphite, with a hollowed-out central cylindrical cavity. The fuel and lasing gas mixture flows through the cavity section of the modules. The graphite provides internal neutron moderation and fission density leveling within the core. The reference reactor configuration has a unit cell length of 200 cm, cavity diameter of 20 cm, and a dimension of 30 cm between any two parallel surfaces of the unit cell. The minimum wall thickness of the graphite cell is 4.5 cm. The gas mixture within the cells was assumed to be composed primarily of helium and UF_6 in the mole ratio of 10:1. The mixture ratio was selected based on the experimental results of Ref. 15. A gas operating pressure of 10 atm and temperature of 600 K were selected in order to size the radial dimension of the unit cell.

The manner in which the high energy fission products lose energy is such that the median light fission product, possessing a higher initial kinetic energy, has a longer range for slowing down than does the median heavy fission product. The median light fission product range in helium was used along with the mixture range-energy relationship to calculate the mixture fission product range as a function of pressure and temperature. The results are shown in Fig. 5. For an operating pressure between 5 and 10 atm and temperature of 600 K, a fission product range of approximately 10 mm (1 cm) results. For a fuel cell in which approximately 95 percent of the kinetic energy of the fission product is to be deposited in the gaseous core volume, a cell radius of approximately 10 cm is required.

Neutronics Calculations

A series of neutronics calculations were performed to establish the critical mass and critical fuel density for the reference design (Fig. 3). The calculations were performed for twenty neutron energy groups using the one-dimensional neutron transport theory computer program ANISN (Ref.16). The results of these calculations are shown in Fig. 6. Each of the cores was made up of unit cells having a cross section as shown in Fig. 4. U-235 clean critical masses of 6.6, 2.5, 4.4, and 16.1 kg were calculated for core gas volumes of 0.032, 0.32, 3.2, and 32.0 m^3, respectively. These core volumes correspond to configurations which have 3, 10, 51, and 204 individual cells, having cell lengths of 34, 100, 200, and 500 cm, respectively. The range in critical mass density varied from 0.2 to 5 x 10^{-4} g/cm^3.

For the reference design (fifty-one cells), a critical mass calculation was performed in which Xe gas was included in the fuel region in an amount equal to 0.5 percent of the He concentration. Also included was the equilibrium Xe^{135} fission product poisoning produced at a neutron flux level of approximately 10^{15} n/cm^2-s, assuming no Xe^{135} fission product removal. The equilibrium amount of Xe^{135} is equal to 29.4 mg. The critical mass was then calculated to be 4.88 kg of U-235, or an approximate 11 percent increase over the clean critical mass obtained with no Xe present. The reference configuration with Xe contained 0.34 atm UF_6 partial pressure based on the assumed fuel temperature of 600 K. The He core partial pressure was assumed to be approximately 10 times greater than the UF_6 pressure, resulting in a total fuel region pressure of 3.8 atm.

A relatively uniform fission energy distribution was obtained across the entire radius of the configuration for the reference core volume of 3.2 m^3. A uniform power density should aid in achieving a large lasing volume within each fuel cavity. The calculated fission energy distribution across the entire cell matrix is shown in Fig. 7. The two largest core volumes have a fission distribution which peaks at the center of the matrix, indicating that these fuel regions are relatively transparent to neutrons. The two smallest core volumes exhibit the effect of fuel self-shielding as expected since an individual cell of these configurations showed self-shielding. The 3.2 m^3 volume was selected as the reference configuration primarily because it appeared to have the most uniform fission distribution of the four configurations investigated.

Two additional calculations were performed in which the heavy water reflector-moderator was replaced with a beryllium moderator. Solid moderator materials would be a better choice than heavy water for DNPL reactors designed for space applications. Beryllium thicknesses equal to approximately one and two thermal neutron diffusion lengths (20 and 40 cm) were used in the calculations. The internal graphite wall thickness was held fixed at 4.5 cm as in the reference design. The calculated U-235 critical masses are 7.6 and 6.3 kg for beryllium thicknesses of 20 and 40 cm, respectively.

Optical Configuration

As previously described, in the reference design cell matrix (Fig. 3) the central cell operates as a self-excited master oscillator and is optically coupled to other amplifier cells. The central cell is configured in an unstable resonator geometry which results in the formation of a large donut-shaped beam such that lasing occurs in most of the fuel cavity volume. This increases the utilization efficiency of the fissioning gain medium, and allows high peak powers to be achieved together with good quality beams.

The output beam of the central cell oscillator is split by a series of mirrors located in the lower optics region. The split beams are amplified in parallel within the remaining fuel cavities and then upon leaving the amplifier cells are recombined into a nominal single beam within the upper optics region. The recombined output laser beam exits from the reactor region through the power extraction channel which is located in the top reflector-moderator region (see Fig. 3).

There are advantages of using a laser oscillator-amplifier configuration over that of a more intense all oscillator configuration. The control and design of a low-power oscillator should be simpler than that of an oscillator with high power potential. A low-power oscillator can be designed with confinement of excitation to its fundamental mode, and low beam steering sensitivity of the output to misalignment of the resonator mirrors (Ref. 17).

The possibility exists that the UF_6 is not a broadband absorber such that there may be narrow optical windows in the spectrum of UF_6 at any wavelength. Also, candidate lasing systems (as yet unidentified) which operate at wavelengths greater than 400 nm would also be attractive if the UF_6 spectral absorption cross section continues to decrease. Unfortunately, quantitative results are not available in this part of the UF_6 spectrum. A determination of UF_6 absorption in this region of the spectrum should be part of the effort to identify potential nuclear pumped laser systems to be developed in conjunction with a self-critical UF_6-fueled reactor.

Power Cycles

For a self-critical reactor system, which is operating cw or quasi-cw, a laser efficiency of greater than approximately 5 percent is desirable. A part of the thermal energy deposited in the lasing gases and reactor structure could be used to produce electricity and the remainder rejected via a space radiator. The fuel (UF_6/He) circuit for the reference design operates at a pressure of 3.8 atm and between temperatures of 351 K and 656 K. Schematic diagrams which show the important features of Rankine and Brayton cycles are presented in Fig. 8. The Rankine cycle would use an organic working fluid which offers the potential for good efficiency over the range of cycle temperatures of interest. Cycle efficiencies in the range of 25 to 35 percent (Ref. 18) appear possible at temperatures which correspond to those of the reference laser reactor configuration. For the cycle configuration shown in Fig. 8a an overall efficiency of 30 percent was determined. If an organic fluid such as Monsanto CP-27 were used, the maximum pressure in the cycle would be about 27 atm. In the Rankine cycle thermal energy is rejected via a condenser/radiator which operates at the lowest temperature present in the cycle. For the cycle conditions in Fig. 8a, the radiator/condenser must reject heat at 317 K. A large radiator would be needed to dissipate the 63 MW produced at the reference configuration design point.

Details of the Brayton thermal energy conversion cycle for the reference reactor configuration are shown in Fig. 8b. The working fluid used in the cycle is helium. The estimated efficiency of the simple Brayton cycle in Fig. 8b is only 9 percent. However, approximately 8 MW of electrical power would be produced via the cycle to meet the requirements of pumps and associated equipment of the laser reactor system. In the Brayton cycle, heat is rejected at higher average temperature than in the Rankine cycle. The ability to reject heat at a higher temperature in the Brayton cycle configuration should allow the size of the radiator required to be reduced relative to the Rankine cycle configuration radiator.

CONCLUDING REMARKS

The self-critical DNPL reactor may be an attractive candidate for a very high power laser system. Principal features of the reactor are the ability to pump a large gaseous lasing volume, self-contained excitation, and the potential for multi-megawatt continuous power output. However, there are important technical questions concerning the feasibility of the DNPL concept which are unresolved, and which require further research. An effort should be continued to identify potential lasing systems which can function in a UF_6 environment. Based on the known UF_6 optical absorption coefficient values in the 200 to 400 nm wavelength range, lasers which operate near the absorption minimum of 340 nm should be sought. Increased efforts should be made to identify systems that will operate at wavelengths longer than 400 nm because of the apparent low absorption in this spectral region. Sufficiently quantitative optical absorption data for UF_6 are not available in this part of the spectrum. Spectroscopic experiments and calculations are needed to quantify the UF_6 spectral absorption. DNPL experiments should continue to be performed in subcritical configurations but with UF_6 added to the lasing cell in quantities which are consistent with the expected range of critical density. It is important to identify laser enhancement or quenching effects due to the presence of UF_6 for specific candidate systems.

REFERENCES

1. Thom, K. and F. C. Schwenk: Gaseous-Fuel Reactor Systems for Aerospace Applications. J. of Energy, Vol. 1, No. 5, Sept.-Oct. 1977.

2. Thom, K., R. J. Schneider, and H. H. Helmick: Gaseous-Fuel Nuclear Research for Multimegawatt Power in Space. International Astronautical Federation, XXVIIIth Congress, Prague, Sept. 25-Oct. 1, 1977.

3. Rodgers, R. J.: Initial Conceptual Design Study of Self-Critical Nuclear Pumped Laser Systems. NASA CR-3128, April 1979.

4. DeYoung, R. J., W. E. Wells, G. H. Miley, and J. T. Verdeyen: Direct Nuclear Pumping of a Ne-N_2 Laser. Applied Physics Letters, Vol. 28, No. 9, May 1976, pp 519-521.

5. DeYoung, R. J., N. W. Jalufka, and F. Hohl: Nuclear-Pumped Lasing of ^{3}He-Xe and ^{3}He-Kr. Applied Physics Letters, Vol. 30, No. 1, Jan. 1977, pp 19-21.

6. Akerman, M. A. and G. H. Miley: A Helium-Mercury Direct Nuclear Pumped Laser. Applied Physics Letters, Vol. 30, No. 8, April 1977, pp 409-412.

7. Prelas, M. A., M. A. Akerman, F. P. Boody, and G. H. Miley: A Direct Nuclear Pumped 1.45 μ Atomic Carbon Laser in Mixtures of He-CO and He-CO_2. Applied Physics Letters, Vol. 31, No. 7, Oct. 1977, pp 428-430.

8. Jalufka, N. W., R. J. DeYoung, F. Hohl, and M. D. Williams: Nuclear-Pumped ^{3}He-Ar Laser Excited by the ^{3}He(n,p)^{3}H Reaction. Applied Physics Letters, Vol. 29, No. 3, Aug. 1976, pp 188-190.

9. McArthur, D. A. and P. B. Tollefsrud: Observation of Laser Action in CO Gas Excited Only by Fission Fragments. Applied Physics Letters, Vol. 26, No. 4, Feb. 1975, pp 187-190.

10. Gudzenko, L. I. and S. I. Yakovlenko: A UF_6+TlF+F_2 Nuclear-Reaction Laser. Soviet Physics-Lebedev Institute Reports, No. 12, Allerton Press, Inc., New York, 1975, pp 11-14.

11. Mansfield, C. R., P. F. Bird, J. F. Davis, T. F. Wimett, and H. H. Helmick: Direct Nuclear Pumping of a ^{3}He-Xe Laser. Applied Physics Letters, Vol. 30, No. 12, June 1977, pp 640-641.

12. DePoorter, G. L. and C. K. Rofer-DePoorter: The Absorption Spectrum of UF_6 from 2000 to 4200 A. Spectroscopy Letters 8 (8), 1975, pp 521-524. Also LASL Report LA-HR-75-792.

13. Tellinghuisen, J., A. K. Hays, J. M. Hoffman, and G. C. Risone: Spectroscopic Studies of Diatomic Noble Gas Halides. II Analysis of Bound-Free Emission from XeBr, XeI, and XeF. J. of Chemical Physics, Vol. 65, No. 11, Dec. 1976, pp 4473-4482.

14. Ewing, J. J. and C. A. Brau: Laser Action on the $^2\Sigma^+_{1/2} \rightarrow {}^2\Sigma^+_{1/2}$ Bands of KrF and XeCl. Applied Physics Letters, Vol. 27, No. 6, Sept. 1975, pp 350-352.

15. Lorents, D. C., M. V. McCusker, and C. K. Rhodes: Nuclear Fission Fragment Excitation of Electronic Transition Laser Media. Proceedings of the Princeton University Conference on Partially Ionized Plasmas Including the Third Symposium on Uranium Plasmas. (Ed. M. Krishnan) NASA Headquarters, Sept. 1976.

16. Engle, W. W., Jr.: A User's Manual for ANISN, A One-Dimensional Discrete Ordinates Transport Code with Anisotropic Scattering. Union Carbide Corp. Report K-1693, 1967.

17. Dyer, P. E. and D. J. James: High-Power Mode-Locked Tea CO_2 Laser Using an Unstable Resonator. Applied Physics Letters, Vol. 26, No. 6, Mar. 1975, pp 331-334.

18. Bjerklie, J., and S. Luchter: Rankine Cycle Working Fluid Selection and Specification Rationale. SAE Paper No. 690063, International Automotive Engineering Congress, Detroit, Michigan, Jan. 13-17, 1969.

LIST OF SYMBOLS

a	Length of side for hexagon fuel cell, cm
$FD/\overline{FD}$	Ratio of fission density to average value of fission density, dimensionless
L/D	Length-to-diameter ratio of core matrix, dimensionless
ℓ	Fuel cell length, cm
M_{crit}	Critical mass, kg
P	Pressure, atm
Q_T	Total power, MW
R	Radius, cm
R_{cell}	Radius of fuel cell, cm
R_{ff}	Median-light fission fragment range, mm
R_{hex}	One-half minimum chord length for hexagon cross section, cm
R_{sph}	Radius of core fuel cell matrix in spherical model, cm
T_F	Average fuel mixture temperature, deg K
V_F	Gaseous core volume, m^3
α	Optical absorption cross section, cm^2
λ	Wavelength, nm or Å
ρ	Density, g/cm^3

TABLE I

CHARACTERISTICS OF NUCLEAR PUMPED LASERS

Lasing Medium	Pressure Atm	Wave-Length Å	Thermal Flux Threshold n/cm^2-s	Average Thermal Flux n/cm^2-s	Power Density	Reference Number
$Ne-N_2$ $B^{10}(n,\alpha)Li^7$	0.2	8629 9393 (N)	$1x10^{15}$	$4.8x10^{15}$ (peak)	3.3 W/cm^3	4
^3He-Xe $^3He(n,p)^3H$	0.5	20270 (XEI)	$4x10^{15}$	$6x10^{15}$		5
^3He-Kr $^3He(n,p)^3H$	0.5	25000 (KRI)	$1.1x10^{17}$			5
He-Hg $B^{10}(n,\alpha)Li^7$	0.8	6150 (Hg^+)	$1x10^{16}$	$3.8x10^{16}$ (peak)	0.2 kW/cm^3	6
He-CO He-CO_2 $B^{10}(n,\alpha)Li^7$	0.8	14550 (C)	$4x10^{14}$	$2.5x10^{15}$ (peak)		7
^3He-Ar $^3He(n,p)^3H$	1.0	17900 (Ar)	$1.4x10^{16}$	$1.2x10^{17}$		8
CO $U(n,\nu n)FF$	0.1	51000→ 56000 (CO)		$1x10^{17}$ (peak)	2 kW/cm^3	9
UF_6-TlF-F_2 $U(n,\nu n)FF$		4000 (Tl)			1-6 W/cm^3	10
^3He-Xe $^3He(n,p)^3H$	0.8	20270 35080 36520 (XEI)		$3x10^{16}$	0.200 kW/cm^3	11

RELATIONSHIP BETWEEN KEY NUCLEAR PUMPED LASER SYSTEM PARAMETERS

T_F = 600 K

ASSUMED CRITICAL MASS: 6.0 kg

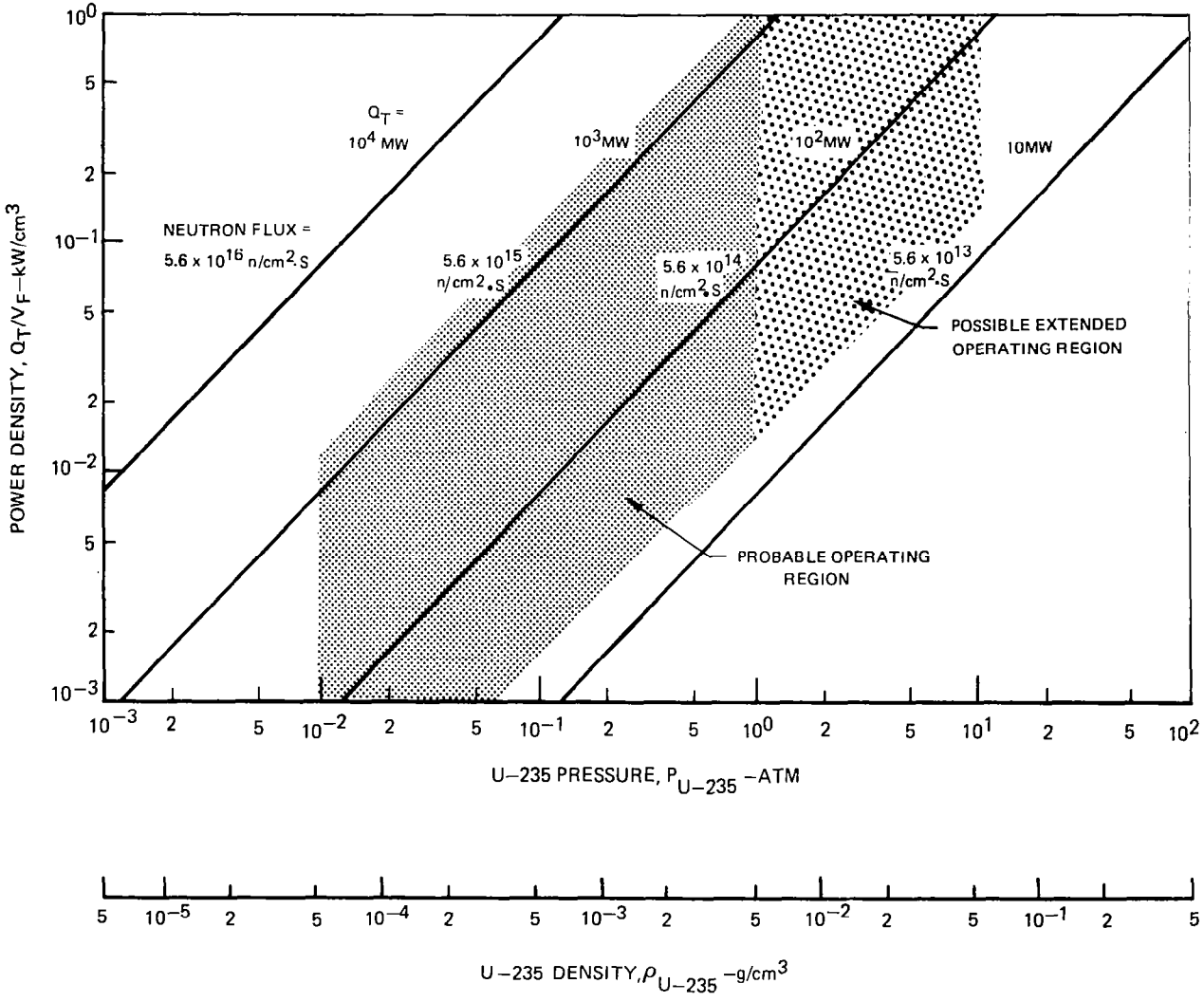

Figure 1

VARIATION OF UF_6 ABSORPTION CROSS–SECTION WITH WAVELENGTH

SEE REF. 12

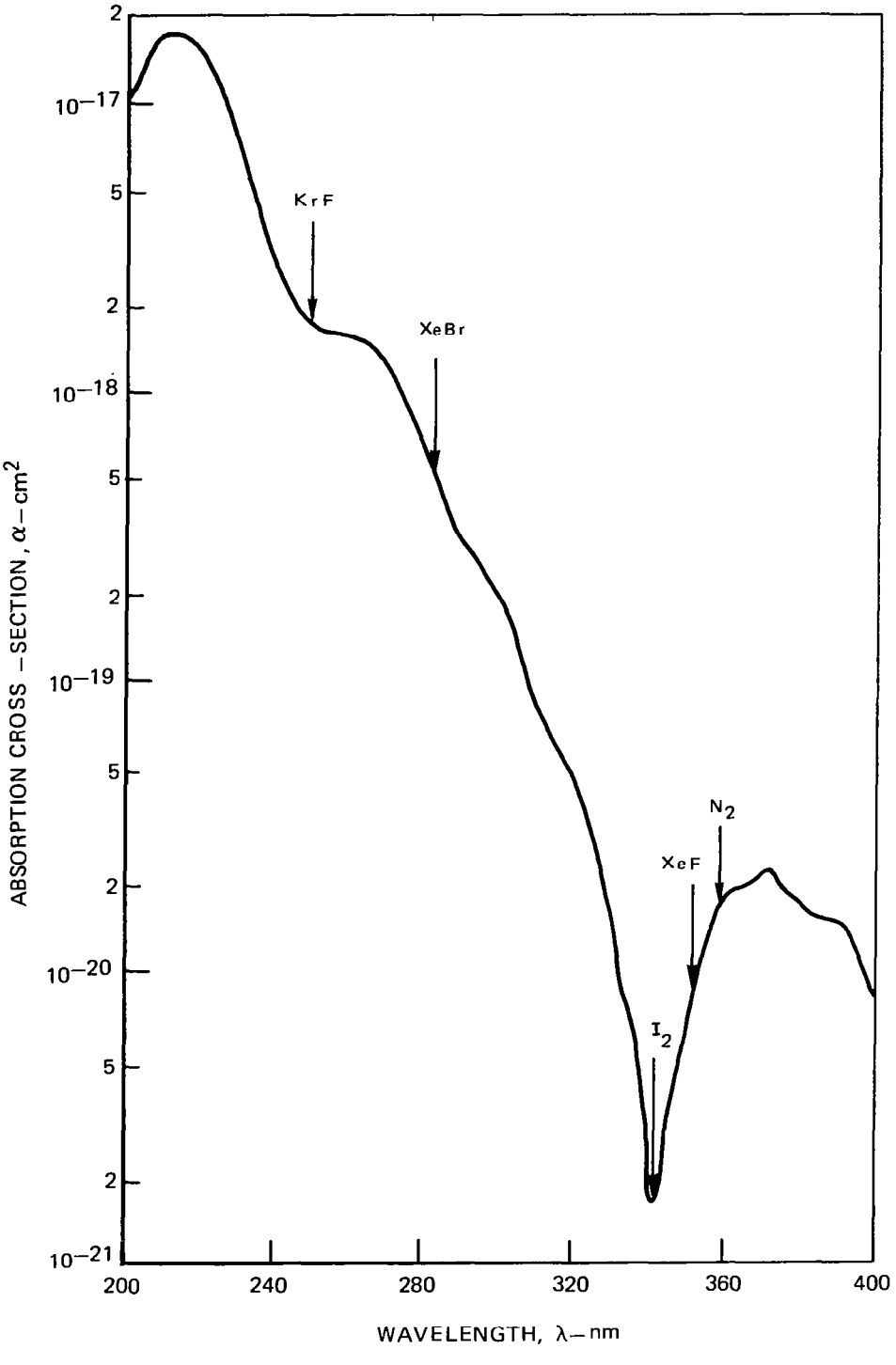

Figure 2

CONCEPTUAL UF_6 GASEOUS NUCLEAR PUMPED LASER REACTOR

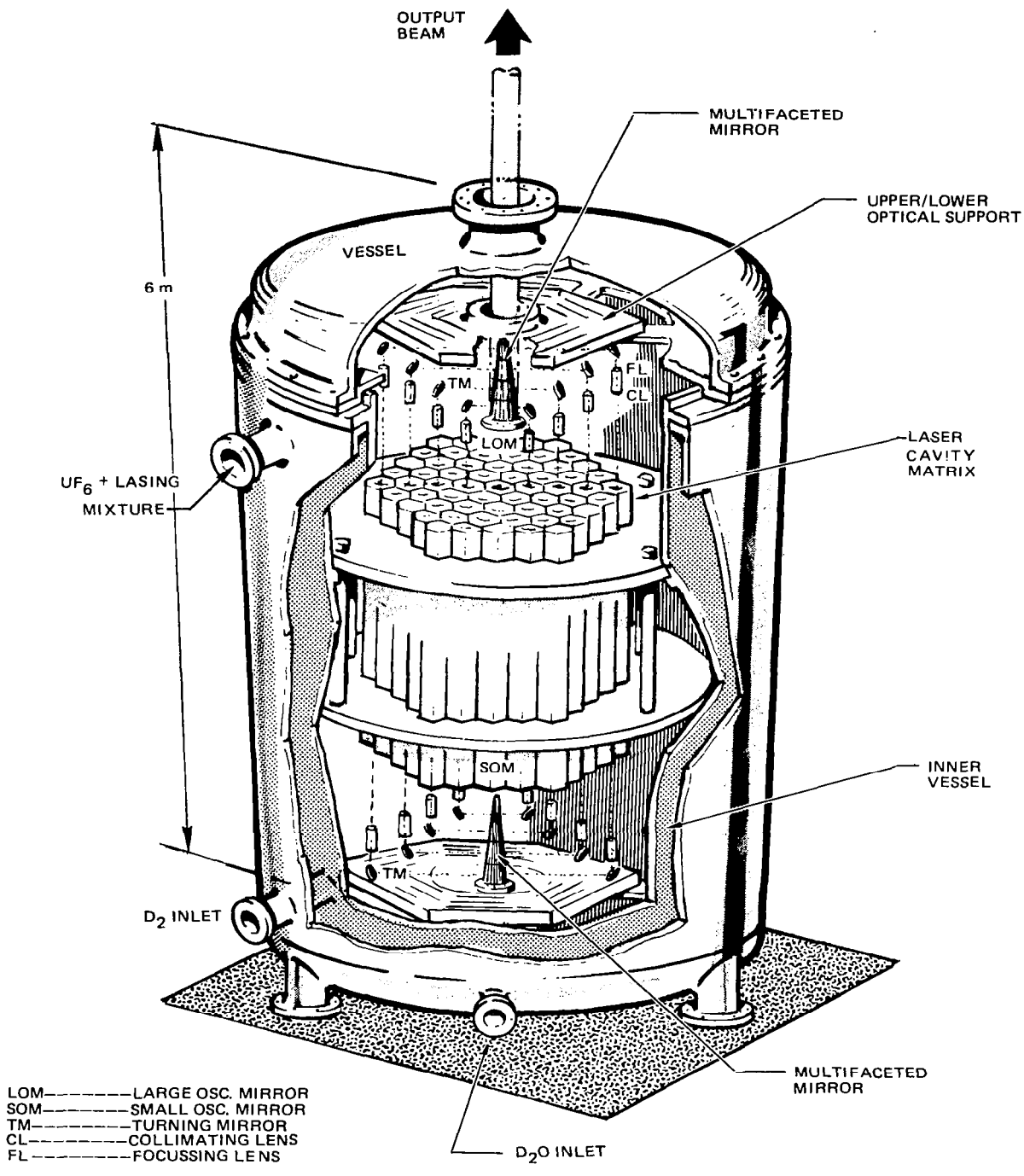

Figure 3

UNIT FUEL CELL FOR LASING REACTOR MATRIX

REF. CELL LENGTH: 200 cm

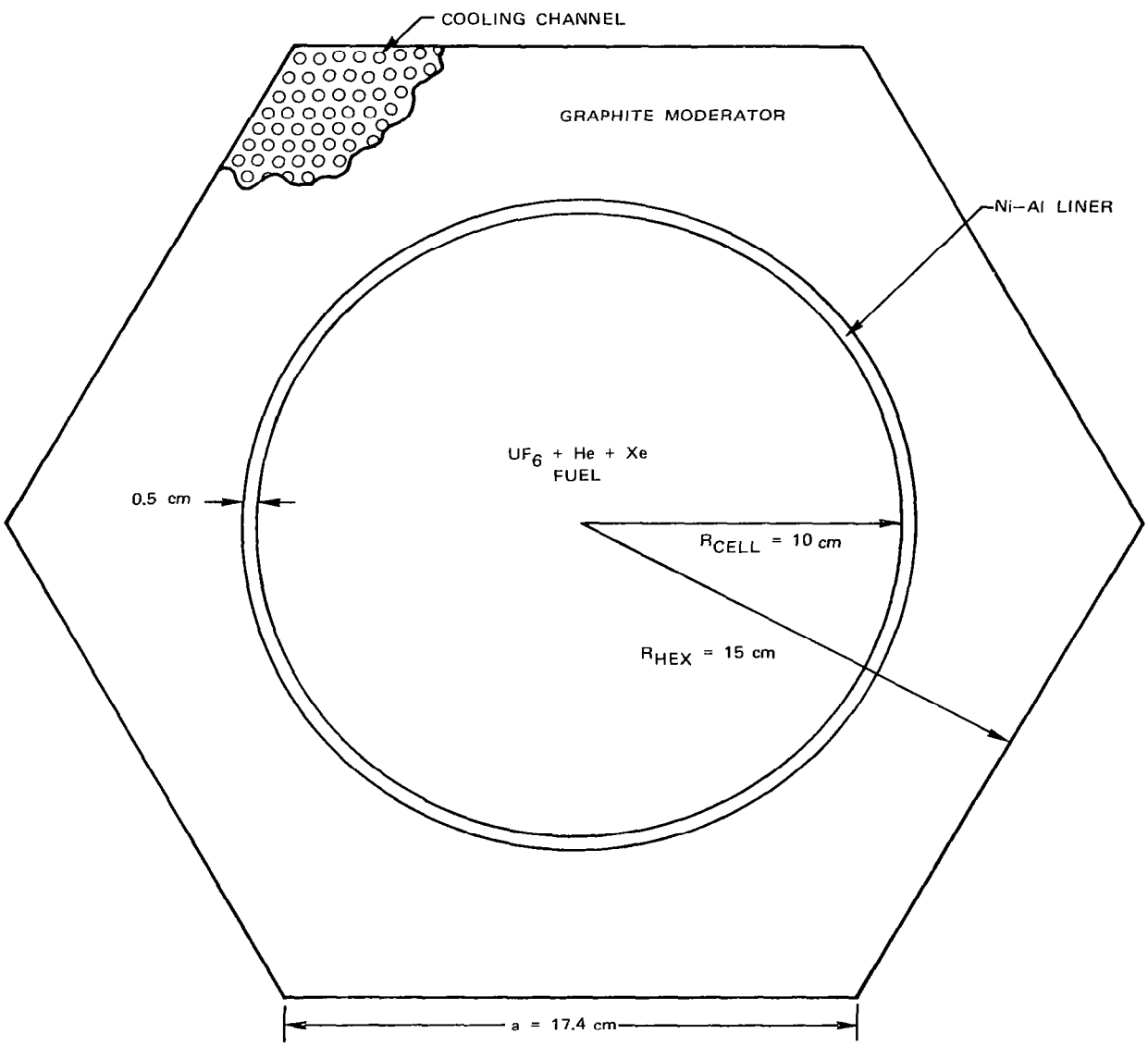

Figure 4

MEDIAN–LIGHT FISSION FRAGMENT RANGE IN UF_6–He MIXTURE

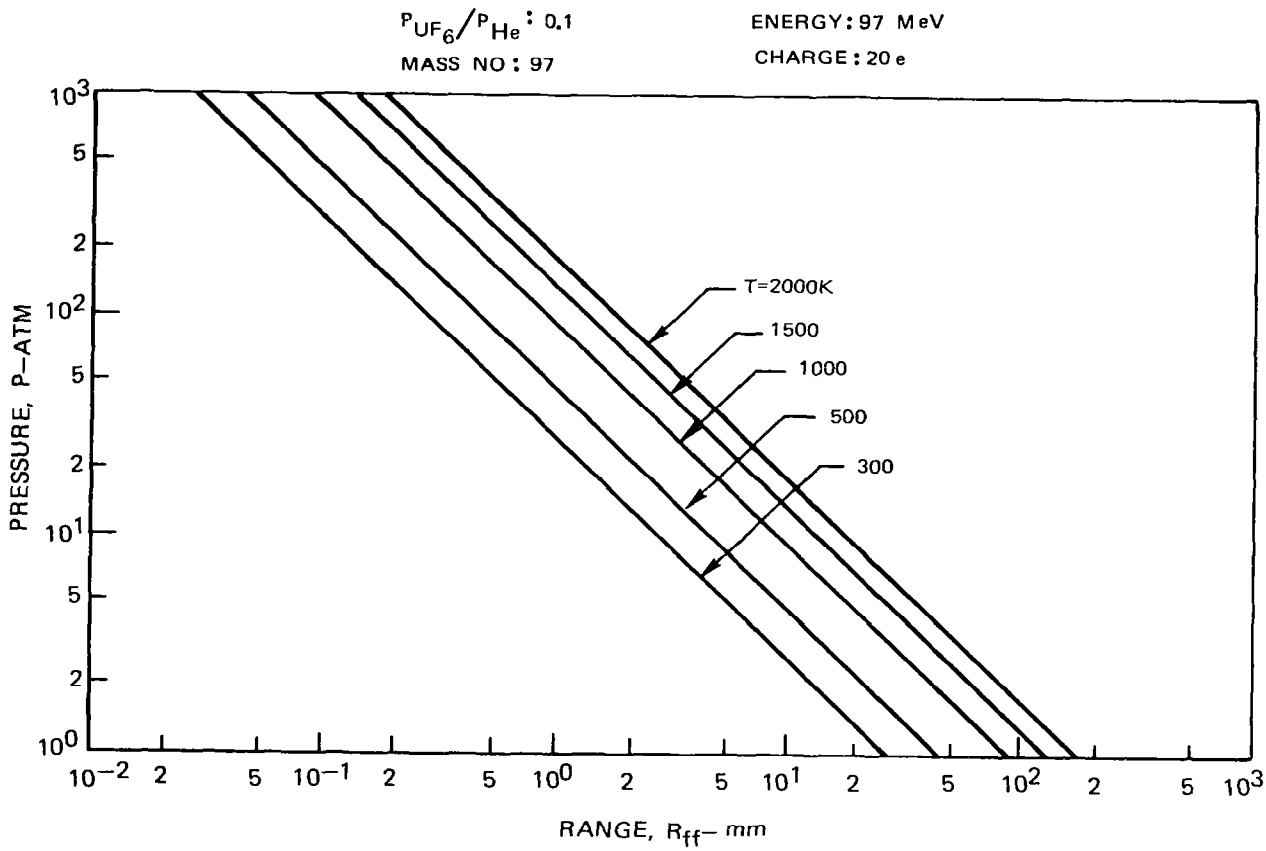

Figure 5

VARIATION OF CALCULATED CLEAN CRITICAL MASS WITH FUEL DENSITY

FUEL MATRIX REGION L/D≈1

FUEL CELL RADIUS = 10 cm

REFERENCE CONFIGURATION INCLUDES 29.4 mg OF Xe^{135} EQUILIBRIUM FISSION PRODUCT POISONING

AND ≈131 g (0.5%) Xe^{NAT} LASING GAS

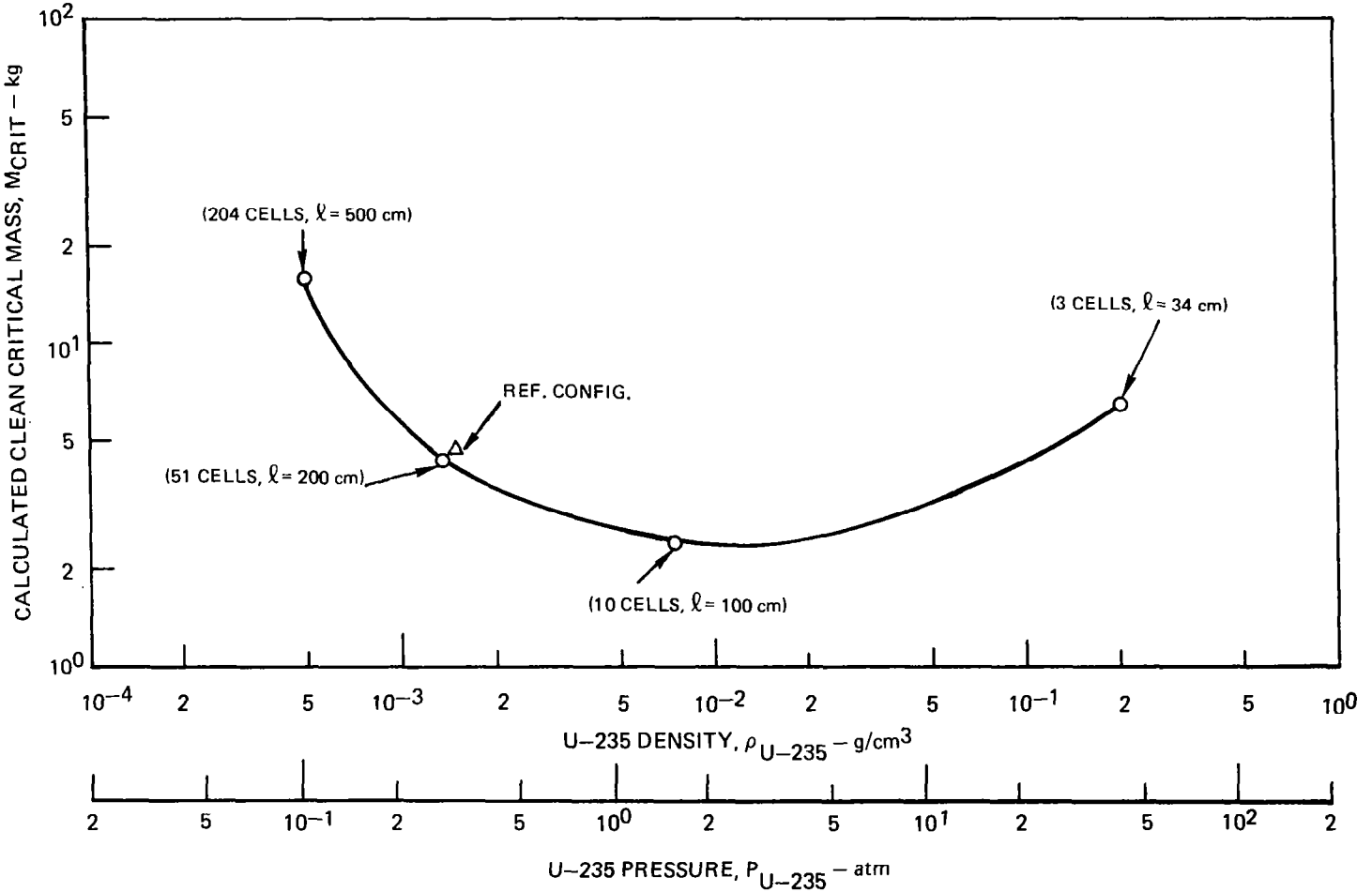

Figure 6

VARIATION OF FISSION DENSITY RATIO WITH SPHERICAL RADIUS OF MATRIX OF FUEL CELLS FOR SEVERAL REACTOR CONFIGURATIONS

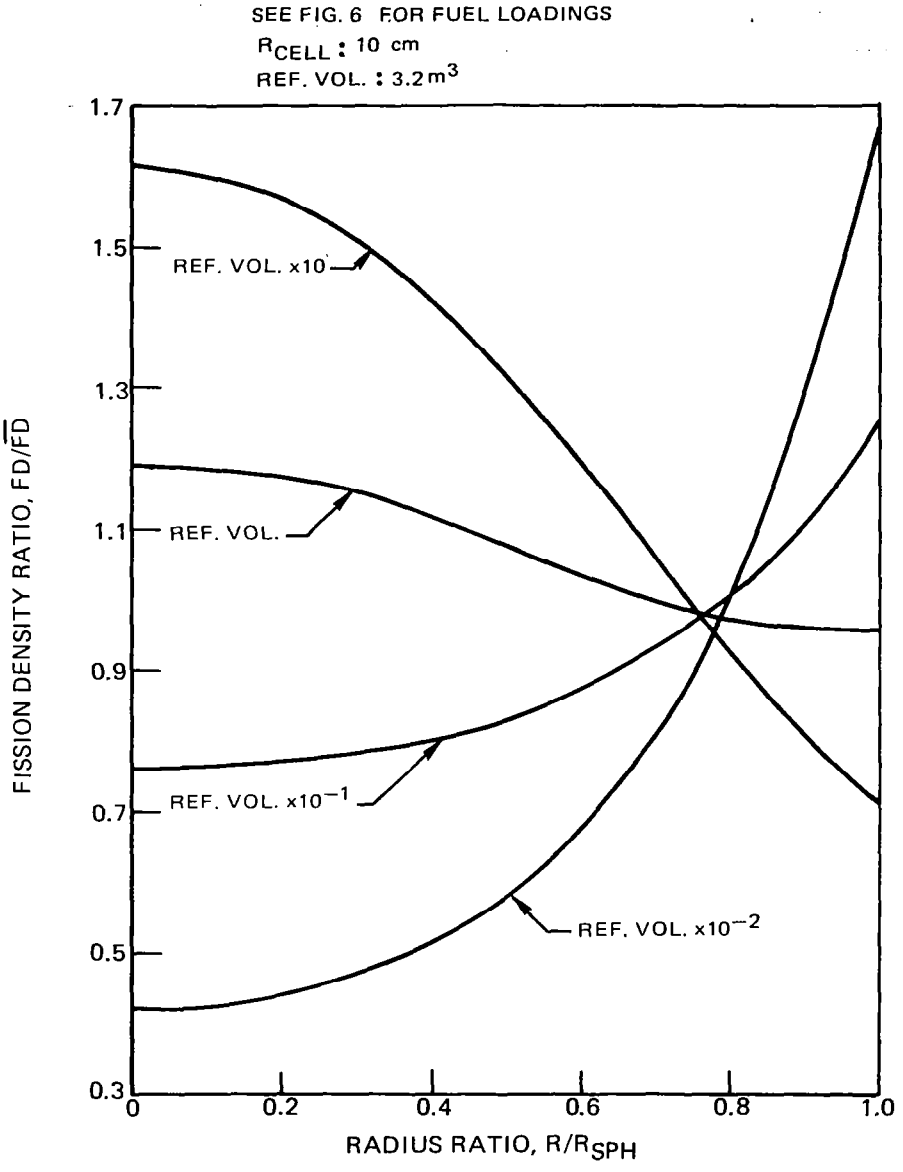

Figure 7

CYCLE SCHEMATICS FOR NUCLEAR PUMPED LASER POWER EXTRACTION SYSTEMS

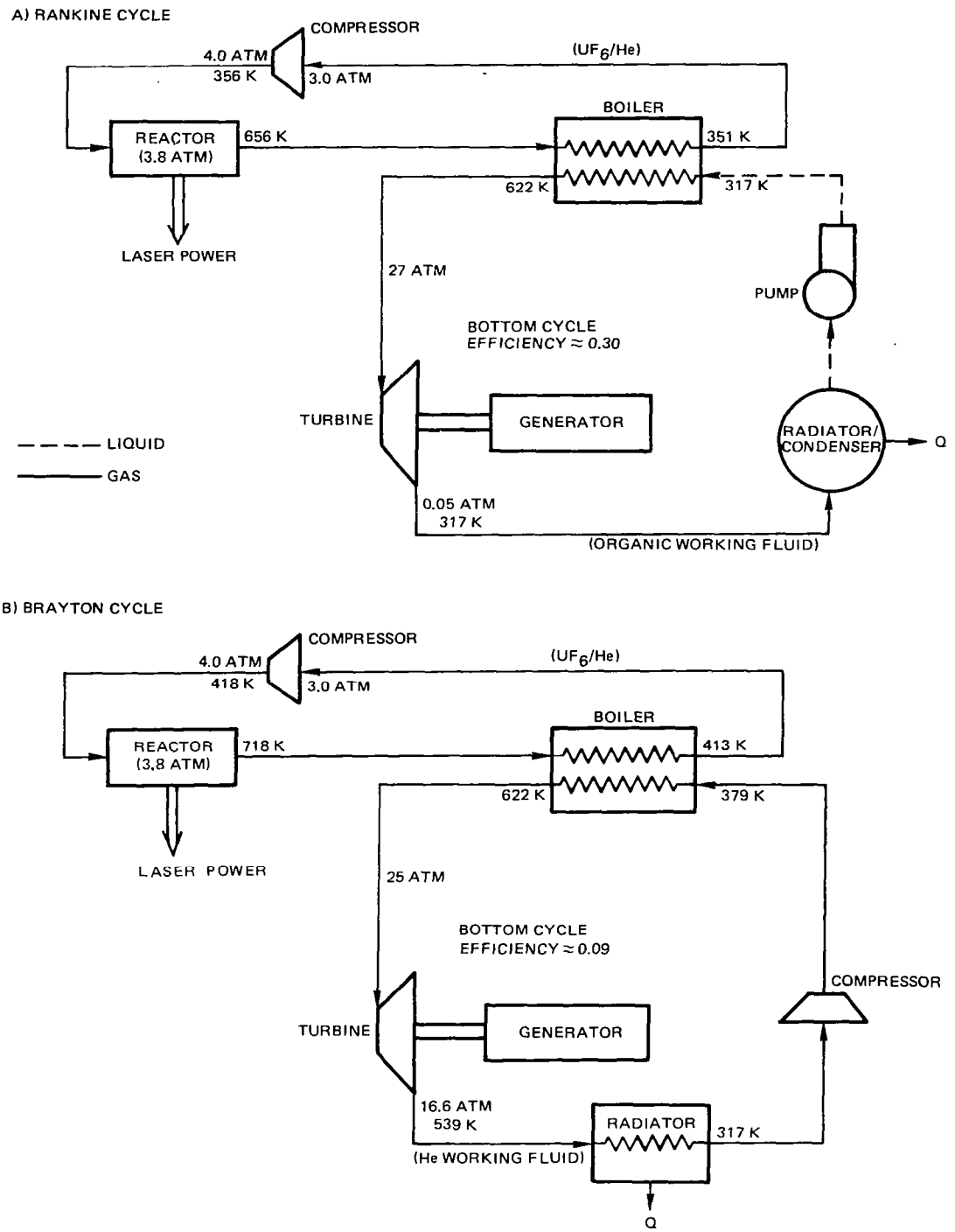

Figure 8

LIST OF PARTICIPANTS

B. D. Carter	Department of Nuclear Engineering, Nuclear Engineering Center, University of Florida, Gainesville, FL 32601
R. J. DeYoung	NASA Langley Research Center, Mail Stop 160, Hampton, VA 23665
J. G. Eden	Gaseous Electronics Laboratory, University of Illinois, Urbana, IL 61801
E. Gulari	Research Institute for Engineering Sciences, Wayne State University, Detroit, MI 48202
H. A. Hassan	Department of Mechanical and Aerospace Engineering, N.C. State University, P. O. Box 5246, Raleigh, NC 27607
F. Hohl	NASA Langley Research Center, Mail Stop 160, Hampton, VA 23665
W. M. Hughes	Los Alamos Scientific Laboratory, P. O. Box 1663, Q-14 MS-560, Los Alamos, NM 87545
N. J. Jalufka	NASA Langley Research Center, Mail Stop 160, Hampton, VA 23665
S. Lim	Research Institute for Engineering Sciences, Wayne State University, Detroit, MI 48202
W. E. Meador	NASA Langley Research Center, Mail Stop 160, Hampton, VA 23665
G. H. Miley	Nuclear Engineering Program, University of Illinois, 214 Nuclear Engineering Laboratory, Urbana, IL 61801
T. G. Miller	Redstone Arsenal, Attn: DRSMI-HS(R&D), Huntsville, AL 35809
W. B. Olstad	NASA Langley Research Center, Mail Stop 367, Hampton, VA 23665
M. A. Prelas	University of Illinois, 214 Nuclear Engineering Laboratory, Urbana, IL 61801
L. P. Randolph	NASA Headquarters, Mail Code RTS-6, Washington, DC 20546
M. Rowe	Department of Nuclear Engineering, University of Florida, Gainesville, FL 32611

G. R. Russel	Jet Propulsion Laboratory, Mail Code 122-123, 4800 Oak Grove Drive, Pasadena, CA 91103
R. T. Schneider	Department of Nuclear Engineering, University of Florida, Gainesville, FL 32611
A. Shapiro	NASA Langley Research Center, Mail Stop 160, Hampton, VA 23665
Y. Shiu	NASA Langley Research Center, Mail Stop 160, Hampton, VA 23665
J. J. Taylor	Air Force Weapons Laboratory, PGA, Kirtland Air Force Base, Albuquerque, NM 87117
M. Tougeau	Department of Physics, Miami University, Oxford, OH 45056
J. T. Verdeyen	Gaseous Electronics Laboratory, University of Illinois, Urbana, IL 61801
R. Walters	Department of Nuclear Engineering, Nuclear Engineering Center, University of Florida Gainesville, FL 32601
W. R. Weaver	NASA Langley Research Center, Mail Stop 160, Hampton, VA 23665
W. E. Wells	Department of Physics, Miami University, Oxford, OH 45056
M. D. Williams	NASA Langley Research Center, Mail Stop 160, Hampton, VA 23665
J. W. Wilson	NASA Langley Research Center, Mail Stop 160, Hampton, VA 23665

1. Report No.	2. Government Accession No.	3. Recipient's Catalog No.
NASA CP-2107		

4. Title and Subtitle	5. Report Date
Nuclear-Pumped Lasers	December 1979
	6. Performing Organization Code
7. Author(s)	8. Performing Organization Report No. L-13366
9. Performing Organization Name and Address NASA Langley Research Center Hampton, VA 23665	10. Work Unit No. 506-25-33-05
	11. Contract or Grant No.
12. Sponsoring Agency Name and Address National Aeronautics & Space Administration Washington, DC 20546	13. Type of Report and Period Covered Conference Publication
	14. Sponsoring Agency Code

15. Supplementary Notes

16. Abstract

The NASA Langley Research Center sponsored the NASA "Nuclear-Pumped Laser Workshop" in Hampton, Virginia, on July 24-25, 1979. The objectives of the workshop were to provide an interchange of recent research results and ideas among researchers in the field of nuclear-pumped lasers and to review the NASA Nuclear-Pumped Laser Program. A synopsis of the talks and the figures presented at the workshop are included in this publication. The presentations covered nuclear-pumped laser modeling, nuclear volume and foil excitation of laser plasmas, proton beam simulations, nuclear flashlamp excitation, and reactor laser systems studies.

17. Key Words (Suggested by Author(s))	18. Distribution Statement
Nuclear-Pumped Lasers	Unclassified-Unlimited Subject Catagory 36

19. Security Classif. (of this report)	20. Security Classif. (of this page)	21. No. of Pages	22. Price*
Unclassified	Unclassified	142	$7.25

* For sale by the National Technical Information Service, Springfield, Virginia 22161

NASA-Langley, 1979